

ABSTRACT

BECKER, SCOTT KARL. Assessing the Use of Dissolved Silicon as a Proxy for Groundwater Age: a Critical Analysis of Published Data and New Data from the North Carolina Coastal Plain. (Under the direction of Prof. David Genereux.)

Groundwater age dating tracers are used in studies investigating land management practices, contaminant transport, watershed mass-balance, and a variety of other topics. Many of the age-dating tracers used involve complicated collection procedures and have considerable cost associated with them (collection, analysis, materials, etc.). I investigated the potential for the use of dissolved silicon concentration in groundwater, [Si], as a cost-effective and simple alternative for estimating groundwater age, based on the observed linear increase of [Si] with increasing groundwater age in new and previously-published data. I performed a critical review on 11 published data sets that contained both groundwater age and [Si]. In addition, new results are presented on the groundwater age-[Si] relationship for the West Bear Creek watershed in the coastal plain of North Carolina. The data from these studies were used to build a series of regressions of age vs. [Si] for 10 different locations (6 in the Atlantic Coastal plain, 2 in the piedmont, and 2 elsewhere in the US) which could in principle be used to estimate groundwater age from groundwater [Si]. Across sites, the range in [Si] acquisition rate by groundwater (inverse of the slope on a regression of age vs. [Si]) was 3.0-232.6 $\mu\text{M}/\text{yr}$ (mean for the coastal plain was about 9.9 $\mu\text{M}/\text{yr}$), and 95% prediction intervals (for predicting age from [Si]) were ± 1 -30 yr (mean for the coastal plain was approximately ± 17.2 yr). Common state of the art age-dating tracers (CFCs, SF_6 , $^3\text{H}/^3\text{He}$) typically have a predicted age uncertainty of ± 1 -4 yr at best. Two sites in the NC coastal plain, Lizzie and West Bear Creek, are 30-40 km distant from each other and had [Si]

acquisition rates of 7.2 and 6.1 $\mu\text{M}/\text{yr}$, respectively. For the Fairmount and Willards coastal plain sites located in MD (which are approximately 60 km apart and are approximately 630 km north of the NC studies), the [Si] acquisition rates were 9.3 and 22.7 $\mu\text{M}/\text{yr}$, respectively. Thus, in the coastal plain, variation in the age-[Si] relationship may be large or small over distances of tens to hundreds of kilometers. These and other findings are consistent with geological and mineralogical properties of a study location as important controlling factors for [Si] acquisition. When the expected range of groundwater age is assessed for two intermediate values of [Si] using a combined plot showing all of the best regressions for the coastal plain, the range of expected groundwater ages for 50 μM of [Si] was found to be approximately 2.4-11.2 yr, and for 250 μM of [Si] the range was approximately 10.6-69.8 yr. It seems there is potential for using [Si] as an indicator of groundwater age within an area that has been "calibrated" through an observed age-[Si] relationship, and perhaps in similar but distant areas, depending on the acceptable magnitude for uncertainty in the age estimate (which would be determined by the specific problem or application for the age information). Areas of piedmont geology had better-defined age-[Si] linear relationships (r^2 of 0.8980 and 0.9140) compared to the coastal plain ($r^2 = 0.2096$ -0.6842). Lastly, [Si] acquisition rates estimated from the age-[Si] regressions were found to typically be about 1-4 orders of magnitude smaller than estimates of lab-based plagioclase dissolution rates for aquifer material, saprolite, and soils.

Assessing the Use of Dissolved Silicon as a Proxy for Groundwater Age: a Critical Analysis
of Published Data and New Data from the North Carolina Coastal Plain

by
Scott Karl Becker

A thesis submitted to the Graduate Faculty of
North Carolina State University
in partial fulfillment of the
requirements for the degree of
Master of Science

Marine, Earth, and Atmospheric Sciences

Raleigh, North Carolina

2013

APPROVED BY:

Prof. Dean Hesterberg

Prof. Helena Mitasova

Prof. David Genereux
Chair of Advisory Committee

DEDICATION

To my family, whose support and dedication has always been a source of inspiration.

BIOGRAPHY

Scott Karl Becker obtained a B.S. in Earth and Space Sciences from the University of Washington in March of 2010, and, with this thesis, an M.S. in geology (with a focus on hydrogeology) from N.C. State University. If opportunity allows, Mr. Becker will pursue a doctoral degree in the field of hydrology.

ACKNOWLEDGMENTS

I am thankful to my adviser Dr. David Genereux for all his contributions in the form of corrections, suggestions, and for his invaluable experience and guidance. I would also like to thank Dr. Helena Mitsova and Dr. Dean Hesterberg for their thoughtful comments and suggestions. I would like to thank Troy Gilmore for all of his hard work and dedication in organizing and orchestrating the field campaigns without which this project would not have been possible. Lastly, I would like to thank Dong-Chan Koh of the Korea Institute of Geosciences and Mineral Resources, South Korea, for his advice and insight.

TABLE OF CONTENTS

LIST OF TABLES	viii
LIST OF FIGURES	xi
1. INTRODUCTION	1
2. BACKGROUND	5
2.1. Applications of Age-dating Tracers.....	5
2.2. Tritium/Helium-3 ($^3\text{H}/^3\text{He}$) Method of Age-dating	7
2.3. Chlorofluorocarbons (CFCs) as Age-dating Tracers	8
2.4. Sulfur hexafluoride (SF_6) as an Age-dating Tracer	10
2.5. Sources of Error	10
2.6. Cost Comparison.....	11
2.7. Chemical Dissolution Reactions Contributing to Dissolved Silicate Concentration.....	11
3. PREVIOUS STUDIES OF GROUNDWATER AGE AND SILICON CONCENTRATION.....	15
3.1. Studies Used in the Analysis of [Si] vs. Groundwater Age.....	15
3.2. Effects of Screen Interval on Interpretation of Groundwater Age.....	19
3.3. Kenoyer and Bowser (1992).....	24
3.4. Tesoriero et al. (2005).....	27
3.4.1. Study Site.....	27
3.4.2. Dissolved Solute Sampling and Analysis Method.....	28
3.4.3. Age-dating Method	28
3.4.4. Data Analysis	30
3.5. Böhlke & Denver (1995)	35
3.5.1. Study Site.....	35
3.5.2. Dissolved Solute Sampling and Analysis Method.....	36

3.5.3. Age-dating Method	36
3.5.4. Data Analysis	37
3.6. Shapiro et al. (1999) and Savoie et al. (1998).....	42
3.6.1. Study Site	42
3.6.2. Dissolved Solute Sampling and Analysis Method.....	43
3.6.3. Age-dating Method	44
3.6.4. Data Analysis	45
3.7. Denver et al. (2010)	56
3.7.1. Study Site	56
3.7.2. Dissolved Solute Sampling and Analysis Method.....	58
3.7.3. Age-dating Method	59
3.7.4. Data Analysis	59
3.8. Rademacher et al. (2001)	74
3.8.1. Study Site	74
3.8.2. Dissolved Solute Sampling and Analysis Method.....	75
3.8.3. Age-dating Method	75
3.8.4. Data Analysis	76
3.9. Lindsey et al. (2003)	78
3.9.1. Study Site	78
3.9.2. Dissolved Solute Sampling and Analysis Method.....	79
3.9.3. Age-dating Method	80
3.9.4. Data Analysis	81
3.10. Burns et al. (2003).....	84
3.10.1. Study Site	84
3.10.2. Dissolved Solute Sampling and Analysis Method.....	85
3.10.3. Age-dating Method	86
3.10.4. Data Analysis	86
4. WEST BEAR CREEK STUDY SITE	91

4.1. Site Location, Land Use, and Previous Research	91
4.2. Hydrogeology	97
5. METHODS	103
5.1. Sample Collection Methods, West Bear Creek, April 2007 and July 2012	
Sampling	103
5.1.1. Sample Collection Strategy.....	103
5.1.2. [Si] Sample Field Collection Method	104
5.1.3. CFC and SF ₆ Field Collection Method	106
5.2. Lab Methods and Analysis.....	108
5.2.1. [Si] Analysis of April 2007 Samples	108
5.2.2. [Si] Analysis of July 2012 Samples	108
5.2.3. Lab Analysis of CFCs and SF ₆	111
6. WEST BEAR CREEK RESULTS	112
6.1. Existing and New Data from West Bear Creek (2007/2012)	112
6.1.1. Study Site.....	112
6.1.2. Data Analysis	112
6.2. West Bear Creek, July 2012 Samples	115
7. ANALYSIS OF AGE-Si RELATIONSHIPS IN GROUNDWATER	125
7.1. Sources of Dissolved Silicon in Groundwater	125
7.2. Relationships Between Groundwater [Si] and Groundwater age	126
7.3. Comparison of Lab-based and Field-based [Si] Kinetics	144
7.4. Effect of Biological Activity on [Si].....	161
7.5. Summary and Conclusions	162
REFERENCES CITED.....	165

LIST OF TABLES

Table 2.1. Prices for analysis and sampling containers for the three leading age-dating methods and for [Si].....	11
Table 3.1. Regression results (groundwater age vs. groundwater [Si]) for published studies	17
Table 3.2. Groundwater age and groundwater [Si] for the study by Kenoyer and Bowser (1992)	26
Table 3.3. Groundwater age and groundwater [Si] for the study by Tesoriero et al. (2005).....	34
Table 3.4. Groundwater age and groundwater [Si] for the study by Böhlke and Denver (1995).....	40
Table 3.5. Groundwater age and groundwater [Si] the studies by Shapiro et al. (1999) and Savoie et al. (1998).....	47
Table 3.6. Groundwater age and groundwater [Si] for wells upgradient of Ashumet pond for the study by Shapiro et al. (1999) and Savoie et al. (1998).....	50
Table 3.7. Groundwater age and groundwater [Si] for wells adjacent to Ashumet pond for the study by Shapiro et al. (1999) and Savoie et al. (1998).....	52
Table 3.8. Groundwater age and groundwater [Si] for wells downgradient of Ashumet pond for the study by Shapiro et al. (1999) and Savoie et al. (1998).....	54

Table 3.9. Groundwater age and groundwater [Si] for the study by Denver et al. (2010)	63
Table 3.10. Regression results (groundwater age vs. groundwater [Si]) for the Lizzie Site, NC, including a regression of the combined data from Tesoriero et al. (2005) and Denver et al. (2010).....	70
Table 3.11. Regression results (groundwater age vs. groundwater [Si]) for the Locust Grove site in MD, based on (1) data in Böhlke and Denver (1995) alone, (2) data in Denver et al. (2010) alone, and (3) the combined data from both papers.....	72
Table 3.12. CFC-11 and CFC-12 groundwater age and groundwater [Si] for the 1999 sampling event by Rademacher et al. (2001)	77
Table 3.13. Polecat Creek groundwater age data and groundwater [Si] for the study by Lindsey et al. (2003).....	82
Table 3.14. Groundwater age data and groundwater [Si] for the study by Burns et al. (2003).....	89
Table 5.1. Values for lab determined and calculated (true) [Si] for four standards	110
Table 6.1. West Bear Creek data set showing groundwater age data collected by Kennedy et al. (2009a) in 2007, and [Si] values determined by Koh at KIGAM in 2012	114

Table 6.2. West Bear Creek data set showing SF ₆ determined groundwater age and [Si] data collected in July 2012	117
Table 6.3. West Bear Creek data set showing CFC-11 and CFC-113 determined groundwater age and [Si] data collected in July 2012	119
Table 7.1. Regression results (groundwater age vs. groundwater [Si]) for published studies	129
Table 7.2. . Mineral weathering rates in the units commonly reported in the scientific literature (mol•m ⁻² s ⁻¹), as estimated from [Si] accumulation rates (μM/yr, inverse of the slopes of the age-[Si] regressions).....	157
Table 7.3. Grain size results from the core collected near West Bear Creek in Wayne County, NC.....	159

LIST OF FIGURES

Figure 2.1. Historic atmospheric concentrations for three varieties of CFCs, SF ₆ , and tritium	6
Figure 3.1. Elevation vs. groundwater [Si] from Bau et al. (2004)	19
Figure 3.2. Histogram showing the distribution of screen lengths for 225 wells or piezometers	22
Figure 3.3. Range of groundwater ages intercepted by well screens of different lengths using a recharge of 20 cm/yr, a porosity of 0.30, and an aquifer thickness of 20 m	23
Figure 3.4. Range of groundwater ages intercepted by well screens of different lengths using a recharge of 30 cm/yr, a porosity of 0.30, and an aquifer thickness of 30 m	24
Figure 3.5. Groundwater age vs. groundwater [Si], with values estimated from Figure 7 of Kenoyer and Bowser (1992)	27
Figure 3.6. Map showing well locations at the Lizzie Research station where cores and groundwater samples were collected	29
Figure 3.7. Groundwater age vs. groundwater [Si] based on 9 points of highest confidence from Tesoriero et al. (2005)	35
Figure 3.8. Groundwater age vs. groundwater [Si] for Chesterville Branch and Morgan Creek based on data from Böhlke and Denver (1995)	41

Figure 3.9. Groundwater age vs. groundwater [Si] for Chesterville Branch and Morgan Creek based on data from Böhlke and Denver (1995) combined into a single regression.....	42
Figure 3.10. Groundwater age vs. groundwater [Si] based on all 62 points from Shapiro et al. (1999) and Savoie et al. (1998).....	49
Figure 3.11. Groundwater age vs. groundwater [Si] based on 14 points from Shapiro et al. (1999) and Savoie et al. (1998) representing wells upgradient to Ashumet pond.....	51
Figure 3.12. Groundwater age vs. groundwater [Si] based on 8 points from Shapiro et al. (1999) and Savoie et al. (1998) representing wells adjacent to Ashumet Pond.....	53
Figure 3.13. Groundwater age vs. groundwater [Si] based on 40 points from Shapiro et al. (1999) and Savoie et al. (1998) representing wells downgradient to Ashumet Pond.....	56
Figure 3.14. Groundwater age vs. groundwater [Si] for Fairmount, Locust Grove, the Lizzie Site, and the Willards area	65
Figure 3.15. Groundwater age vs. groundwater [Si] for the Fairmount based on 20 points from Denver et al. (2010).....	66
Figure 3.16. Groundwater age vs. groundwater [Si] for Locust Grove based on 13 points from Denver et al. (2010).....	67

Figure 3.17. Groundwater age vs. groundwater [Si] for the Lizzie Site based on 15 points from Denver et al. (2010).....	68
Figure 3.18. Groundwater age vs. groundwater [Si] for the Willards site data based on 9 points from Denver et al. (2010).....	69
Figure 3.19. Groundwater age vs. groundwater [Si] at the Lizzie site in NC, based on combining 24 points from Tesoriero et al. (2005) and Denver et al. (2010)	71
Figure 3.20. Groundwater age vs. groundwater [Si] at the Locust Grove site in MD (For the Chesterville Branch and Morgan Creek), based on combining 45 points from Böhlke and Denver (1995) and Denver et al. (2010)	73
Figure 3.21. Exponential fit to the groundwater age and [Si] data for the Fairmount site based on 20 points from Denver et al. (2010)	74
Figure 3.22. Groundwater age vs. groundwater [Si] based on 10 points from the data presented in Rademacher et al. (2001)	78
Figure 3.23. Groundwater age vs. groundwater [Si] based on 12 points from Lindsey et al. (2003)	83
Figure 3.24. Piston flow model for CFC-12 and SF ₆ constructed from historic atmospheric concentrations.....	84
Figure 3.25. Groundwater age vs. groundwater [Si] based on 20 points from Burns et al. (2003).....	90

Figure 4.1. Map of the area around the West Bear Creek Study reach.....	95
Figure 4.2. Map showing exact location of the West Bear Creek Study reach	96
Figure 4.3. Stratigraphic columns representing the hydrogeology underlying the study reach	100
Figure 4.4. Stratigraphic column produced by the study conducted by Kennedy et al. (2009a).....	101
Figure 5.1. Representation of sampling strategy and equipment for the West Bear Creek channel.....	106
Figure 5.2. Calculated true values of [Si] standards vs. lab-determined values of [Si] standards	110
Figure 6.1. Groundwater age vs. [Si] based on 24 samples collected in 2007 from beneath the streambed of West Bear Creek	115
Figure 6.2. SF ₆ determined groundwater age vs. [Si] based on 10 samples collected in July of 2012 from beneath the streambed of West Bear Creek.....	118
Figure 6.3. CFC-11 determined groundwater age vs. [Si] based on 10 samples collected in July of 2012 from beneath the streambed of West Bear Creek.....	120
Figure 6.4. CFC-113 determined groundwater age vs. [Si] based on 10 samples collected in July of 2012 from beneath the streambed of West Bear Creek.....	121

Figure 6.5. CFC-11, CFC-113, and SF₆ determined groundwater age vs. [Si] for samples collected from 10 points in July of 2012 from beneath the West Bear Creek streambed.....122

Figure 6.6. Groundwater age vs. [Si] for West Bear Creek based on 24 samples collected in April 2007 combined with all July 2012 data (CFC-11, CFC-113, and SF₆).....123

Figure 6.7. Groundwater age vs. [Si] for West Bear Creek based on 24 samples collected in April 2007 combined with CFC-113 determined groundwater age and [Si] for 10 samples collected in July 2012124

Figure 7.1. Approximate positions for the seven studies located in the coastal plain, as determined from GIS data and relative positions from the published figures presented in the literature for the studies shown.....128

Figure 7.2. [Si] acquisition rate per year for 13 age-[Si] regressions from 10 studies132

Figure 7.3. Regression slopes for all of the studies which have been conducted in the coastal plains area142

Figure 7.4. The uncertainty in groundwater age prediction based on the age-[Si] regressions in Table 7.1143

Figure 7.5. Grain-size distribution for sample Wayne-2013-01-E, representing

a depth of approximately 16 ft below the land surface.....155

Figure 7.6. Grain-size distribution for sample Wayne-2013-01-J, representing
a depth of approximately 48 ft below the land surface156

Figure 7.7. Mineral dissolution rates for the studies reported in Table 4 in
White and Brantley (2003), and rates from Table 7.2 of this report, and rates
representing two scenarios for the dissolution of plagioclase160

1. INTRODUCTION

Groundwater age-dating tracers have a wide variety of uses in the field of hydrology, hydrogeology, and groundwater resources, such as: determining velocity and direction of groundwater flow, determining hydraulic conductivity on a large spatial scale (Bethke and Johnson 2008), determining residence time of groundwater (Bauer et al. 2001), and in general they allow for the integration of chemical and physical hydrology. Groundwater age-dating tracers have been applied to studies dealing with contaminant transport (Kennedy et al. 2009a,b, Böhlke et al. 2007, Katz 2004, Tesoriero et al. 2000), aquifer recharge and baseflow discharge studies (Plummer et al. 2001, Cherry 2000, Szabo et al. 1996), land management studies (Stoner et al. 1997), recent climate-change studies (Rademacher et al. 2002), as well as a myriad of other hydrological studies (Puckett et al. 2002, Cook & Solomon 1995). Many of the existing age-dating methods in use today, however, are complicated and expensive.

This project explored the potential for using dissolved silicon concentration, [Si] (present in groundwater mainly as silicic acid, chemical formula $\text{Si}(\text{OH})_{4(\text{aq})}$ (Iler 1979)), as a proxy for groundwater age. Relationships between [Si] and groundwater age have been previously recognized (e.g., Tesoriero et al. 2005), but to our knowledge no exhaustive studies of the application for age-dating groundwater have been conducted. Other studies (Bau et al. 2004, Scanlon et al. 2001, Day and Nightingale 1984) show an increase in [Si] with depth, which can serve as a possible indicator of increasing [Si] with increasing

groundwater age, since it has been observed that groundwater age typically increases with depth below the water table (Solomon et al. 1992). If [Si] does increase with increasing groundwater age, then it is possible that this correlation is strong enough to have predictive power, which is very useful in that it suggests that there is potential to estimate age from [Si], a solute which has proven much easier and less expensive to analyze than other age dating tracers. This correlation between increasing [Si] with increasing groundwater age leads to the main research question addressed in my study: how useful is [Si] as an age-dating proxy for shallow groundwater in the coastal plain? Supporting research questions addressed in this study include:

1. What is the relationship between groundwater [Si] and groundwater age, based on evidence in the existing scientific literature?
2. What is the relationship between groundwater [Si] and groundwater age, based on new data collected in the NC coastal plain?
3. How does this correlation vary between different areas in the North Carolina coastal plain in relation to geology or hydrogeology?
4. Compared to other groundwater age-dating methods, what are the pros and cons of using [Si] content as a proxy for groundwater age (e.g., uncertainty, cost, etc.)?
5. From the scientific literature, how do lab-determined Si dissolution rates compare to field-determined Si dissolution rates that are based on [Si] and age-dating tracer data?

This method of age-dating groundwater is attractive because it may provide an inexpensive (few dollars per age determination) alternative to other age-dating methods that require more

complex and expensive analyses (several hundred dollars per age determination) of dissolved gases and/or isotopes. This cost-effective age-dating method allows for a greater sampling point density or for a larger area to be assessed more efficiently and inexpensively.

This thesis includes a critical review and synthesis of published data and a collection of new data showing the relationship between [Si] and groundwater age. Three collections of data have been included:

- West Bear Creek, NC, 2007: 23 samples of groundwater collected in April 2007 from near West Bear Creek in the NC coastal plain (Kennedy et al. 2009a). Age dating of the groundwater was done by the CFC method in 2007, at the USGS CFC Lab in Reston, VA. [Si] analyses were done in 2012, at the Korea Institute of Geosciences and Mineral Resources (KIGAM).
- West Bear Creek, NC, 2012: 10 samples of groundwater collected in July 2012 from a different area near West Bear Creek (part of a larger 39-sample data set for which analysis was still underway at the time of completion of this thesis). Age dating of the groundwater was done by the CFC method.
- Literature data: Data from 8 sources from the scientific literature. All sources include data pertaining to dissolved silicon concentration and groundwater ages determined by gaseous tracer age dating methods.

It is important to note that application of [Si] as an age-dating tracer may require "calibration" with other tracers such as those mentioned above (i.e., a plot of age determined by $^3\text{H}/^3\text{He}$, CFCs, or other means vs. [Si]), but once that line is available it may be possible to

realize cost-savings on further age estimates by using [Si]. The predictive power and geological or geographical limits on such calibration lines would be important questions, and are addressed to some extent in this report. This thesis will answer the main research question and supporting research questions by discussing the evidence from previously published literature and the evidence from new data collected from the North Carolina coastal plain.

For the purposes of this proposal, groundwater age refers to what is commonly called the “apparent age”, the age calculated assuming the groundwater and tracer moved through the aquifer to the sample collection point by simple piston flow (so that the groundwater sample does not contain a mixture of waters of different ages). This study is part of a larger collaborative research project being conducted by the University of Utah, the U.S. Geological Survey, and North Carolina State University.

2. BACKGROUND

2.1. Applications of Age-dating Tracers

There are three primary methods for the dating of young groundwater: CFCs, SF₆, and ³H/³He, all of which can be used to date groundwater that was recharged into the aquifer less than 30-50 years ago (Plummer et al. 2003). All of the age-dating methods discussed in this section depend on atmospherically-derived environmental tracers. These atmospherically-derived environmental tracers are fairly ubiquitous worldwide, although SF₆ is produced predominately in the mid-latitudes of the Northern hemisphere (Busenberg & Plummer 2000). In addition, most studies using the ³H/³He age-dating method should consider local ³H concentration via precipitation records to improve accuracy, due to the possibility of local sources of contamination (Solomon & Cook 2000).

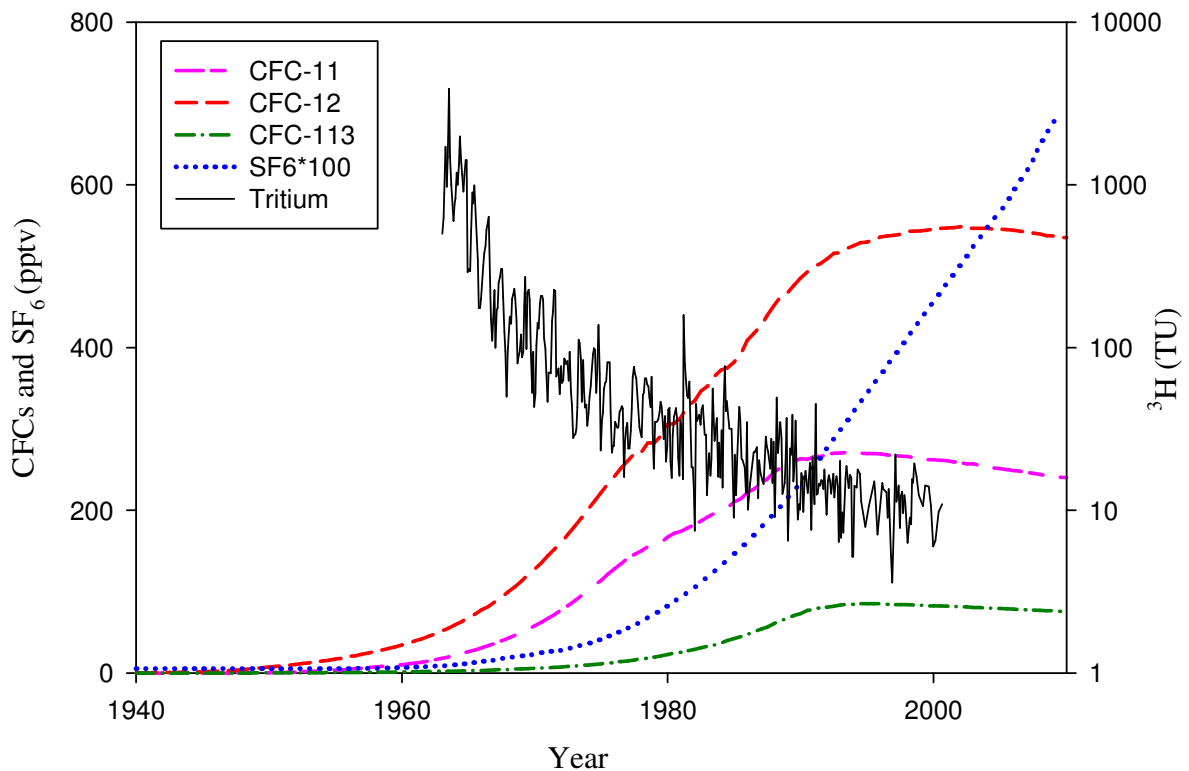


Figure 2.1. Plot showing historic atmospheric concentrations for three varieties of CFCs, SF₆, and tritium. Tritium data measured in Washington D.C. and analyzed at the USGS Reston Stable Isotope Laboratory (<http://www-naweb.iaea.org/napc> 2012); CFC and SF₆ data measured in Niwot Ridge, Co, and analyzed by USGS Chlorofluorocarbons Laboratory, Reston, VA (Busenberg and Plummer 2011).

There are several main concepts and assumptions involved in determining groundwater age using gaseous age-dating tracers. To begin, environmental tracers are recharged into the groundwater at the water table, and it is assumed that groundwater does not exchange these tracers with the atmosphere after the time of recharge through the water table, i.e., the groundwater is a closed system (Bethke & Johnson 2008). It is also assumed that the time spent in the unsaturated zone is not significant (true if the unsaturated zone is not thick) (Cook & Böhlke 2000). Movement through the saturated zone assumes a piston

flow model (Plummer et al. 2003). Temperature, pressure, and dissolved solute concentration (at time of recharge for gaseous tracers) must be known in order to define the parameters of the gas solubility function (Plummer et al. 2006). It is assumed that the water sample was in solubility equilibrium with the atmosphere at the time of recharge, though additional gases may be added soon after recharge by dissolution of trapped bubbles ("excess air"), requiring additional analysis in the age estimation process (Stute and Schlosser 2000). These assumptions allow for the water gas-content to be compared to historic atmospheric concentrations (Figure 2.1), which can be used to determine an "apparent age".

2.2. Tritium/Helium-3 ($^3\text{H}/^3\text{He}$) Method of Age-dating

$^3\text{H}/^3\text{He}$ dating is based on the introduction of ^3H into the atmosphere via the testing of nuclear weapons (which peaked in the 1960s) and on the decay of ^3H to ^3He (referred to as ^3He in-growth, the half-life of ^3H is 12.4 years) (Plummer et al. 2003). This dating technique is useful because the age of the young groundwater is yielded by a ratio of the parent and daughter isotopes, and is thus theoretically unaffected by the introduction of or mixing with older groundwaters (Plummer et al. 2003). This method of age-dating young groundwaters is also dependent on the comparison to historic atmospheric concentrations, and was shown to agree within 3 years when compared to other age-dating methods (Ekwurzel et al. 1994).

Tritium is measured by the radiometric method involving low level liquid scintillation or gas proportional counting after electrolytic enrichment or by measuring the amount of the

daughter product (^3He) produced in a sealed water sample in the lab which is subsequently measured via mass spectrometry (Solomon & Cook 2000). This method must account for mantle helium (typically not a concern in shallow groundwater systems) and atmospheric helium-4 (Kazemi et al. 2006). Tritium is expressed in the units “TU”, representing one tritium-containing water molecule to 10^{18} normal water molecules (Solomon & Cook 2000).

The method of using only tritium has been used in the past, but becomes more inefficient as time progresses (as it requires several samples from a vertical profile in the ground to determine progression of tritium). As can be seen in Figure 2.1, the atmospheric concentration of tritium has peaked and is now in decline. Use of $^3\text{H}/^3\text{He}$ was found to be more effective because this method involves the measurement of a parent daughter-ratio, which does not require the tritium input function be known (Kazemi et al. 2006, Han et al. 2006).

2.3. Chlorofluorocarbons (CFCs) as Age-dating Tracers

CFCs have been in existence since the 1930s, and had a wide variety of uses for industry and household appliances. Detectable limits of CFCs are present in groundwaters recharged after 1945, and the three common varieties of CFCs (CFC-11, CFC-12, and CFC-113) have historically increased in atmospheric concentration, peaked at different times in the 1990s, and are now in a decline as a result of protocols which limit or forbid their use due to their destruction of stratospheric ozone (Busenberg & Plummer 1992). CFCs have been a

useful groundwater age-dating tool (although their decline in the atmosphere is now complicating their use in age-dating) because the concentration of each variety of CFC in groundwater can be compared to atmospheric concentrations to estimate the year of groundwater recharge.

When CFCs enter the groundwater system as recharge through the water table, the temperature and barometric pressure (i.e. altitude) must be known at the time of recharge (Plummer and Busenberg 2006). The three dominant varieties of CFCs (listed above) that were introduced into the atmosphere at different times allow for the use of ratios of any two of the three CFC species, which can assist in identifying degradation or contamination of CFCs that may have occurred in the sample since the time of recharge (Plummer et al. 2003). CFC-11 is commonly not used, as this species is prone to significant amounts of microbial degradation (Cook et al. 2006). Concentration of CFCs in a sample is converted from concentration in water to atmospheric concentration (pptv), and then compared to historic atmospheric concentrations to determine recharge date and apparent age (Plummer and Busenberg 2006).

Groundwater samples for CFC dating are collected in the field using a meticulous sampling process to insure that they represent historic recharge, as there is a possibility that the “clock” may be reset (the age information altered) if there is gas exchange during sample collection. In the lab, CFCs are measured by pre-concentrating using purge and trap

procedures, separating via gas chromatography, and are then measured with an electron capture detector (Buesenberg and Plummer 2006).

2.4. Sulfur hexafluoride (SF₆) as an Age-dating Tracer

SF₆ is an odorless, colorless, stable anthropogenic gas used as an insulator in high voltage switches, or for magnesium metal production. SF₆ is rapidly increasing in the atmosphere (see Figure 2.1), and can be used to date groundwaters that are younger than 40 years (Busenberg & Plummer 2000). Much like CFCs, SF₆ concentrations in groundwater can be compared to historic atmospheric concentrations. SF₆ is useful in that it is not as susceptible to microbial degradation (less so than CFC-11, for example), and can be analyzed in groundwater with a precision of 1-3% (Plummer et al. 2003). SF₆ is measured in the lab by gas chromatography, and the method has the same underlying principles as the CFC method, but requires a larger sample size of 1 liter.

2.5 Sources of Error

Sources of error or complications inherent to the gaseous age-dating methods include: gas exchange with the atmosphere after the time of original recharge (especially during sample collection), mixtures of groundwater of multiple ages, presence of "excess air" in the samples, sample contamination (e.g., CFCs from discarded equipment rather than the atmospheric source), and dispersion (Bethke & Johnson 2008, Kazemi et al. 2006, Plummer et al. 2003).

2.6. Cost Comparison

The costs of sample analysis and sampling containers are much more expensive for the age-dating methods discussed above than for [Si] (Table 2.1).

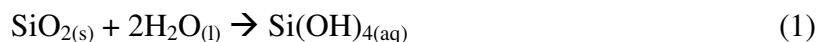
Table 2.1. Prices for analysis and sampling containers for the three leading age-dating methods and for [Si].

Age-Dating Method	Laboratory	Cost of Analysis	Receptacle/Cost
[Si]	NCSU Environmental and Agricultural Testing Service (ICP-AES)	\$2.65 per site	20 mL plastic scintillation vial/ ~\$0.35 per sample bottle ¹
[Si]	NCSU Center for Applied Aquatic Ecology (Colorimetric)	\$7.67 per site	20 mL plastic scintillation vial/ ~\$0.35 per sample bottle ¹
³ H/ ³ He	University of Utah Noble Gas Lab	\$620 per site ²	Copper tube/ ~\$2.00 per sample ⁶ , steel clamp/ \$40.00 (reusable) ⁶ , 500 mL polypropylene bottle/\$2.80 per sample bottle ³
CFC	USGS Reston CFC	\$550 per sample ⁴	3-4 125 mL clear glass bottle/~\$4.90 per sample bottle ¹
SF ₆	USGS Reston CFC	\$550 per sample ⁴	1 liter sized, plastic safety coated, amber glass bottle/~\$5.00 per sample bottle ⁵

¹Fischer Scientific; ²for both the ³H and ³He analysis; ³Wheaton; ⁴includes the cost of analysis of other dissolved gases needed for estimation of excess air in the groundwater ⁵Qorpak Lab Glassware, Supplies, Containers, and Packaging; ⁶personal communication with Kip Solomon, January of 2012.

2.7. Chemical Dissolution Reactions Contributing to Dissolved Silicate Concentration

The dissolution of silica in an excess of water occurs via the following reaction (Iler 1979):

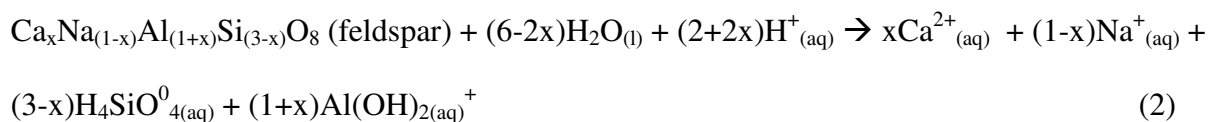


This reaction creates the soluble form of silica referred to as monosilicic acid. It is a weak acid, and is essentially nonionic in neutral and weakly acidic solutions (Iler 1979).

Polysilicic acids (also known as oligomers-typically smaller than 50Å) and colloidal silica (larger than 50Å) can also be present in a water sample if the water is saturated in regards to monosilicic acid. These particles can range in size from approximately 0.001µm to larger than 0.005µm (Iler 1979) and are reported as “dissolved silica” according to the analysis method commonly used. Groundwater samples for the analysis of [Si] are typically filtered with 0.2-0.45 µm filters.

The most common crystalline form of silica is quartz (SiO₂). The solubility of quartz, commonly present as sand, is 6 ppm SiO₂. For naturally weathered primary silicate minerals, quartz generally has the lowest dissolution rate, potassium feldspar has a higher dissolution rate, and plagioclase has the highest dissolution rate of all three (Brantley & Mellott 2000).

The dissolution of plagioclase feldspars occurs via the following reaction (Velbel 1985):



However, as is exhibited in the reaction below showing the second stage of weathering of plagioclase feldspar (Kittrick 1970), the formation of secondary minerals (such as smectite, montmorillonite, or kaolinite) results in the uptake of some of the aqueous silica:



The secondary mineral kaolinite can also be produced by the dissolution of the primary mineral biotite, a common constituent in granites and pegmatites. Biotites weather easily and thus will most likely not be found far from the parent source. Kenoyer and Bowser (1992) note the weathering of plagioclase feldspar to kaolinite and smectite as another important silicate weathering reaction.

It has been shown that in the presence of polyvalent metal cations such as Fe, Al, and other metals, colloidal silicates or clays are formed, and have a significantly reduced solubility compared to monosilicic acid (Iler 1979). Stated differently, this means that the formation of secondary minerals in a natural system (such as a shallow aquifer) can result in the lowering of or stabilization of [Si] when compared to increasing groundwater age. In the study done by Kenoyer and Bowser (1992) looking at a shallow aquifer system between two lakes, [Si] was observed to increase along a flow path, then the [Si] held constant for a portion of the flow path, then values were observed to increase again. This was attributed to the formation of secondary minerals (such as kaolinite or smectite) in a layer of strata along a portion of the path traveled by groundwater.

Increasing specific surface area (with decreasing grain size) has shown to parallel with increasing dissolution rates for primary silicate minerals (Brantley and Mellott 2000). This is because a greater surface area allows for an increased area on which chemical reactions may occur, increasing the weathering rate. The affect is exacerbated by pitting and striations, which are the result of weathering, and further increase the amount of weathering surface. This implies that in a crystalline silica-rich system, finer grain size may lead to an increased weathering rate, which results in an accelerated creation of [Si].

3. PREVIOUS STUDIES OF GROUNDWATER AGE AND SILICA CONCENTRATION

3.1. Studies Used in the Analysis of [Si] vs. Groundwater Age

This section reviews 9 previously published studies reporting data for both groundwater [Si] and groundwater age (Table 3.1). New results on [Si] and age from the WBC study site are presented in Chapter 6: West Bear Creek Results and Discussion. For each study, a plot was made of groundwater age vs. groundwater [Si], and linear regression was used to estimate the slope, intercept, and correlation statistics r^2 and p . With regards to slope, the p -value indicates the probability of being wrong in rejecting the null hypothesis that the regression slope equals zero, i.e., a low p indicates a high probability there is some relationship between the two variables (Zar 1999, p. 328-329). In the SigmaPlot® 10 users manual (2006, p. 672), the p -value is described as the probability of being wrong in concluding that the coefficient (for our purposes the slope and intercept coefficient) is not zero. The smaller the p -value, the greater the probability that the coefficient is not zero. It is usually concluded that the independent variable can be used to predict the dependent variable when $p < 0.05$.

The study by Bau et al. (2004) is not in Table 3.1 because it does not include groundwater age data, but it does show a positive relationship between groundwater [Si] with increasing depth in groundwater (Fig. 3.1), which is consistent with a positive relationship between [Si] and age because groundwater age typically increases with depth. The study by

Bau et al. (2004) took place in Ashumet Valley, northeastern Falmouth, Cape Cod, Massachusetts. The aquifer under study was the Cap Cod aquifer, and the samples and depth data presented in the study were obtained from multilevel samplers that had been installed in the area for the USGS study described by Savoie et al. (1998). [Si] was analyzed using ICP-AES (Bau et al. 2004).

Table 3.1. Regression results (groundwater age vs. groundwater [Si]) for published studies. "n" = number of data points in the regression. In each cell of the last column, the P values apply to the slope and intercept, respectively.

Study	Study Area	n	Geology/Geologic Formations	slope (yr/ μ M)	intercept (yr)	r ²	P
Kenoyer and Bowser (1992)	Crystal Lake, Vilas County, WI	6	Glacial sediments overlying Precambrian bedrock comprised of gneisses, amphibolite, schists, granites, monzonites, mafic metavolcanics, and quartzose and feldspathic sandstones	0.0186	0.566	0.9555	0.0005/ 0.0219
Tesoriero et al. (2005)	Contentnea Creek sub-basin of the Neuse River, NC	9	Yorktown aquifer material overlain by sandy-clayey silt	0.1965	-14.401	0.8500	0.0004/ 0.0385
Böhlke and Denver (1995)A	Delmarva Peninsula, MD (Chesterville Branch/ Morgan Creek)	18; 14	Permeable sand and gravel units of the fluvial Pensauken Formation and the marine glauconitic Aquia Formation	0.3693/ 0.3831	-13.979/ -22.743	0.4604/ 0.5880	(<0.0020/ 0.1474) /(0.0014/ 0.0572)
Shapiro et al. (1999) B and Savoie et al. (1998)B	Ashumet Valley, Falmouth, MA	62; 14; 8; 40	Carbonate-free silicate Pleistocene sediments (90% quartz) deposited during last glacial regression	0.0995/ 0.0607/ 0.0811/ 0.1278	-1.422/ -2.360/ -2.570/ -2.259	0.3357/ 0.0659/ 0.2795/ 0.6751	<(0.0001/ 0.6742) /(0.3755/ 0.8603) /(0.1179/ 0.8122)/ (<0.0001/ 0.3887)
Denver et al. (2010)C	Fairmount, DE/ Locust Grove, MD/ Lizzie, NC/ Willards, MD	20; 13; 15; 9	Fairmount: primarily permeable sand and gravel (Beaverdam Formation) underlain by the sandy Bethany Formation; Locust Grove:	0.1074/ 0.2429/ 0.1070/ 0.0440	-16.170/ -26.172/ 1.138/ 0.520	0.4863/ 0.6605/ 0.6425/ 0.6077	(0.0006/ 0.0414) /(0.0007/ 0.0271)

Table 3.1 Continued

			permeable quartz sand and gravel sediments of the Pennsuaken Formation, underlain by highly weathered fine-grained glauconitic sands of the Aquia Formation; Lizzie: described above (Tesoriero 2005). Willards: Beaverdam sand overlain by 3-8 m the clay, silt, peat, and sand of the Omar Formation, which is overlain by 3-8 m of the Parsonsburg Sand, which is a sandy unit with interspersed clay, silt, and organic matter.				/(0.0003/ 0.7630) /(0.0132/ 0.8474)
Rademacher et al. (2001)	Sagehen Basin, Nevada County, CA-eastern Sierra Nevada	10	Glacial till deposits derived from a combination of andesite and granodiorite basement rocks	0.0043	23.914	0.0030	0.8802/ 0.1111
Lindsey et al. (2003)	VA Piedmont	12	Piedmont Crystalline consisting primarily of garnet-biotite gneiss	0.0572	-4.3432	0.9140	<0.0001/ 0.0183
Burns et al. (2003)	Piedmont, southern GA	20	Panola Granite intruded into the Clairmont Formation	0.0490	-5.088	0.8980	<0.0001/ <0.0001

A: Results in this row are reported for two different regressions from two different watersheds: Chesterville Branch (n=18) and Morgan Creek (n=14), respectively.

B: Results in this row are reported for 4 different regressions: all data points (n=62), data points from wells upgradient of Ashumet pond (n=14), data points from wells adjacent to Ashumet pond (n=8), and data points from wells down gradient of Ashumet pond (n=40), respectively.

C: Results in this row are reported for 4 different regressions from four different watersheds: Fairmount (n=20), Locust Grove (n=13), Lizzie (n=15), and Willards (n=9), respectively.

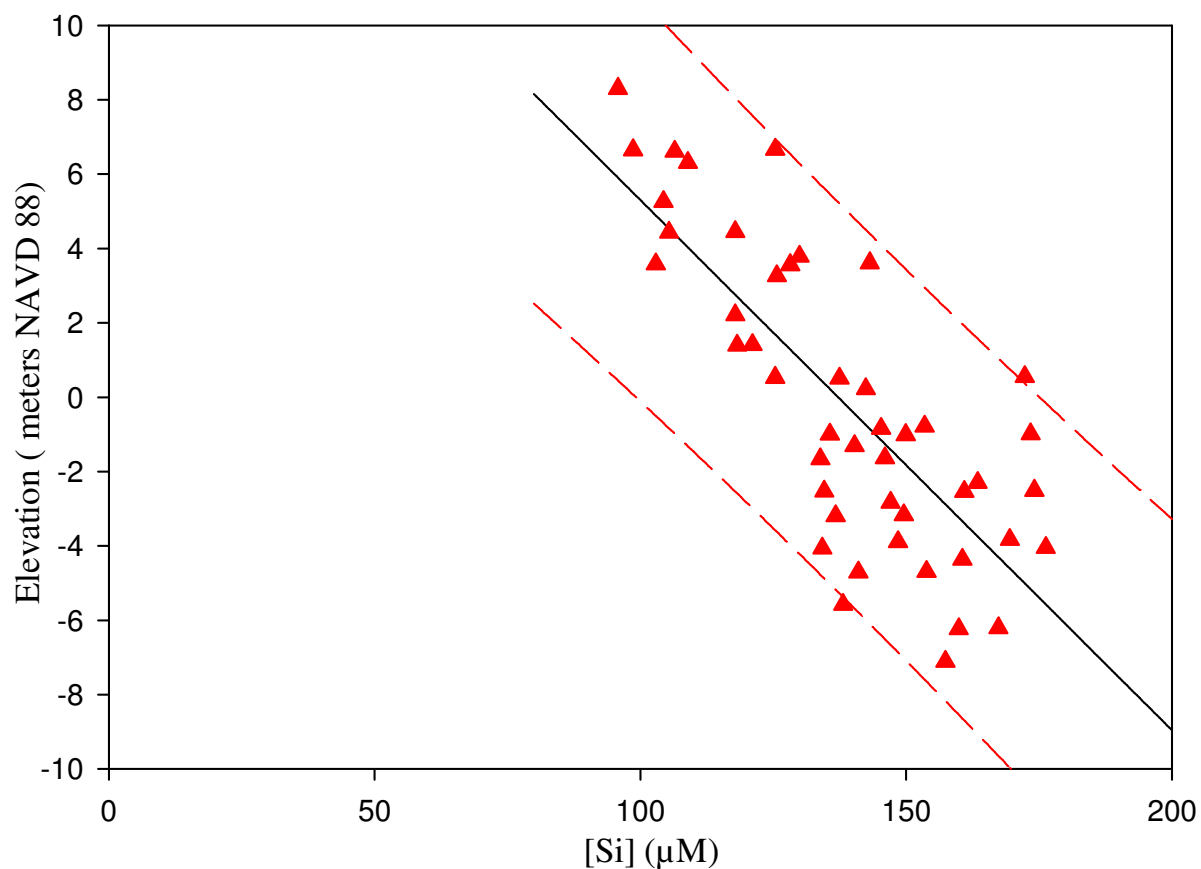


Figure 3.1. Elevation (relative to average sea level, taken as North American Vertical Datum of 1988 (NAVD 88)) vs. groundwater [Si] ($n = 46$) from Bau et al. (2004). Regression analysis yielded a slope of $-0.1426 \text{ m}/\mu\text{M}$, an intercept of 19.5614 m , an r^2 of 0.5997 , and p -values of <0.0001 for both the slope and intercept. Red dashed lines are 95% prediction intervals.

3.2. Effects of Screen Interval on Interpretation of Groundwater Age

For the purposes of this study it was necessary to evaluate the effect that the screened interval of wells or piezometers had on the distribution of groundwater age. For an unconfined aquifer receiving recharge over its upper surface, such as the surficial aquifer, groundwater age increases with increasing depth (Solomon et al. 2006). Due to this principle, groundwater intercepted during sampling through a vertical well screen can represent a range

of ages, with the extent of the range depending on the length of the screened interval and the depth at which the well or piezometer is screened (groundwater age contours are increasingly compressed nearer to the bottom of the aquifer, e.g., Solomon et al. 2006). For this reason, I considered whether some Si-age data should be excluded from the regression analysis due to uncertainty in the age estimates arising through the collection of groundwater samples from wells with long screens (such samples could represent complex mixtures of groundwater with a range of ages). Most of the data reported in the studies in Table 3.1 are based on samples collected through screens <1 m long, but some samples were collected through longer screens (Fig. 3.2).

To give an approximate idea of the magnitude of screen length effects, I created plots showing the range of groundwater ages that would be intercepted by screens of different length at different depths, based on the equation predicting the distribution of groundwater ages in an unconfined aquifer of uniform thickness receiving uniform recharge:

$$t = (L\Theta/R)\ln(L/(L-z)) \quad (3.1)$$

where L is aquifer thickness, R is recharge rate, Θ is porosity, and z is depth below the water table (Solomon et al. 2006). As shown in the equation, recharge rate, porosity, and aquifer thickness are relevant parameters. I made plots (Figs. 3.3, 3.4) using reasonable values for the Atlantic coastal plain. The plots do not show any age ranges that include groundwater recharged before approximately 1940, as a limit of approximately 73 yr before the present was used. This limit was used because the tracers used to estimate ages do not reliably

distinguish among recharge years older than that and so there are no older dates in the literature (e.g., no dates from the 1920s or 1910s). Thus, there is no use in considering effects of screen length on ages in that range (roughly pre-1940).

For example, Figure 3.3 shows the effects of screen length for an aquifer with a thickness of 20 m, a recharge of 20 cm/yr, and a porosity of 0.30. It shows that, at depth of about 17 m, a well with a 60 cm screen interval will intercept groundwater with a range of ages of about 7 yr (producing error margin of approximately ± 3.5 yr in the estimate of apparent age). Error margins of ± 2 -6 yr are typical for CFC, SF₆, and ³H/³He age dates (Busenberg and Plummer et al. 2003; Solomon and Cook 2000; Plummer and Busenberg 2000).

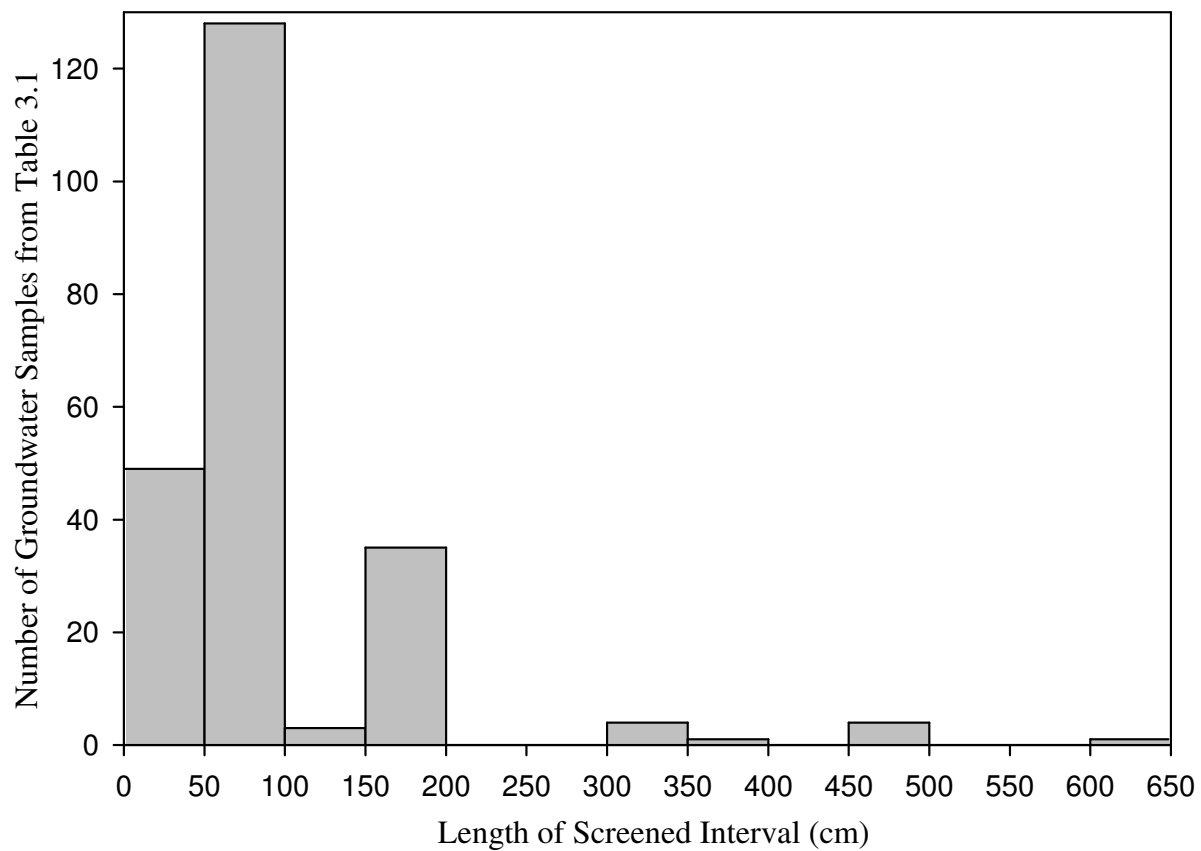


Figure 3.2. Histogram showing the distribution of screen lengths for 225 wells or piezometers from the 9 studies listed in Table 3.1.

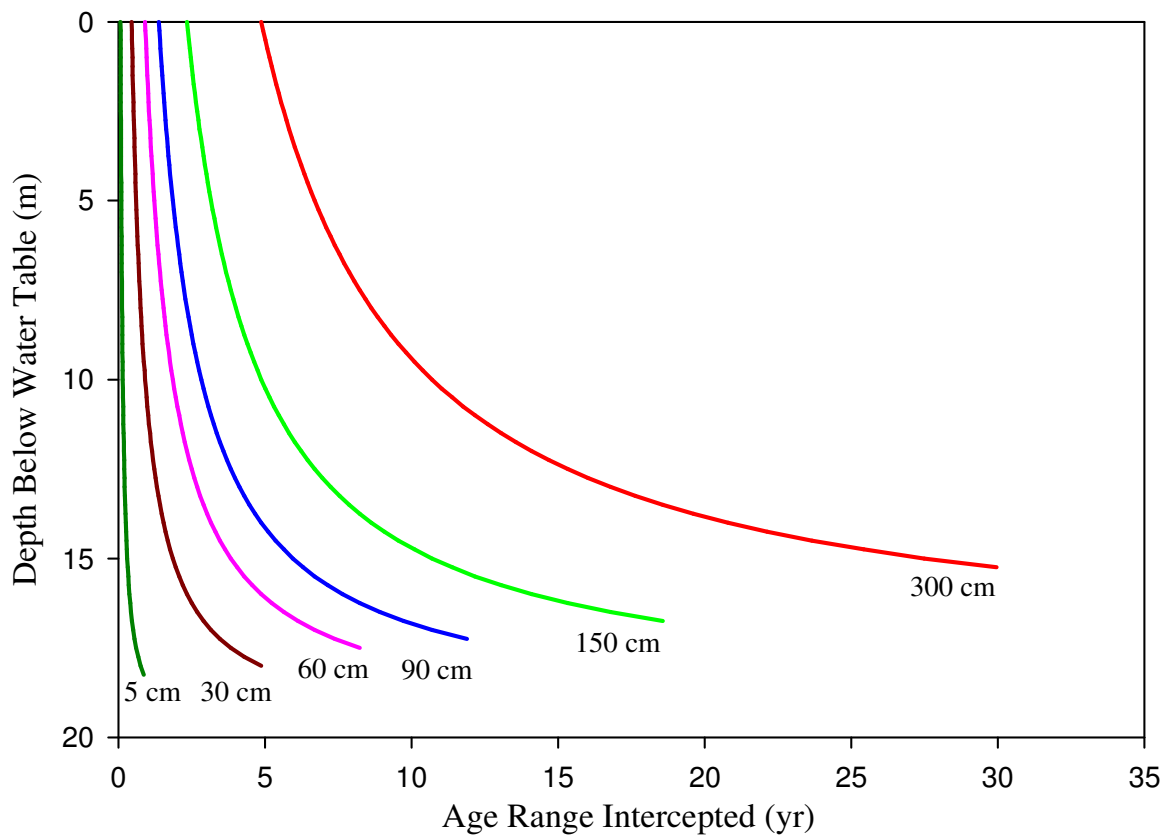


Figure 3.3. Range of groundwater ages intercepted by well screens of different lengths, as a function of depth below the water table. Each curve is labeled with its screen length. Recharge of 20 cm/yr, aquifer porosity of 0.30, and aquifer thickness of 20 m were assumed; see text for details.

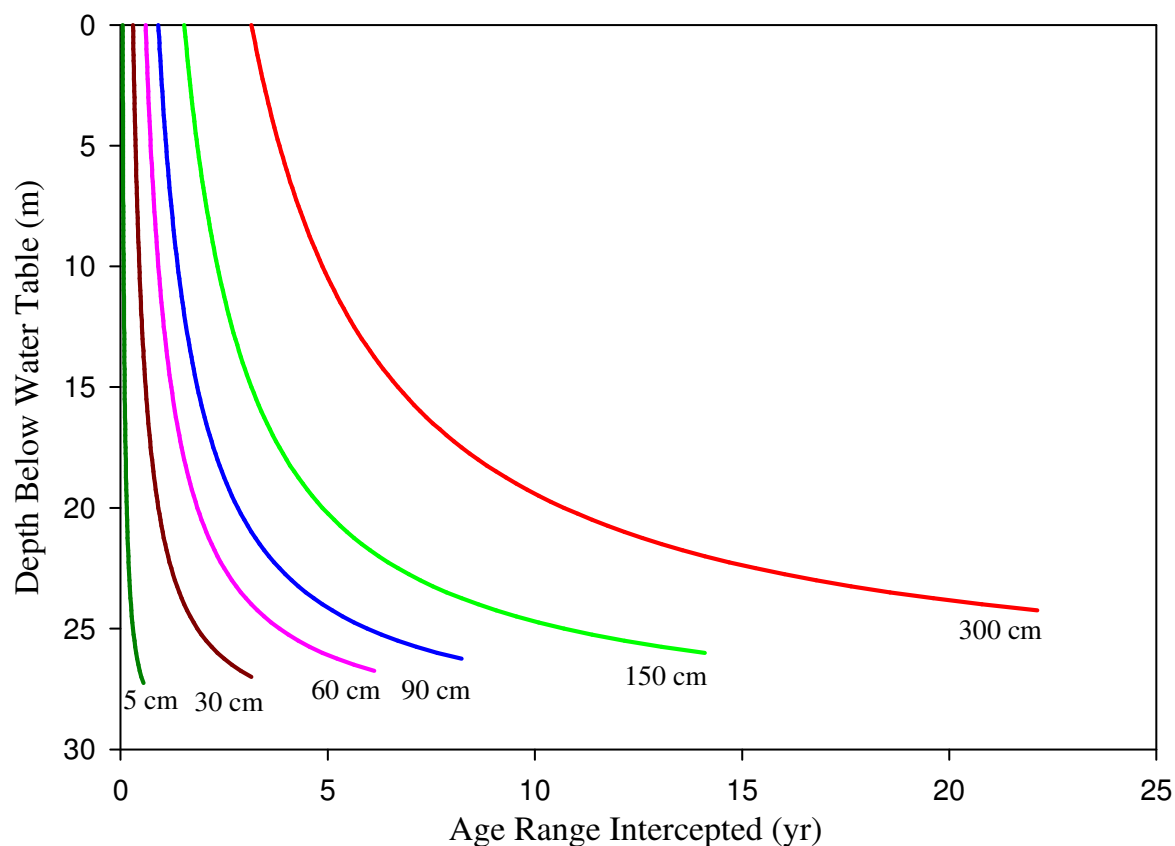


Figure 3.4. Range of groundwater ages intercepted by well screens of different lengths, as a function of depth below the water table. Each curve is labeled with its screen length. Recharge of 30 cm/yr, aquifer porosity of 0.30, and aquifer thickness of 30 m were assumed; see text for details.

3.3. Kenoyer and Bowser (1992)

The study by Kenoyer and Bowser (1992) was conducted near Crystal Lake, Vilas County, located in central Wisconsin. The topography is predominately small lakes set in hummocky glacial terrain, the geology is comprised of approximately 50 m of glacial sediment overlying Precambrian bedrock. The glacial sediment is comprised of predominately sand-sized material (85-95%) with minor amounts of silt and clay-sized particles, eroded from various rock types, including: gneiss, amphibolite, granites,

monzonites, mafic metavolcanics, and quartzose and felspathic sandstones. The sand-sized fraction is largely quartz (50-75%), with some calcic plagioclase (9-15%), sodic plagioclase (9-15%), orthoclase (2-10%), and biotite (1-2%). Clay minerals include smectite (30-40%), illite (30-40%), chlorite and kaolinite (15-30%). Permeability is generally high in the sandy drift composing the surficial aquifer. A network of 54 piezometers were installed around Crystal Lake to determine head configuration in the surficial aquifer, and 28 piezometers (24 constructed of 1.9 cm diameter PVC pipe with 15 cm screened intervals, 4 constructed of 3.1 cm diameter PVC pipe with 30 cm screened intervals) were constructed along a vertical plane between Crystal Lake and Big Muskellunge Lake to monitor groundwater flow paths. Samples were collected in July of 1982, and sampling strategy included purging at least two well volumes from wells (or until temperature, dissolved oxygen, and specific conductance stabilized), collecting samples for [Si] analysis using a peristaltic pump, filtering with an in-line 0.45 micron (μm) Nucleopore filter, then acidifying samples to 1%, and storing samples at 4°C. The analysis of [Si] was performed using the colorimetric molybdate blue method.

The study by Kenoyer and Bowser (1992) is considered in this report because it contains both [Si] and groundwater ages, but it should be noted that the method of determination of groundwater age differs from that of the other studies. In the study conducted by Kenoyer and Bowser (1992) groundwater age was determined by calculating the magnitude and direction of groundwater velocity along a cross-section. Groundwater flow velocities were determined by application of Darcy's law to point measurements of

head and hydraulic conductivity for 28 piezometers, and the groundwater velocities were checked by using flow nets and tracer tests. By assuming that the flow lines were constant in time (which the authors thought justified for the purpose), the mean annual flow velocity was used to calculate the travel time of groundwater between any two points. Kenoyer and Bowser (1992) estimate that this method can predict groundwater ages to within 40% accuracy.

The study by Kenoyer and Bowser (1992) displays the lowest age-uncertainty for all the studies presented in this study. The results of the regression are highly linear but over a very small range of ages (0.75-3.4 yr). The minimum age uncertainty (i.e., the minimum vertical distance on the regression plot between the upper and lower 95% prediction limits) for my regression based on Kenoyer and Bowser (1992) is approximately ± 0.7 yr.

Table 3.2. Groundwater age and groundwater [Si] for the study by Kenoyer and Bowser et al. (1992). No specific well data, screen interval data, or depth data was available for this study.

GW Age (yr)	[Si] (μM)
0.75	20.0
1.2	30.0
1.25	40.0
1.6	45.0
3	145.0
3.4	140.0

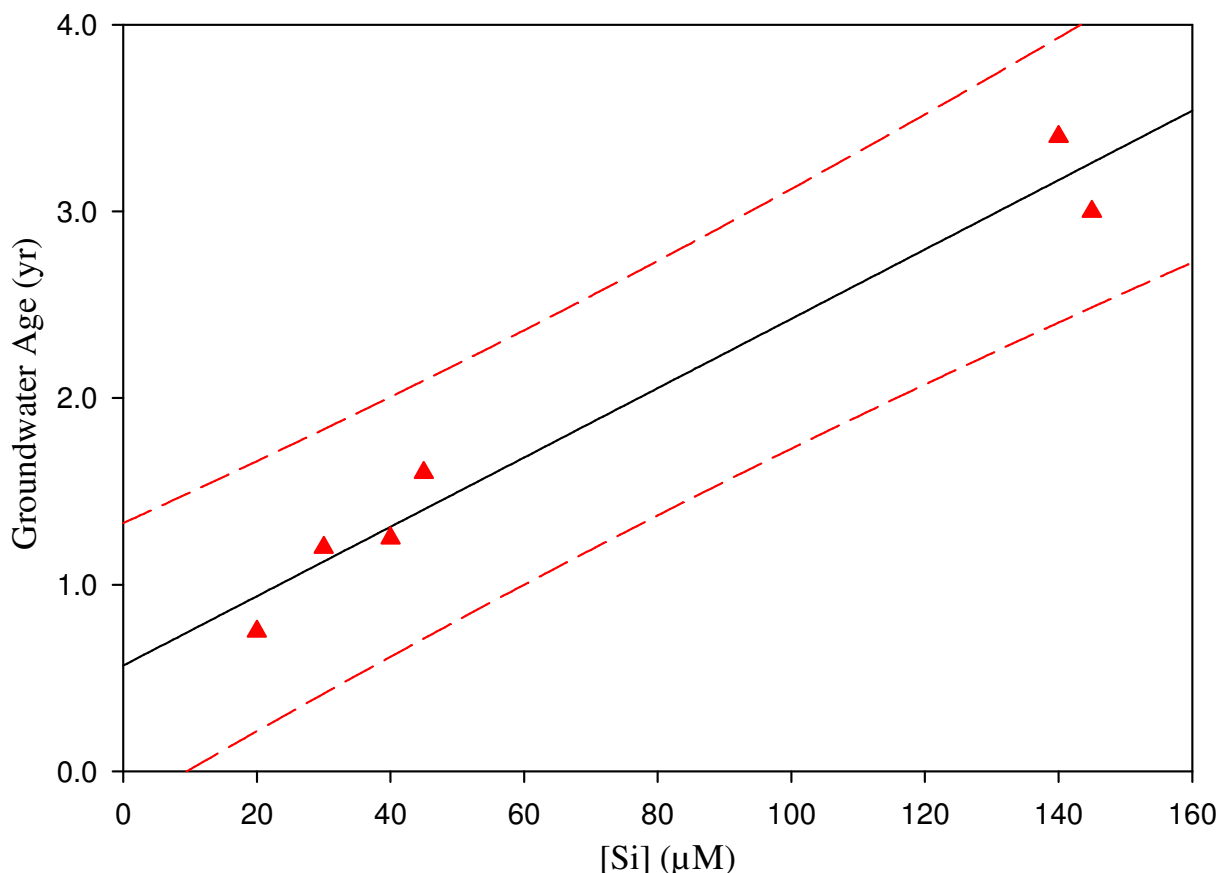


Figure 3.5. Groundwater age vs. groundwater [Si], with values estimated from Figure 7 of Kenoyer and Bowser (1992). Regression analysis yielded a slope of 0.0186 yr/ μM , an intercept of 0.5664 yr, an r^2 of 0.9644, and p-values of 0.0005 and 0.0219 for the slope and intercept, respectively. Red dashed lines are 95% prediction intervals.

3.4. Tesoriero et al. (2005)

3.4.1. Study Site: The study by Tesoriero et al. (2005) took place in the 180 ha Lizzie research site, located in the Contentnea Creek sub-basin of the Neuse River, North Carolina. The Lizzie Research station lies south of the confluence of the Sandy Run and Middle Slope headwater streams, and drains into Sandy Run. The site is located in the coastal plain physiographic province, which is characterized by paleoshores and intervening terraces.

Sandy run is characterized by alluvial paleovalley geology. The hydrogeology of the site is late Cretaceous marine shelf deposits overlain by the Yorktown Formation of Pliocene age and poorly exposed Pliocene to Pleistocene units. The lithology of the Yorktown aquifer is composed of gravelly sands and phosphitic gravelly, shelly sands overlain by sandy, clayey silt. Tidally bedded surficial deposits (of the Wicomico plain) lie stratigraphically above the Yorktown aquifer, forming the upland surficial aquifer at the Lizzie site. These deposits are medium to fine-grained sand and silts that were originally deposited in low-lying depressions. Overlying these deposits is a 1-3 m thick surficial layer of tidal flat or bay-like deposits that evolve upwards into salt marshes.

3.4.2. Dissolved Solute Sampling and Analysis Method: Water samples for [Si] were collected from several wells that were installed and maintained by the North Carolina Division of Environmental and Natural Resources (NC DENR). The samples were collected from the wells using submersible or peristaltic pumps and Teflon lines (with the exception of samples for CFCs, which require copper tubing to avoid contamination). Samples collected for [Si] were filtered using a 0.45 μm capsule filter. [Si] samples were analyzed using inductively coupled plasma mass spectrometry (ICP-MS).

3.4.3. Age-dating Method: Age dating tracers used in this study include CFCs (CFC-11, CFC-12, and CFC-113), SF₆, and tritium. Tritium analyses were performed using electrolytic enrichment and liquid scintillation.

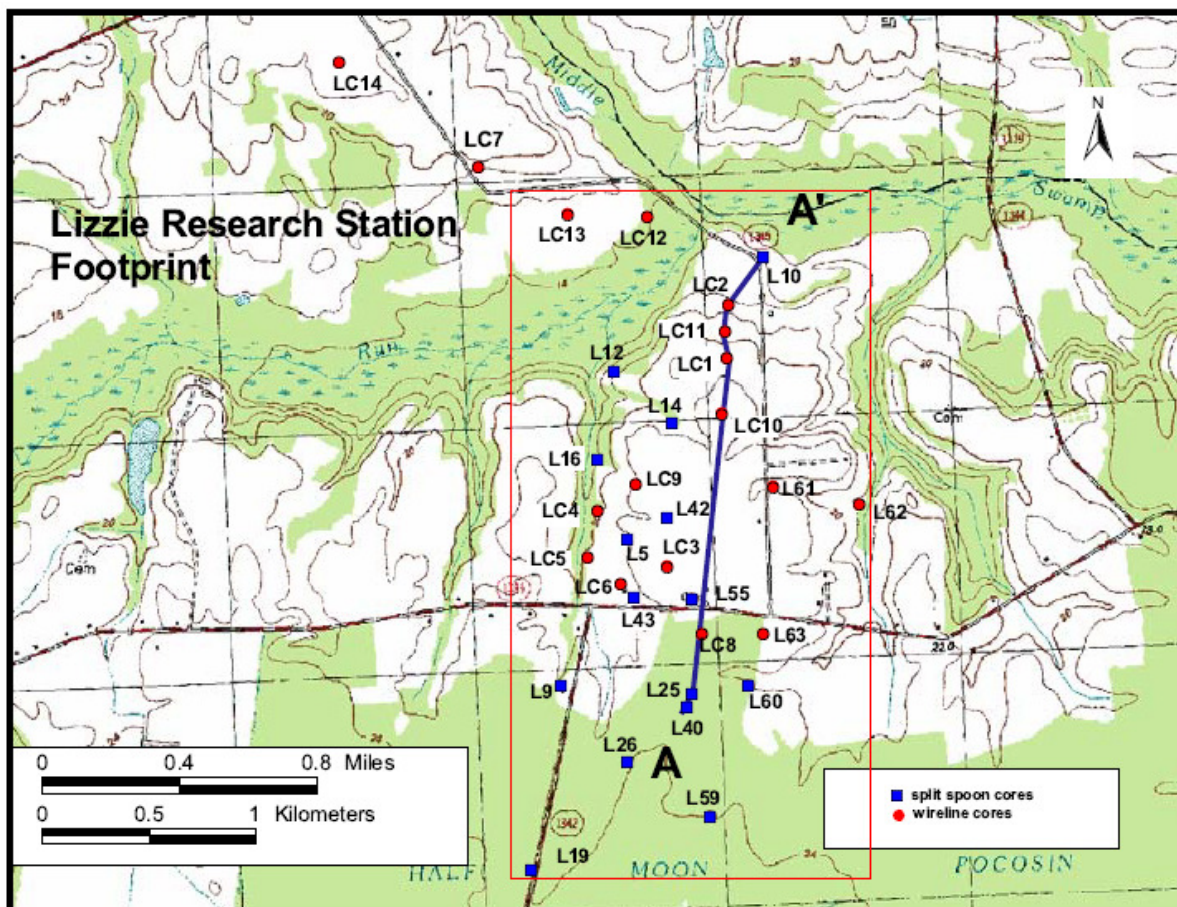


Figure 3.6. Map showing well locations at the Lizzie Research station where cores and groundwater samples were collected (from Tesoriero et al. 2005).

Because only tritium was analyzed (i.e., $^3\text{H}/^3\text{He}$ dating was not done), this tracer was used primarily to determine if water samples were recharged before or after the onset of widespread atmospheric testing of nuclear weapons (~1953, according to Tesoriero et al. 2005). There is no discussion in Tesoriero et al. (2005) of the sampling and analysis procedure for SF_6 ; however, it is listed as an age-dating method for well L11D in Table 2 of Tesoriero et al. (2005).

3.4.4. Data Analysis: Tesoriero et al. (2005) state that SiO_2 (represented as [Si] in my study) is an excellent indicator of groundwater residence time but also discuss scenarios in which the [Si]-age relationship could be altered, such as algal blooms of diatoms (a photosynthetic organism which absorbs silica from the water to build its skeletal structure). Although not specifically stated, this would only affect samples collected from a stream or spring outlet, and not groundwater samples collected from a well or sampling probe pushed through a streambed. Tesoriero et al. (2005) have attributed low [Si] values in their dataset to seasonal algal blooms that affect stream water samples. Another scenario considered in which [Si] values can be altered is the mixing of older groundwater with younger groundwater that may have migrated downwards. Tesoriero et al. (2005) attribute low [Si] values obtained for the sample from well L10 to this process.

In creating a plot of groundwater age vs. [Si] from the data presented in Tesoriero et al. (2005), it was necessary to critically evaluate and compare the data included in their Table 2 and Figure 8 and other sources (an Excel data file and email received from Tesoriero in August of 2012) in order to identify data points that could be used to create a plot and perform a regression analysis with the greatest confidence possible. Critical analysis has led to elimination of some data points present in the plot from Tesoriero et al. (2005), and other points not in the Tesoriero et al. (2005) plot have been included in my plot. A detailed explanation of the points that were included in my groundwater age vs. [Si] plot and those that were excluded follows.

The following data points, listed by well name, are included: L2D, L3, L6S, L6D, L15D, L20, L27, L7, and L8S. These 9 points have been selected from a total of 16 presented in Table 2 of Tesoriero et al. (2005) which represent samples taken in the surficial and alluvial aquifers at the Lizzie Research Station.

The following points, collected in the alluvial and surficial aquifer, have been excluded due to the ambiguity of the apparent groundwater age:

L4: This point was flagged by Tesoriero et al. (2005) as likely biased old. According to Tesoriero (personal communication, June 2012), this point was not included in the plot or in the regression in Tesoriero et al. (2005).

L18D and L23: The recharge dates for these samples are presented by Tesoriero et al. (2005) as >1953 based on tritium, thus placing only an upper limit (not a best estimate) on groundwater age (indicating only that this sample was "post-bomb pulse").

L24: The recharge date for this point (and two others) was determined via the tritium method and is listed in Table 2 of Tesoriero et al. (2005) as <1955. I have inferred that this date is given to indicate that the water sample at this point was recharged before 1955, and is thus "pre-bomb pulse".

L8D: No recharge date was included in Tesoriero et al. (2005) for this sample.

L11S: The recharge date listed in Table 2 of Tesoriero et al. (2005) is 1994, and the sampling date was 1999. This implies a groundwater age of approximately 5 yr. However, a personal communication (June, 2012) from Tesoriero indicates that N₂O interference may have affected the retention times during the gas chromatographic analysis of CFCs, which could have affected the CFC-12 age. N₂O and CFC-12 retention times are typically very similar (Busenberg et al. 2006), and it may be possible for these peaks to overlap, making it difficult to calculate the concentration of CFC-12. Because of this and other "hydrological and chemical data" Tesoriero et al. (2005) assigned the sample a CFC-113 age estimate of 2 yr. The sample is suspected to be a mixture of groundwaters of different age, according to an email correspondence with Tesoriero (June, 2012).

L11D: The recharge date listed in Table 2 of Tesoriero et al. (2005) is 1992, and the sampling date was 6/1/1999. This implies a groundwater age of 7 yr. However, a personal communication (June, 2012) from Tesoriero indicates that this sample is suspected to be a mixture of groundwaters of different age. Both this sample point and L11S are situated in the alluvial aquifer at the study site. According to Tesoriero et al. (2005) groundwater in the alluvial aquifer is recharged from adjacent streams, and/or directly from the riparian zone. Presumably this is the cause for the mixture of groundwaters sampled at these sites.

In addition, Tesoriero et al. (2005) included the sample point L10 in the unconfined portion of the plot in their Figure 8. In their Table 2 this point is in the Yorktown Aquifer, and the groundwater has a recharge date of 1974. Tesoriero et al. (2005) states that the sample collected at this point is a mixture of confined and unconfined groundwaters, as it was collected at the interface of the alluvial, surficial, and Yorktown aquifers. It is not clear why this sample has been included in the unconfined portion of the plot, although it may serve as a transition point for the regressions of the confined and unconfined aquifers shown in their Figure 8.

The regression of the data points plotted for the surficial aquifer in Figure 8 of Tesoriero et al. (2005) yielded a slope of $0.1580 \text{ yr}/\mu\text{M}$, an intercept of -7.1165 yr , an r^2 of 0.8725 , and p-values of 0.0002 and 0.0986 for the slope and intercept, respectively. The results from my regression (Table 3.1) compare fairly well with the slope, r^2 , and p-values with those from Tesoriero et al. (2005), although the intercept is roughly a factor of two less (intercept of -14.401 yr). When a regression is calculated for only the four wells with short screen lengths ($< 1 \text{ m}$), the slope becomes $0.2875 \text{ yr}/\mu\text{M}$, the intercept is -33.7857 , the r^2 is 0.8541 , and the p-values are 0.0758 and 0.1515 for the slope and intercept, respectively. The minimum age uncertainty for the regression based on all wells (Figure 3.7) is approximately $\pm 14.2 \text{ yr}$.

Table 3.3. Groundwater age and groundwater [Si] for the study by Tesoriero et al. (2005). Top of screen is provided in Tesoriero et al. (2005) as an elevation relative to mean sea level (msl).

Well	Top of Screen (m)	Screen Length (m)	Recharge Date	GW Age (yr)	[Si] (μM)
L2D	18.1	0.6	1981	18	164.6
L3	16.5	4.6	1958	41	282.6
L6S	22.1	0.6	1990	9	159.6
L6D	17.5	0.6	1971	28	216.1
L15D	16	0.6	1987	12	162.9
L20	21.1	3	1957	42	249.4
L27	21.2	3	1989	11	78.1
L7	12.4	6.1	1994	5	103.1
L8S	14	1.6	1995	4	108.1

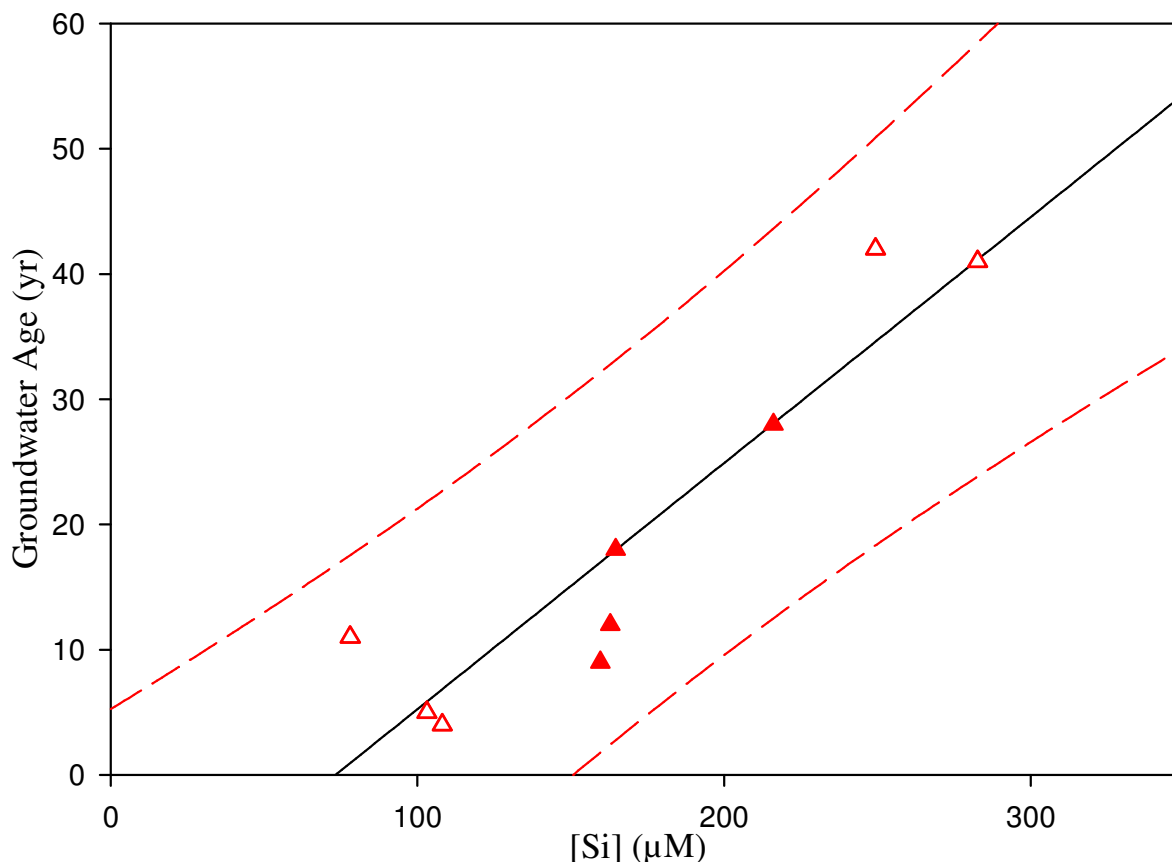


Figure 3.7. Groundwater age vs. groundwater [Si] based on 9 points of highest confidence (see text for details) from Tesoriero et al. (2005). Regression analysis yielded a slope of 0.1965 yr/ μM , an intercept of -14.4011 yr, an r^2 of 0.8500, and p-values of 0.0004 and 0.0385 for the slope and intercept, respectively. Open triangles indicate data point was taken from a well with screen length ≥ 1 m, and filled triangles indicate data point was taken from a well with screen length < 1 m. Red dashed lines are 95% prediction intervals.

3.5. Böhlke & Denver (1995)

3.5.1. Study Site: This study was conducted in the Locust Grove watershed, located within the Delmarva Peninsula of the Atlantic coastal plain, Maryland. The Locust Grove area is underlain near the surface by permeable sand and gravel units of the fluvial Pensauken Formation and the marine glauconitic Aquia Formation. Drill cores taken during

the study revealed that most of the surficial material is oxidized (ferric oxides and silicates have largely replaced Fe^{2+} -bearing glauconite). The Aquia Formation is underlain by unoxidized marine sediments, primarily glauconitic sands. Below this unit is a 2-3 m thick unit containing a large proportion of interstitial fine-grained material, and is considered to be the lower boundary of the surficial aquifer, although it is not fully confining.

3.5.2. Dissolved Solute Sampling and Analysis Method: Groundwater samples were collected from below the stream bed using a pushable minipiezometer, and from permanently installed observation wells. Groundwater was collected using 6 mm nylon or Teflon tubing and a peristaltic pump containing Tygon tubing from approximately 1 m below the streambed with a stainless steel minipiezometer with a 5 cm screened tip. Wells were constructed of PVC with an inside diameter of 5.1 cm and a screen length 0.9 m. Minipiezometer sites were selected to represent discharge to different segments of the stream (i.e., from higher headwater streams to second and third order reaches, and sampling points from the center to the sides of the channel). Samples from the streambed were typically collected from sandy layers overlain by less permeable silt, sand, and organic-rich material. Samples for [Si] were acidified and filtered with a 0.1 μm membrane. Samples were analyzed for [Si] at the USGS Reston laboratory using directly coupled plasma emission spectroscopy.

3.5.3. Age-dating Method: The age-dating tracers employed in this study were primarily CFC-11, CFC-12, and tritium. Groundwater samples for CFCs were collected using

the method described above, but with the use of a copper tube instead of nylon or Teflon tubing. The sampling process typically took 1-3 hours with one set of unfiltered splits for the sampling of CFCs collected and sealed in glass ampoules at the beginning of the sampling period, and a second set collected at the end of the sampling period (after all other samples had been collected). Untreated and unfiltered samples were taken for the collection of groundwater for tritium analysis. Tritium was concentrated by electrolysis and measured by liquid scintillation counting. The detection limit for tritium analysis was 0.5 Tritium Units (TU). CFC-11 and CFC-12 concentrations were measured by gas chromatography with an electron capture detector, after the samples had gone through purge-and-trap separation. Dissolved CFC concentrations were then converted to equilibrium partial pressure using the local average recharge temperature of 9°C (Dunkle et al. 1993), and were compared to historic atmospheric concentrations.

3.5.4. Data Analysis: The CFC analyses for separate samples from a given well had a standard deviation of ~5-10%. Uncertainties associated with the gas-liquid equilibration in the laboratory are on the order of 2-4%. The authors state tentatively that there were varying amounts of CFC-11 contamination as a result of storage and subsequent release from contaminated Nylon and Tygon tubing. This source of contamination did not contain CFC-12, however, and so should not have affected any of the CFC-12 groundwater ages. The authors also note that sites 173d, 180d (which were sampled twice, with age and [Si] determined both times), and 182d had tritium activities that were too low to be consistent

with their associated CFC-12 ages. These samples were interpreted to be mixtures of mostly relatively old water and small amounts of young water and for this reason have been excluded from my regression (Fig. 3.8) of age vs. [Si]. In Figure 5 of Böhlke and Denver (1995), sample site 159d is also mentioned as possibly being comprised of a mixture of groundwater of different ages. Sample site 159d was sampled on three separate occasions, with one $^3\text{H}/^3\text{He}$ age reported in Table 1 of Böhlke and Denver (1995), and two CFC ages reported in Table 2 of Böhlke and Denver (1995). An additional anomaly concerning sample site 159d is that in Table 1 of Böhlke and Denver (1995), the TU units are 0.0, but in Figure 5 of Böhlke and Denver (1995) they are reported as being somewhere between 5-10 TU. Two of the three sampling events included [Si].

The rate of [Si] acquisition (i.e., the regression slopes) for Chesterville Branch and Morgan Creek compare fairly well (0.3693 and 0.3831 yr/ μM , respectively), but the r^2 and p-values for Chesterville Branch are lower than for Morgan Creek. The minimum age uncertainty for Chesterville branch is approximately ± 18.7 yr and the minimum age uncertainty for Morgan Creek is approximately ± 27.0 yr. When the two studies are combined in a single regression, the slope becomes 0.3327 yr/ μM , the intercept is -13.5125 yr, the r^2 is 0.4853, and the p-values are < 0.0001 and 0.04555 for the slope and intercept, respectively. Slope and r^2 for the combined regression are not significantly different from either the Chesterville Branch or Morgan Creek regression, but the p-values for the combined regression have improved, which is reflected by the improved minimum age uncertainty

value of approximately ± 21.7 yr. In addition, because most of the surficial aquifer material is oxidized at this site, there is a possibility that oxide mineral coatings are inhibiting or slowing the dissolution of silicate minerals, which may in part account for the notably higher slopes (lower Si acquisition rates) of these sites, compared to other areas in the coastal plain.

Table 3.4. Groundwater age and groundwater [Si] for the study by Böhlke and Denver (1995). There is no indication in Böhlke and Denver (1995) whether the depth is measured from the top, bottom, or center of the screened interval.

Site ID	Depth below Water Table (m)	Screen Length (cm)	GW Age (yr)	[Si] (μM)
<u>Chesterville Branch</u>				
62r	4.7	90	4	61.2
53r	1.3	90	6	68.2
64r	3.2	90	7	85.5
52r	5.1	90	9	100.9
163r	10.1	90	10	77.5
163r	10.1	90	10	77.5
161r	4	90	13	77.5
170r	0.9	90	18	93.4
169d	0.7	90	20	85.5
63r	10.4	90	19	85.5
61r	9.7	90	20	85.5
160d	9.9	90	15	93.4
162r	17.3	90	37	100.9
162r	17.3	90	32	101.3
176d	0.8	5	18	82.7
174d	1	5	32	85.5
175d	0.9	5	34	90.1
177d	1	5	40	161.1
<u>Morgan Creek</u>				
167r	2.8	90	1	107.9
50r	2.8	90	2	132.2
59r	3.8	90	6	85.5
166r	6.1	90	6	93.4
51r	3.8	90	10	93.4
60r	1.6	90	11	68.2
165r	12	90	17	86.4
164r	10.5	90	24	93.4
158r	2.3	90	4	60.7
179d	0.8	5	18	104.6
178d	1.3	5	52	143.8
178d	1.4	5	44	158.3
172d	1.3	5	40	163.5
147d	0.8	5	45	170.9

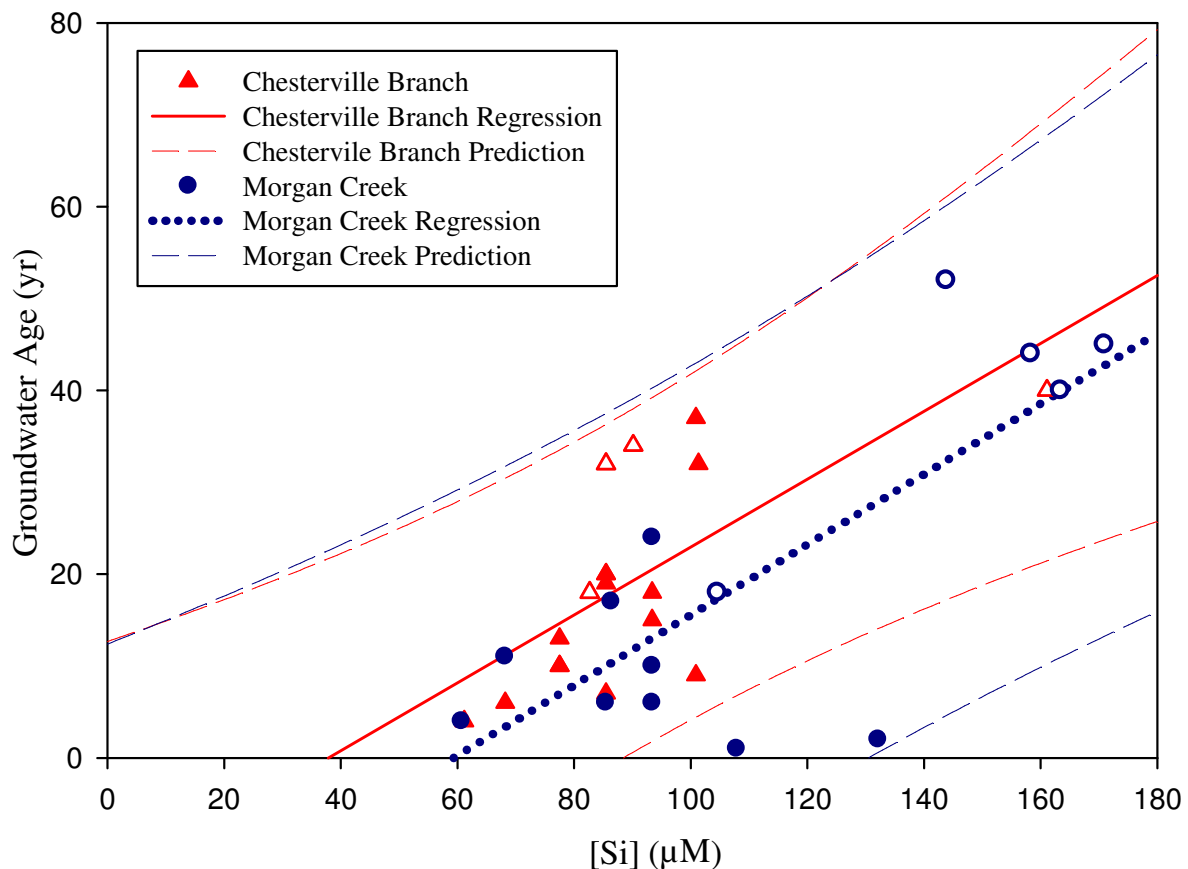


Figure 3.8. Groundwater age vs. groundwater [Si] for Chesterville Branch and Morgan Creek based on data from Böhlke and Denver (1995). Triangles represent Chesterville Branch, and circles represent Morgan Creek. The regression for Chesterville Branch yielded a slope of $0.3693 \text{ yr}/\mu\text{M}$, an intercept of -13.9786 yr , an r^2 of 0.4604 , and p-values of 0.0020 and 0.1474 for the slope and intercept, respectively. The regression for Morgan Creek yielded a slope of $0.3831 \text{ yr}/\mu\text{M}$, an intercept of -22.7433 yr , an r^2 of 0.5880 , and p-values of 0.0014 and 0.0572 , respectively. Open shapes indicate data point was taken from a well with screen length $\geq 1 \text{ m}$, and filled shapes indicate data point was taken from a well with screen length $< 1 \text{ m}$. Dashed lines are 95% prediction intervals.

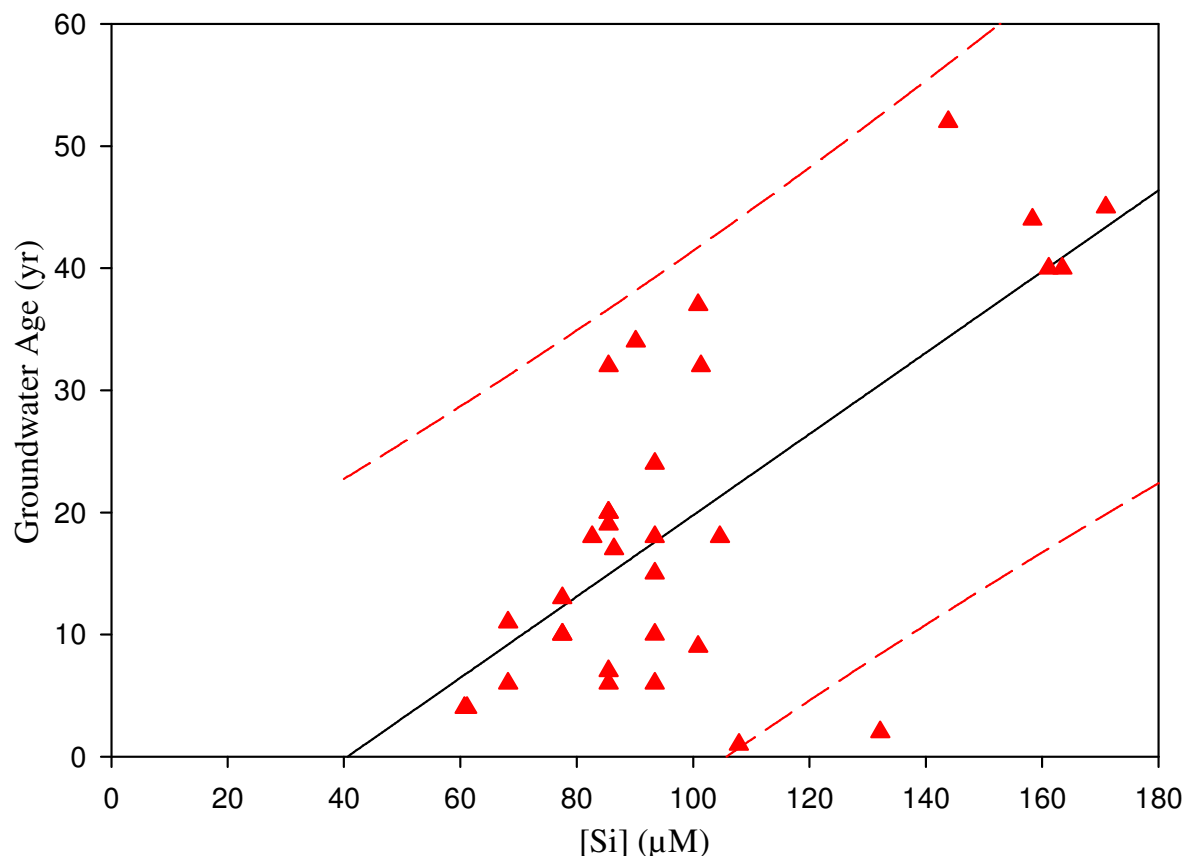


Figure 3.9. Groundwater age vs. groundwater [Si] for Chesterville Branch and Morgan Creek (n=32) based on data from Böhlke and Denver (1995) combined into a single regression. The regression yielded a slope of 0.3327 yr/ μM , an intercept of -13.5125 yr, an r^2 of 0.4853, and p-values of <0.0001 and 0.0455, respectively. Dashed lines are 95% prediction intervals.

3.6. Shapiro et al. (1999) and Savoie et al. (1998)

3.6.1. Study Site: The study done by Shapiro et al. (1999) and the Savoie et al. (1998) USGS study took place in Ashumet Valley, Cape Cod, Massachusetts. Data from the two studies could be integrated (1) because of the overlap of the study areas, both of which contained data from wells situated within and around a contaminant plume south of the Otis Air Force Base in Falmouth, Massachusetts, and (2) because the two studies use data from the same sampling events. The numbering scheme for the wells in the two studies is the

same, but the site names are listed differently in the tables presented. For example, the site listed as 300-10 in Shapiro et al. (1999) is referred to as site FSW 300-0010 in Savoie et al. (1998). The Shapiro et al. (1999) study provided age dates, while the Savoie et al. (1998) study provided [Si] data. The shallow Cape Cod aquifer consists of glacial deposits of boulders, sand, gravel, silt, and clay of Pleistocene age that were deposited during the last retreat of glacial ice sheets. The upper 27-43 m of the aquifer is primarily composed of well sorted sands and gravels. Underlying sands and gravels are finer-grained, and underlain by crystalline bedrock (Shapiro et al. 1999). Pleistocene sediments are approximately 90% quartz, with minor amounts of potassium feldspar, plagioclase, glauconite, and Fe-oxides. Sand and gravel consist of 95% (by weight) quartz and feldspar, and less than 1% silt and clay. The medium grain size of the sediments is 0.5 mm. Sediments with grain size less than 0.1 mm are 90-95% quartz and approximately 5% of plagioclase dominated feldspar (Bau et al. 2004).

3.6.2. Dissolved Solute Sampling and Analysis Method: For these studies USGS installed 315 observation wells at 84 cluster sites as well as 31 multi-level sampling devices over the period of June to December of 1994. Wells were constructed with 1.25, 2.0, or 2.5 in diameter PVC well casing and screens with a protective steel casing at the land surface. Aquifer material was allowed to collapse naturally around the well casing. All pumps and equipment were decontaminated with deionized water after sampling each well. Wells were sampled with either a Keck Model SP-81 submersible pump with Teflon tubing (2 and 2.5 in

wells) or with a GeoPump2 peristaltic pump (1.25 in wells) fitted with Neoprene tubing in the pump head and Teflon tubing to lower into the well. A minimum of 3 well volumes were purged before sampling, and specific conductance, pH, turbidity, and temperature were monitored for stabilization. Groundwater samples for [Si] analysis were filtered in-line with a 0.45 μm Gelman capsule filter, acidified in the field with nitric acid, and were then chilled until transport to the USGS National Water Quality Laboratory in Arvada, Co. All samples were analyzed within three months of collection. [Si] was analyzed with ICP-AES (Savoie et al. 1998).

3.6.3. Age Dating Method: The only age-dating method employed in this study was $^3\text{H}/^3\text{He}$, performed on samples collected from 82 observation wells at 15 different well clusters. In particular, samples were collected from wells situated within and adjacent to a localized contaminant plume that was the focus of the study for Shapiro et al. (1999). Samples were collected primarily along two transects. Wells sampled had 0.61 m screens. Samples were collected using the same equipment and purge methods described above and by following the collection procedures described by Ekwurzel et al. (1994). Samples were then sent to the Lamont-Doherty Earth Observatory Noble Gas Facility in Palisades, New York, for analysis. Tritium concentration in the water was determined using the helium-3 ingrowth method, and was said to have an analytical precision of approximately $\pm 2\%$ (Shapiro et al. 1999).

3.6.4. Data Analysis: Water in well cluster FSW 347 produced young $^3\text{H}/^3\text{He}$ ages when compared to wells upgradient and further downgradient of infiltration beds present in the area. A likely explanation provided by the authors is that regional water is recharged through the infiltration beds, forced down, and then confined by the contaminant plume (resulting in a greater increase in age with depth for these waters), which results in $^3\text{H}/^3\text{He}$ age increases with depth that are not increasing at a constant rate. In general, groundwaters on the eastern side of the study section and downgradient of Ashumet pond tend to have lower $^3\text{H}/^3\text{He}$ ages, due to the interaction of Ashumet pond. Water entering the pond (near well cluster FSW 300) from the groundwater system loses ^3He through the water/air interface. This water, which has been outgassed, is then recharged back into the groundwater system around well cluster FSW 348, with a younger $^3\text{H}/^3\text{He}$ age. Because of outgassing of this water, it was necessary to separately evaluate well clusters that are upgradient, adjacent to, and downgradient of the pond. When evaluated separately, wells that are downgradient of the pond show the best regression (R^2 of 0.6751, Table 3.8). Wells that are upgradient of the pond are nearest to the base and to the infiltration beds, which may complicate the groundwater system in that area (see above). Wells that are adjacent to the pond can receive water that has recently had its ^3He content outgassed by coming into contact with the atmosphere at the ponds surface.

For the study conducted by Shapiro et al. (1999) and Savoie et al. (1998), running three separate regressions for wells upgradient of, adjacent to, and downgradient of Ashumet

pond identified the area downgradient of Ashumet pond as the portion with the most confidence, as the r^2 and p-values for this portion of the study area indicated a much lower age uncertainty. This also makes sense conceptually if we consider that the area upgradient of Ashumet pond contained infiltration beds where intense recharge took place (Shapiro et al. 1999), and the area adjacent to Ashumet pond experienced major interference from Ashumet pond in the form of ^3He outgassing through the pond surface. The minimum age uncertainty for my regression for the downgradient portion is approximately ± 13.0 yr (Table 3.8). However, the main focus of the study conducted by Shapiro et al. (1998) and Savoie et al. (1999) was to explore the extent and effect of a local contaminant plume (which was found had a smaller age gradient with depth than the surrounding groundwater, due to the intense recharge through the infiltration beds). The hydrologic conditions of the Ashumet Valley contaminant plume should not be assumed to be similar to the hydrologic conditions found in other glacial outwash aquifers.

Table 3.5. Groundwater data and groundwater [Si] for the studies by Shapiro et al. (1999) and Savoie et al. (1998). Depth below land surface was calculated as the difference between the land surface and screen elevations reported in Savoie et al. (1998).

Site Name	Depth to Top of Screen (m)	Screen Length (cm)	Groundwater Age (yr)	[Si] (μM)
300-10	2.42	60.96	0.1	101.43
300-30	8.42	60.96	6	216.17
300-50	14.76	60.96	6	232.79
300-73	21.67	60.96	9	216.17
300-99	29.68	60.96	15.9	224.48
300-118	35.40	60.96	28.2	232.79
300-138	41.31	60.96	30.2	199.54
347-20	5.39	60.96	0.5	134.69
347-31	8.78	60.96	2.7	232.79
347-38	10.86	60.96	1.6	216.17
347-46	13.37	60.96	3.1	216.17
347-67	19.62	91.44	5.4	199.54
347-67	19.62	91.44	4.5	216.17
347-101	30.15	60.96	10.7	199.54
347-116	34.73	60.96	13.6	216.17
347-131	39.40	60.96	22.4	249.42
347-145	43.52	57.912	24.9	232.79
348-98	29.04	60.96	1.8	28.27
350-13	3.28	60.96	0.6	84.80
350-52	15.13	60.96	14.8	136.35
350-64	19.24	39.624	24.4	121.39
350-77	22.89	60.96	25.9	166.28
350-84	24.94	60.96	25.9	199.54
350-110	33.10	39.624	28.9	266.05
350-125	37.58	60.96	38.1	282.68
357-79	23.43	60.96	6	138.01
357-99	29.58	60.96	13.9	133.02
357-119	35.87	39.624	21.7	93.12
357-139	41.89	60.96	29.2	249.42
358-49	14.28	60.96	0.6	98.11
358-89	26.42	60.96	14.8	152.98
358-104	31.01	60.96	22.4	159.63
358-132	39.54	60.96	26.6	199.54

Table 3.5 Continued

411-36	10.23	60.96	1.1	66.51
411-54	15.95	60.96	6.7	131.36
411-65	19.31	60.96	13.1	83.14
411-81	24.13	60.96	16.6	156.30
411-94	28.11	60.96	25.6	199.54
411-106	31.57	60.96	28.5	349.19
412-42	12.07	60.96	3.2	94.78
412-64	18.83	60.96	8	114.73
412-78	23.04	60.96	10.5	99.77
412-91	27.14	60.96	11.8	106.42
412-108	32.33	60.96	11	111.41
418-49	14.35	60.96	0.9	99.77
418-89	26.41	60.96	17.8	162.96
418-103	30.91	60.96	25.1	161.29
418-122	36.56	60.96	26.8	266.05
418-141	42.23	60.96	37.3	249.42
436-36	10.26	60.96	5.9	108.08
436-60	17.73	60.96	19.7	143.00
436-76	22.55	60.96	33	249.42
443-104	31.14	60.96	24.4	151.32
443-140	42.06	60.96	32.7	199.54
474-129	38.67	60.96	15.4	139.68
474-147	44.32	60.96	24.6	139.68
501-102	30.40	60.96	29.6	266.05
501-117	34.96	60.96	36	315.93
315-104	31.22	39.624	6.4	139.68
315-126	37.72	60.96	14.7	152.98
315-149	44.92	39.624	22.7	166.28
317-51	14.83	60.96	0.1	166.28

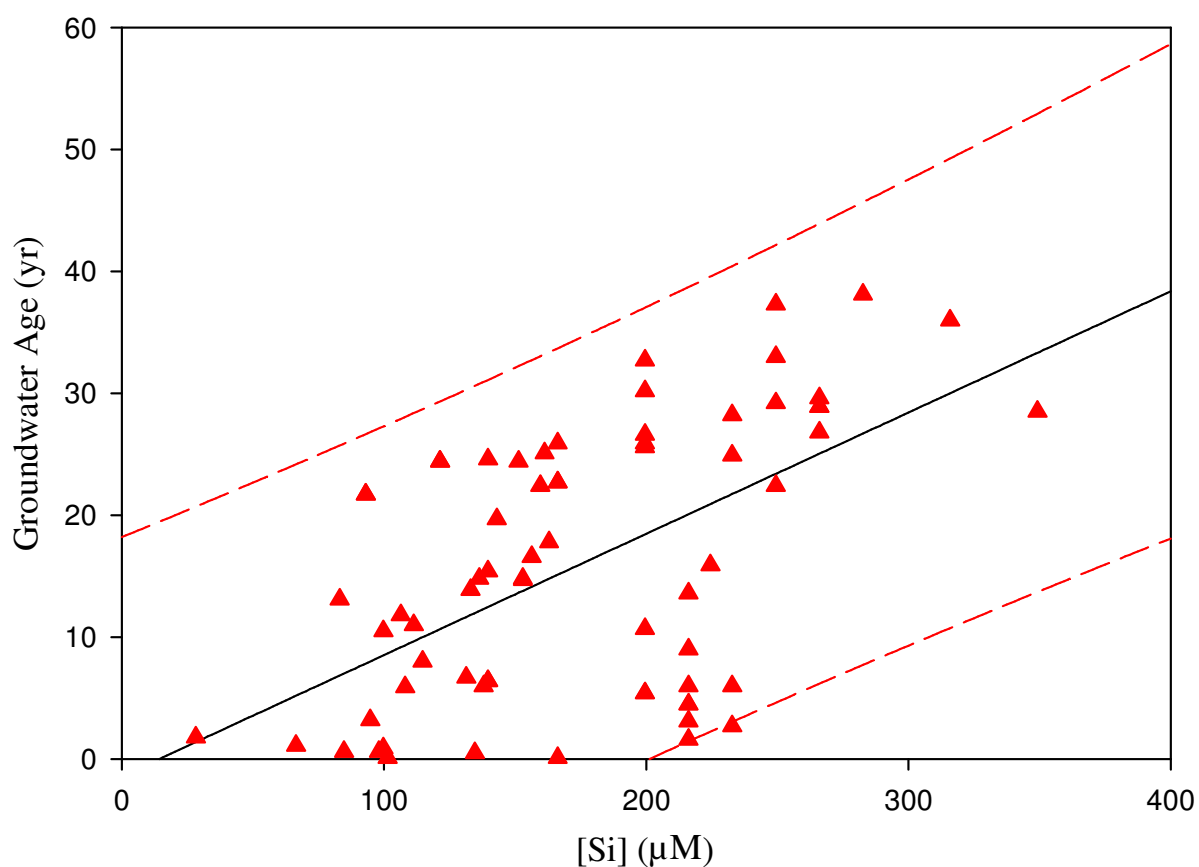


Figure 3.10. Groundwater age vs. groundwater [Si] based on all 62 points from Shapiro et al. (1999) and Savoie et al. (1998). Regression analysis yielded a slope of 0.0995 yr/ μM , an intercept of -1.4224 yr, an r^2 of 0.3357, and p-values of <0.0001 and 0.6742 for the slope and the intercept, respectively. Red dashed lines are 95% prediction intervals.

Table 3.6. Groundwater data and groundwater [Si] for wells upgradient of Ashumet pond, for the studies by Shapiro et al. (1999) and Savoie et al. (1998). Depth below land surface was calculated as the difference between the land surface and screen elevations reported in Savoie et al. (1998).

Site Name	Depth to Top of Screen (m)	Screen Length (cm)	Groundwater Age (yr)	[Si] (μM)
347-20	5.39	60.96	0.5	134.69
347-31	8.78	60.96	2.7	232.79
347-38	10.86	60.96	1.6	216.17
347-46	13.37	60.96	3.1	216.17
347-67	19.62	91.44	5.4	199.54
347-67	19.62	91.44	4.5	216.17
347-101	30.15	60.96	10.7	199.54
347-116	34.73	60.96	13.6	216.17
347-131	39.4	60.96	22.4	249.42
347-145	43.52	57.912	24.9	232.79
315-104	31.22	39.624	6.4	139.68
315-126	37.72	60.96	14.7	152.98
315-149	44.92	39.624	22.7	166.28
317-51	14.83	60.96	0.1	166.28

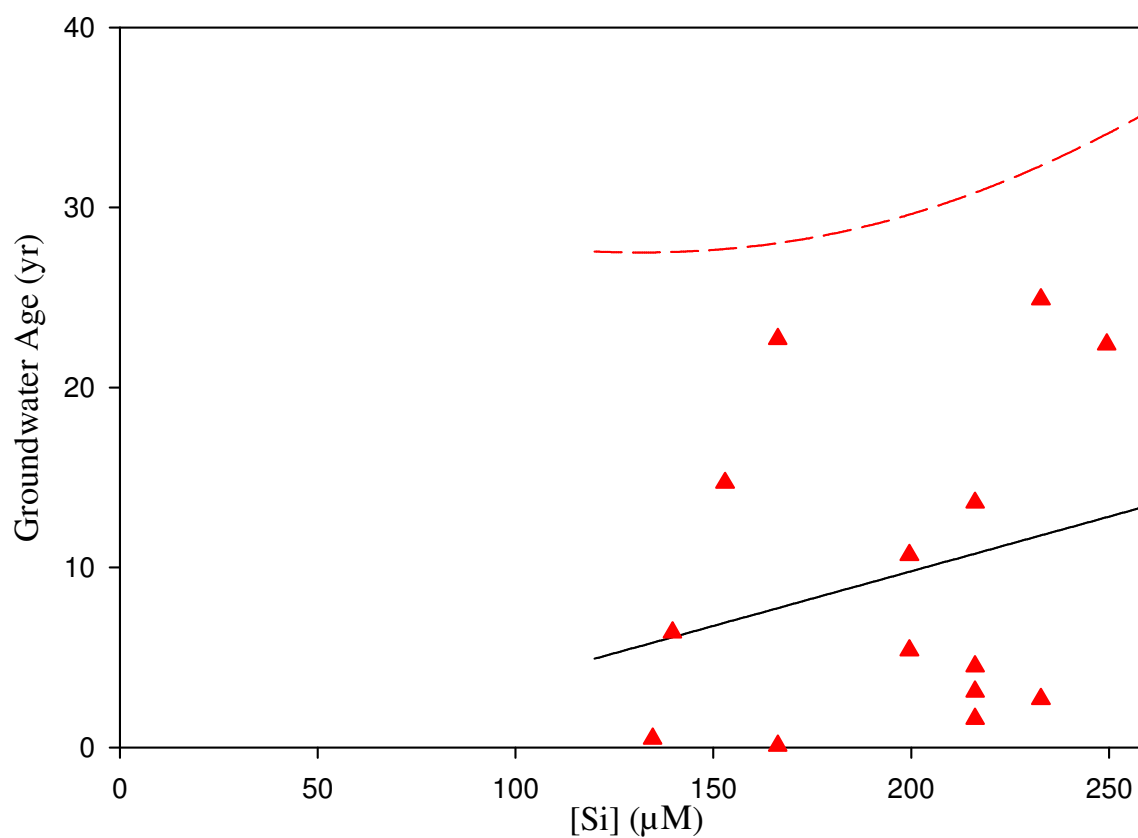


Figure 3.11. Groundwater age vs. groundwater [Si] based on 14 points from Shapiro et al. (1999) and Savoie et al. (1998) representing wells upgradient to Ashumet Pond. Regression analysis yielded a slope of 0.0607 yr/ μM , an intercept of -2.3598 yr, an r^2 of 0.0659, and p-values of 0.3755 and 0.8603 for slope and intercept, respectively. Red dashed lines are 95% prediction intervals.

Table 3.7. Groundwater age and groundwater [Si] for wells adjacent to Ashumet pond, for the studies by Shapiro et al. (1999) and Savoie et al. (1998). Depth below land surface was calculated as the difference between the land surface and screen elevations reported in Savoie et al. (1998).

Site Name	Depth to Top of Screen (m)	Screen Length (cm)	Groundwater Age (yr)	[Si] (μM)
300-10	2.42	60.96	0.1	101.43
300-30	8.42	60.96	6	216.17
300-50	14.76	60.96	6	232.79
300-73	21.67	60.96	9	216.17
300-99	29.68	60.96	15.9	224.48
300-118	35.4	60.96	28.2	232.79
300-138	41.31	60.96	30.2	199.54
348-98	29.04	60.96	1.8	28.27

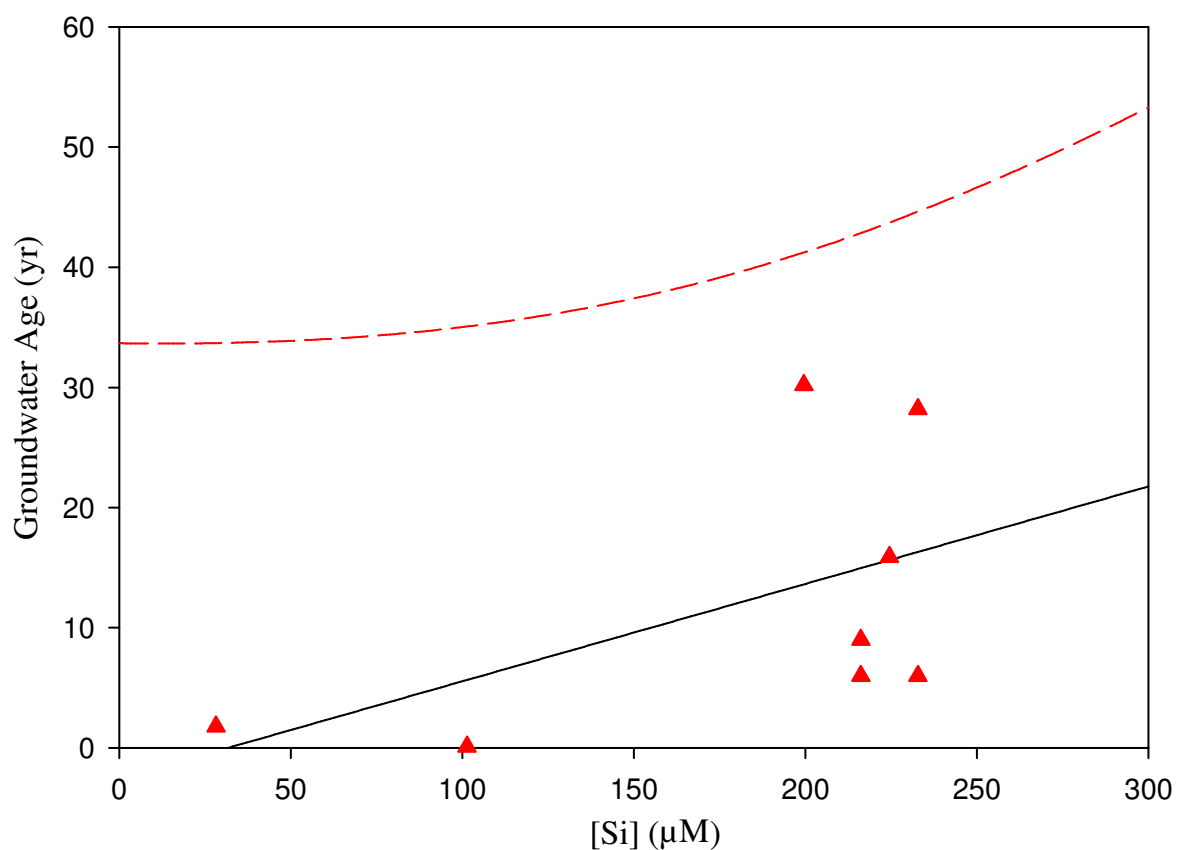


Figure 3.12. Groundwater age vs. groundwater [Si] based on 8 points from Shapiro et al. (1999) and Savoie et al. (1998) representing wells adjacent to Ashumet Pond. Regression analysis yielded a slope of 0.0811 yr/ μM , an intercept of -2.5701 yr, an r^2 of 0.2795, and p-values of 0.1179 and 0.8122 for the slope and intercept, respectively. Red dashed lines are 95% prediction intervals.

Table 3.8. Groundwater age and groundwater [Si] for wells downgradient to Ashumet pond, for the studies by Shapiro et al. (1999) and Savoie et al. (1998). Depth below land surface was calculated as the difference between the land surface and screen elevations reported in Savoie et al. (1998).

Site Name	Depth to Top of Screen (m)	Screen Length (cm)	Groundwater Age (yr)	[Si] (μM)
350-13	3.28	60.96	0.6	84.80
350-52	15.31	60.96	14.8	136.35
350-64	19.24	39.624	24.4	121.39
350-77	22.89	60.96	25.9	166.28
350-84	24.94	60.96	25.9	199.54
350-110	33.10	39.624	28.9	266.05
350-125	37.58	60.96	38.1	282.68
357-79	23.43	60.96	6	138.01
357-99	29.58	60.96	13.9	133.02
357-119	35.87	39.624	21.7	93.12
357-139	41.89	60.96	29.2	249.42
358-49	14.28	60.96	0.6	98.11
358-89	26.42	60.96	14.8	152.98
358-104	31.01	60.96	22.4	159.63
358-132	39.54	60.96	26.6	199.54
411-36	10.23	60.96	1.1	66.51
411-54	15.95	60.96	6.7	131.36
411-65	19.31	60.96	13.1	83.14
411-81	24.13	60.96	16.6	156.30
411-94	28.11	60.96	25.6	199.54
411-106	31.57	60.96	28.5	349.19
412-42	12.07	60.96	3.2	94.78
412-64	18.83	60.96	8	114.73
412-78	23.04	60.96	10.5	99.77
412-91	27.14	60.96	11.8	106.42
412-108	32.33	60.96	11	111.41
418-49	14.35	60.96	0.9	99.77
418-89	26.41	60.96	17.8	162.96

Table 3.8. Continued

418-103	30.91	60.96	25.1	161.29
418-122	36.56	60.96	26.8	266.05
418-141	42.23	60.96	37.3	249.42
436-36	10.26	60.96	5.9	108.08
436-60	17.73	60.96	19.7	143.00
436-76	22.55	60.96	33	249.42
443-104	31.14	60.96	24.4	151.32
443-140	42.06	60.96	32.7	199.54
474-129	38.67	60.96	15.4	139.68
474-147	44.32	60.96	24.6	139.68
501-102	30.40	60.96	29.6	266.05
501-117	34.96	60.96	36	315.93

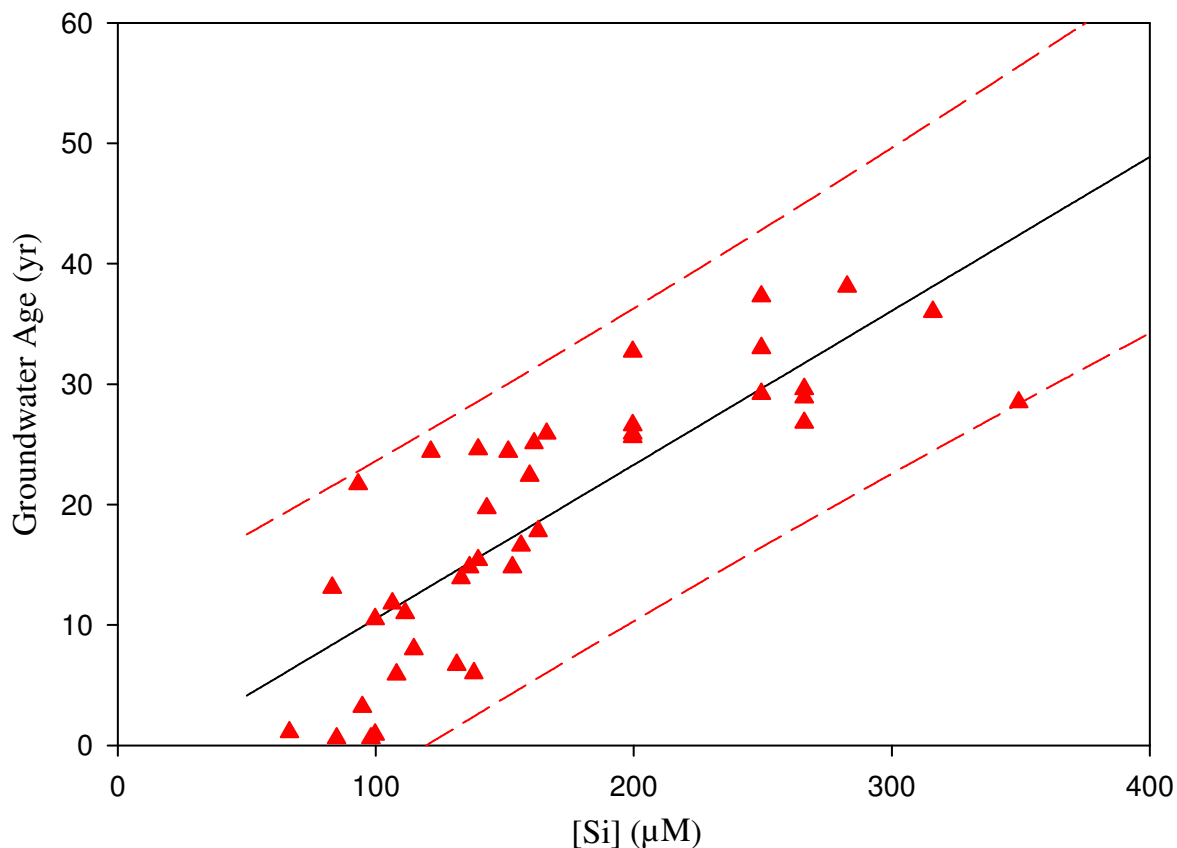


Figure 3.13. Groundwater age vs. groundwater [Si] based on 40 points from Shapiro et al. (1999) and Savoie et al. (1998) representing wells downgradient to Ashumet Pond. Regression analysis yielded a slope of 0.1278 yr/ μM , an intercept of -2.2590 yr, an r^2 of 0.6751, and p-values of <0.0001 and 0.3887 for the slope and intercept, respectively. Red dashed lines are 95% prediction intervals.

3.7. Denver et al. (2010)

3.7.1. Study Site: The study by Denver et al. (2010) concentrates on four study sites located within the Atlantic coastal plain: The Fairmount study site, the Locust Grove study site, the Lizzie study site, and the Willards study site. The Lizzie site was discussed in a previous section covering Tesoriero et al. (2005), and the other three sites are discussed below.

The Fairmount study site is located in southeastern Delaware in the Delaware Inland bays. The soils present at this site are mostly well drained, have a low organic matter content, and are highly permeable. The surficial aquifer at this site ranges in thickness from 25-55 m, and consists primarily of permeable quartz sand and gravel of the Beaverdam Formation and underlying sandy strata of the Bethany Formation. Depth to groundwater ranges from between <0.5 m up to 7 m deep. The land use at this site is primarily agriculture. There are, however, large forested areas upgradient and downgradient of the site. The primary crop grown at this site were corn, soybeans, and small grains.

The Locust Grove study site located in northeastern Maryland in the Chester River Basin is the same site sampled by Böhlke and Denver (1995) and described above in section 3.5.1 of this report. A comparison of the well IDs of the two studies, however, does not yield any matches. Furthermore, a comparison of the distance of the well clusters from the Chesterville Branch channel (Figure 3 in Böhlke and Denver 1995 and Figure 3 in Denver et al. 2010) does not suggest that the two studies collected groundwater from the same wells, although the depths from which samples were collected are similar for the two studies.

The Willards study site is located near the Delaware-Maryland state line, on the west side of the upper part of the Pocomoke River Basin. The soils at this site are typically poorly drained permeable sandy or silt loams containing relatively high amounts of organic matter. The bottom-most unit at this site is the Beaverdam Sand, which is overlain by 3-8 m of thick

clay, peat, silt, and sand of the Omar Formation, which forms a discontinuous confining bed. The Omar formation is subsequently overlain by the Parsonsburg Sand, a sandy unit typically comprised of interspersed clay, silt, and organic matter. When the Beaverdam sand is unconfined, it is considered part of the surficial aquifer. The water table at this site is typically at a depth of 3 m or less. A high density of surface drainage at this site is the result of poor soil drainage (owing to the land being very flat), but relatively high soil permeability. Drainage ditches have been installed to artificially lower the water table. The land use at this site is forested wetland and agriculture. The main crops are corn, soybean, and small grains.

3.7.2. Dissolved Solute Sampling and Analysis Method: The wells sampled in this study were selected from an existing network of wells installed by the USGS for the National Water Quality Assessment Program and associated studies. In most cases, wells were constructed with 5 cm PVC casings and screens (except several wells at the Willards study site that are 2.5 cm in diameter). Wells at the Fairmount, Locust Grove, and Lizzie study sites were installed along the water table gradient which slopes towards local streams. Wells at the Willards study site were installed as single and paired wells, screened to intercept short and intermediate length groundwater flow paths. Chemical data were collected from the Lizzie site in 2003 (1-4 years after the Lizzie sampling reported by Tesoriero et al. 2005), and data from the other 3 sites were collected in 1999. For the Lizzie site there are 5 wells from which usable data (CFC determined groundwater age and [Si]) were collected that are common to both the Tesoriero et al. (2005) and Denver et al. (2010) studies, four of which (L3, L6D,

L8S, and L15D) have been included in my analysis (L11S is not included in this report for reasons discussed above in section 3.4.4). Groundwater samples were collected following the USGS protocols outlined by Koterba et al. (1995). Data presented in Denver et al. (2010) represent a single sampling event. Samples in the field were measured for dissolved oxygen, pH, specific conductance, and temperature using electrodes and probes in a closed-cell flow through chamber. Samples for [Si] were analyzed at the USGS National Water-Quality Laboratory, or at the USGS Organic Geochemistry Laboratory. The instrument and method used for the analysis of [Si] is not mentioned in the paper.

3.7.3. Age-dating Method: The two age-dating methods employed in the Denver et al. (2010) study were CFCs and SF₆. Dissolved-gas analysis was used to determine the concentration of CFCs and SF₆ in groundwater samples collected for analysis. Samples were analyzed at the USGS Chlorofluorocarbon Laboratory in Reston, VA, following procedures used by Busenberg and Plummer (2000, 1992).

3.7.4. Data Analysis: Denver et al. (2010) collected and analyzed four separate data sets pertaining to groundwater age and [Si], and simple linear regression was used to quantify the relations between these two variables. Denver et al. (2010) state that the dissolution of silicate minerals is indicated by the positive correlation between [Si] and groundwater age at all four sites. The number of samples and the published r^2 for the Fairmount study site is 19 and 0.59, respectively; however, only 17 points are visible in the plot in Figure 6 of Denver

et al. 2010. The number of samples and the published r^2 for the Locust Grove site is 13 and 0.66. The number of samples and the published r^2 for the Lizzie site is 16 and 0.63. However, data sent to us from an email communication from Tesoriero (February, 2013) does not show a screen length for well site GR-157 SANDY, and so it has been excluded from my regression. Lastly, the number of samples and r^2 for the Willards site is 9 and 0.61, respectively.

The apparent rate of increase in [Si] over time appears to be greatest at the Willards study site, which Denver et al. (2010) attribute to the mixing of deeper, older water, based on samples collected from confined portions of the Beaverdam formation within the study site. Denver et al. (2010) draws the conclusion that differences in [Si] may be useful for understanding the relative age of groundwater at a local scale, but they doubt the ability of this method to be used on a regional scale.

Figure 3.14 shows my regression for all 4 sites, created from data received via an email correspondence from Tesoriero in January 2013. A personal communication was necessary to obtain the complete dataset for the 2003 Lizzie data (as well as the other three sites) because the Denver et al. (2010) paper contained summary statistics (minimum, maximum, and median values) and not the complete data sets. In addition, there were no values for the screen lengths for individual wells in Denver et al. (2010), though in some cases ranges for screen length were provided. There were two apparent discrepancies

between the emailed data set and the data published in Denver et al. (2010). In the emailed data set there are 20 usable data points that included values for both groundwater age and [Si] for the Fairmount study site, but Denver et al. (2010) list 19 samples as having been collected and 17 are plotted in their Figure 6. Visual comparison of Fig. 3.15 against Fig. 6 in Denver et al. (2010) indicate three points are included in the former graph but not the latter: wells 383854075124801, 383854075122004, and 383929075123105. Similarly, the published data lists the number of samples for the Lizzie location as 15, but 16 values are plotted in Figure 6 of Denver et al. (2010). The emailed data also contained 16 values for the Lizzie study site, 15 of which I used in my analysis. Well GR-157 Sandy was excluded from my regression because there was no information on this well (i.e., screen length) in the Excel file provided by Tesoriero (January 2013). The minimum age uncertainty for the Fairmount site was approximately ± 14.4 yr, the minimum age uncertainty for the Locust Grove site was approximately ± 16.1 yr, the minimum age uncertainty for the Lizzie site was approximately ± 14.4 yr, and the minimum age uncertainty for the Willard site was approximately ± 9.7 yr.

There were two locations presented in the study conducted by Denver et al. (2010) which overlapped with other studies considered in this report. A combined regression (24 points) of the Lizzie data in Tesoriero et al. (2005) and the Lizzie data in Denver et al. (2010) yielded a slope of 0.1385 yr/ μM , an intercept of -4.0127 yr, an r^2 of 0.6979 , and p-values of <0.0001 and 0.2440 for slope and intercept, respectively (Fig. 3.19). A combined regression (31 points) of the Locust Grove data in Böhlke and Denver (1995) and the Locust Grove data

from Denver et al. (2010) for the Chesterville Branch yielded a slope of $0.0780 \text{ yr}/\mu\text{M}$, an intercept of 9.3382 yr , an r^2 of 0.1669 , and p-values of 0.0225 and 0.0556 for slope and intercept, respectively. With the new regressions, the minimum age uncertainty for the Lizzie site becomes $\pm 13.4 \text{ yr}$, and that for Locust Grove becomes $\pm 21.7 \text{ yr}$ (Fig. 3.20). In both cases the age uncertainty has been improved. In addition, there are 4 wells in the Lizzie site that were sampled in both sampling events: L3, L6D, L8S, and L15D. Both sampling events from these wells produced [Si] and groundwater ages that were similar, and well L8S produced [Si] and groundwater ages that are apparently the same. As unlikely as this is, there is no indication from either Tesoriero et al. (2005) or Denver et al. (2010) that the samples from well L8S were from the same sampling event. Tesoriero et al. (2005) states that most of the samples in their study were collected from March 1999 to June 2002. In the data table sent to us by Tesoriero (January 2013), he lists the samples reported in the Denver et al. (2010) study as having been collected in April of 2003.

Visual inspection of the plot of the Fairmount data suggests the possibility that the data from this location may be explained by a non-linear, concave-up model. An exponential fit to the data (Fig. 3.21) gives improved r^2 and p-values, in comparison to the linear regression. While an exponential (or other concave-up) function may be realistic (in the sense that it shows a decreasing rate of Si acquisition by groundwater as [Si] increases), Fairmount is the only site that showed both improved r^2 and p values for an exponential fit, compared to

a linear fit. At this time further investigation of more complex non-linear regressions does not seem warranted by the data.

Table 3.9. Groundwater age and groundwater [Si] for the study by Denver et al. (2010). Depths (where available) have been calculated as depth below land surface elevation (NGVD 29).

Site	Depth to Top of Screen (m)	Screen Length (cm)	GW Age (yr)	[Si] (μM)
<u>Fairmount Site</u>				
383854075122002	No Data	150	11.1	294.92
383854075122003	No Data	150	8.8	293.60
383854075122004	No Data	150	13.8	181.58
383854075124801	No Data	150	2.63	178.80
383854075124802	No Data	150	9.63	291.24
383903075123001	No Data	150	18.1	308.70
383903075123002	No Data	150	16.6	311.71
383903075123003	No Data	150	13.1	293.72
383903075123004	No Data	150	8.8	267.25
383903075123005	No Data	150	7.1	272.42
383907075124101	No Data	150	17.1	316.37
383907075124102	No Data	150	8.8	243.82
383907075124103	No Data	150	7.3	278.40
383907075124104	No Data	150	6.4	163.29
383929075123101	No Data	150	33	360.10
383929075123102	No Data	150	30.4	345.95
383929075123103	No Data	150	34	344.43
383929075123104	No Data	150	12.1	329.40
383929075123105	No Data	150	7.4	284.29
383939075120102	No Data	150	5.6	180.66
<u>Locust Grove</u>				
391720075554601	No Data	60.96-91.44	52	293.37
391720075554602	No Data	60.96-91.44	27	194.85
391720075554603	No Data	60.96-91.44	15	170.52
391720075554701	No Data	60.96-91.44	17	209.38
391721075554501	No Data	60.96-91.44	24	189.03

Table 3.9 Continued

391721075554502	No Data	60.96-91.44	11	200.25
391742075554801	No Data	60.96-91.44	10	124.08
391742075554802	No Data	60.96-91.44	29	213.95
391742075554803	No Data	60.96-91.44	17	153.84
391810075555801	No Data	60.96-91.44	12	191.79
391810075555803	No Data	60.96-91.44	20	176.74
391832075560803	No Data	60.96-91.44	8	180.13
391832075560804	No Data	60.96-91.44	24	198.17
<u>Willards Site</u>				
382452075202901	No Data	60.96-91.44	3.4	130.06
382452075202902	No Data	60.96-91.44	10.7	133.90
382543075212201	No Data	60.96-91.44	7.4	86.67
382611075210601	No Data	60.96-91.44	8.2	260.75
382611075210604	No Data	60.96-91.44	16.2	234.75
382704075224101	No Data	60.96-91.44	7	243.56
382704075224104	No Data	60.96-91.44	16.6	334.45
382745075234301	No Data	60.96-91.44	0.1	49.07
382745075234302	No Data	60.96-91.44	2	46.92
<u>Lizzie Site</u>				
GR-082 L2 LI	1.83	304.8	13	90.29
GR-085 L6LIZ	1.22	91.44	16.2	149.99
GR-090 L3	7.01	457.2	41	290.99
GR-094 L6D	0.27	91.44	28	222.82
GR-097 L8S	4.89	152.4	4	108.08
GR-098 L8D	5.19	152.4	14	109.08
GR-100 L10	9.15	457.2	29	199.54
GR-102 L11S	0.56	304.8	5	61.52
GR-103 L11D	6.16	304.8	15	59.03
GR-107 L15 L	3.04	304.8	15	101.76
GR-109 L15D	6.23	304.8	18	176.26
GR-113 L18D	7.40	304.8	16.3	146.49
GR-168 LWQ70	No Data	121.92	13	119.722272
GR-169 LWQ70	No Data	121.92	17	244.432971
GR-171 LWQ71	No Data	121.92	18	212.839594

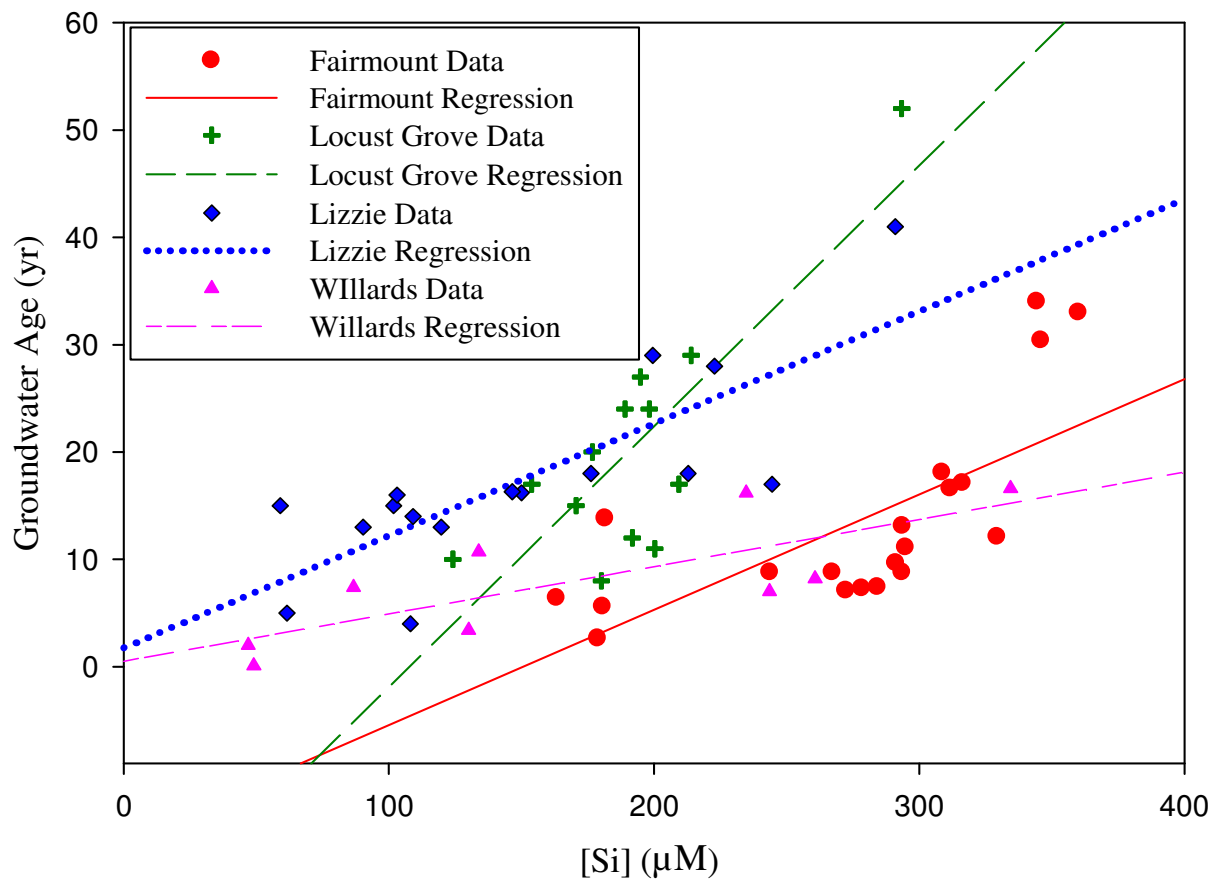


Figure 3.14. Groundwater age vs. groundwater [Si] for Fairmount, Locust Grove, the Lizzie Site, and the Willards area.

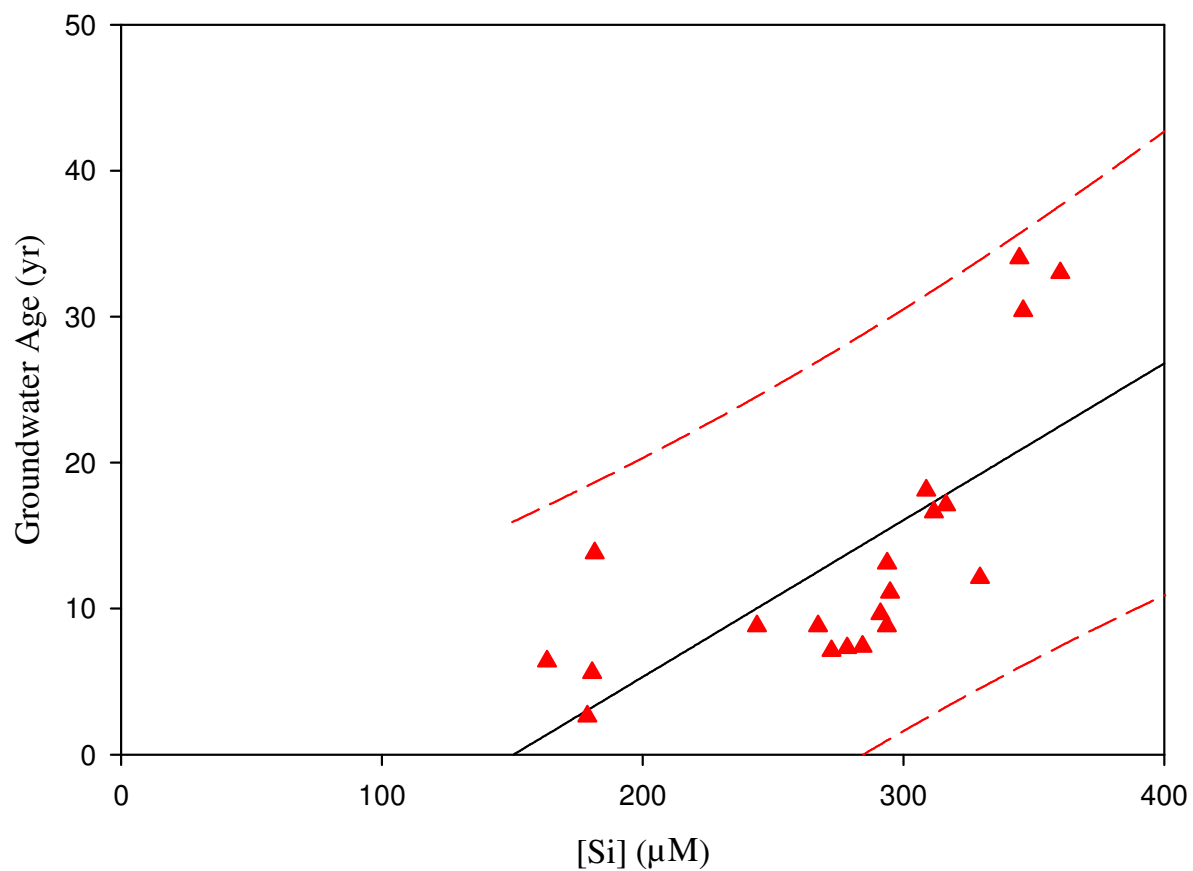


Figure 3.15. Groundwater age vs. groundwater [Si] for the Fairmount site based on 20 points from Denver et al. (2010) yielded a slope of 0.1074 yr/ μM , an intercept of -16.1706 yr, an r^2 of 0.4863, and p-values of 0.0006 and 0.0414 for the slope and intercept, respectively. Red dashed lines are 95% prediction intervals.

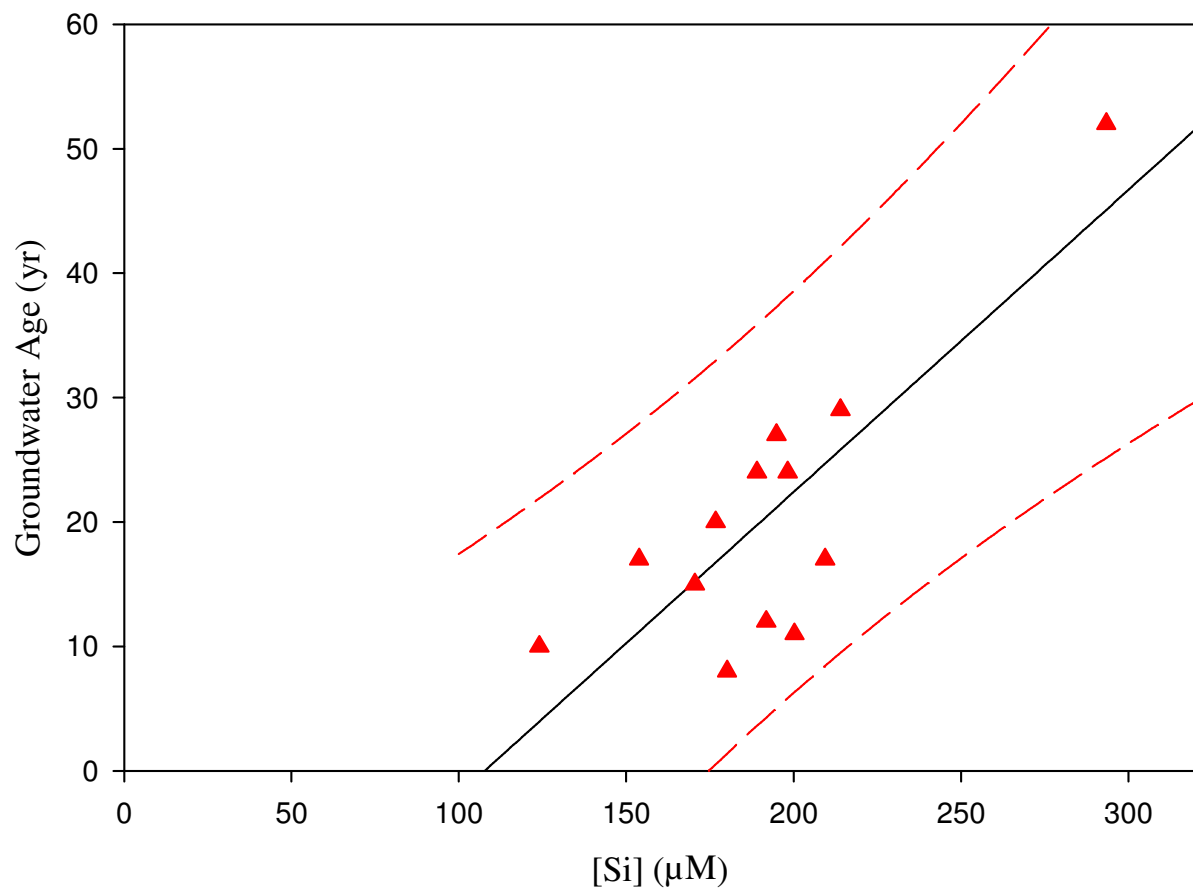


Figure 3.16. Groundwater age vs. groundwater [Si] for Locust Grove based on 13 points from Denver et al. (2010) yielded a slope of $0.2429 \text{ yr}/\mu\text{M}$, an intercept of -26.1716 yr , an r^2 of 0.6605 , and p-values of 0.0007 and 0.0271 for the slope and intercept, respectively. Red dashed lines are 95% prediction intervals.

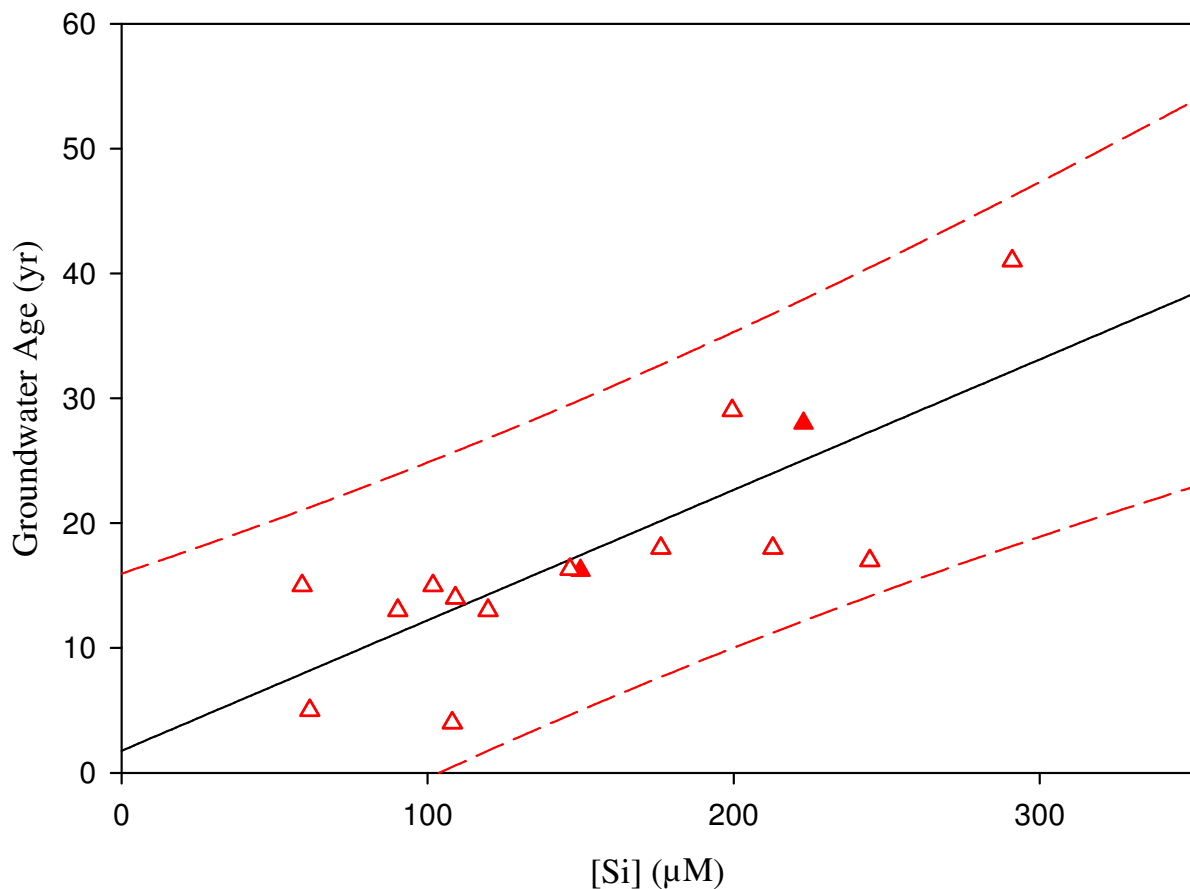


Figure 3.17. Groundwater age vs. groundwater [Si] for the Lizzie Site based on 15 points from Denver et al. (2010) yielded a slope of $0.1070 \text{ yr}/\mu\text{M}$, an intercept of 1.1382 yr , an r^2 of 0.6150 , and p-values of 0.0003 and 0.7630 for the slope and intercept, respectively. Open triangles indicate data point was taken from a well with screen length $\geq 1 \text{ m}$, and filled triangles indicate data point was taken from a well with screen length $< 1 \text{ m}$. Red dashed lines are 95% prediction intervals.

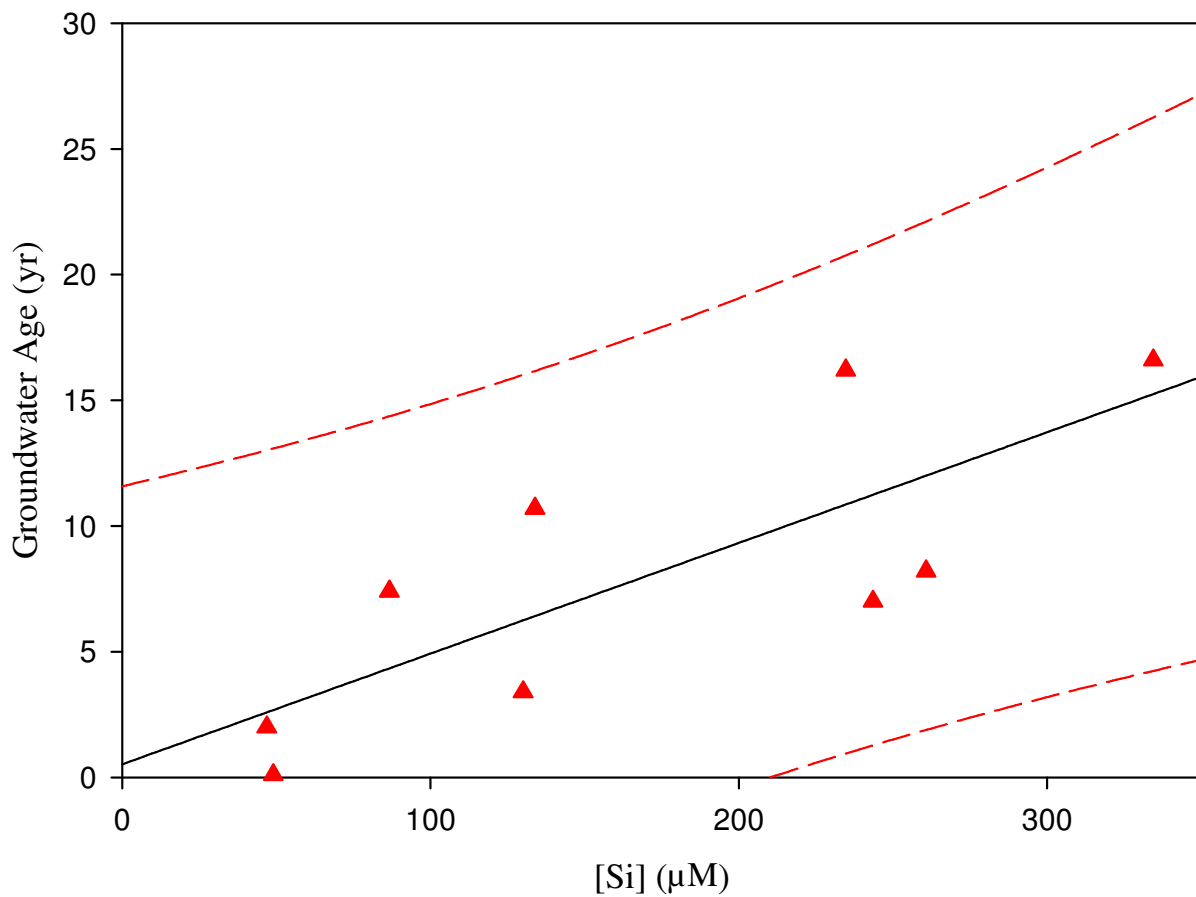


Figure 3.18. Groundwater age vs. groundwater [Si] for the Willards site data based on 9 points from Denver et al. (2010) yielded a slope of 0.0440 yr/ μM , an intercept of 0.5198 yr, an r^2 of 0.6077, and p-values of 0.0132 and 0.8474 for the slope and intercept, respectively. Red dashed lines are 95% prediction intervals.

Table 3.10. Regression results (groundwater age vs. groundwater [Si]) for the Lizzie Site, NC, including a regression of the combined data from Tesoriero et al. (2005) and Denver et al. (2010). "n" = number of data points in the regression. In each cell of the last column, the P values apply to the slope and intercept, respectively.

Study	Study Area	n	slope yr/(μM)	intercept (yr)	r²	P
Tesoriero et al. (2005)	Contentnea Creek sub-basin of the Neuse River, NC	9	0.1965	-14.401	0.8500	0.0004/ 0.0385
Denver et al. (2010)	Lizzie Site, NC	15	0.1070	1.138	0.6425	0.0003/ 0.7630
Tesoriero et al. (2005) and Denver et al. (2010): Lizzie Site	Contentnea Creek sub-basin of the Neuse River, NC	24	0.1385	-4.013	0.6842	<0.0001/ 0.2440

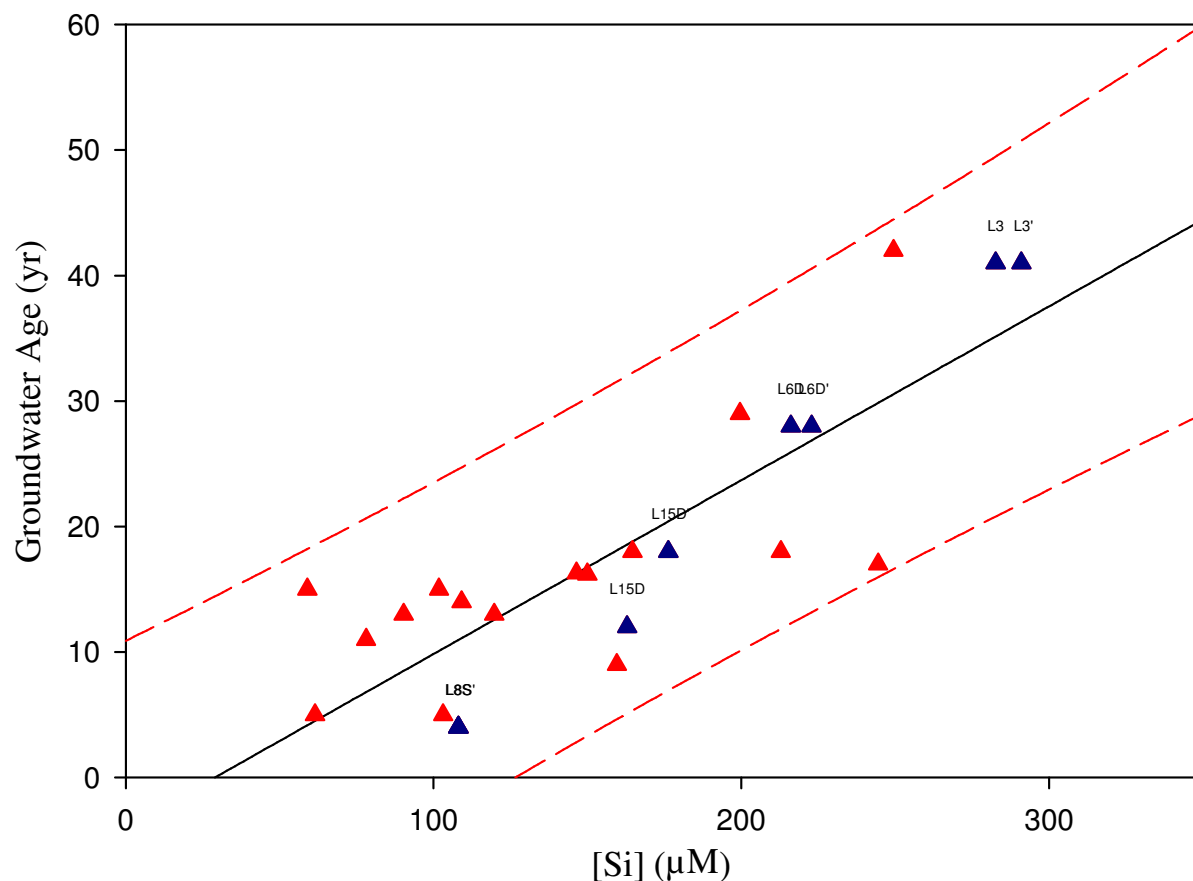


Figure 3.19. Groundwater age vs. groundwater [Si] at the Lizzie site in NC, based on combining 24 points from Tesoriero et al. (2005) and Denver et al. (2010). Regression analysis yielded a slope of 0.1385 yr/ μM , an intercept of -4.0127 yr, an r^2 of 0.6979, and p-values of <0.0001 and 0.2440 for slope and intercept, respectively. Blue triangles are wells common to both studies Red dashed lines are 95% prediction intervals.

Table 3.11. Regression results (groundwater age vs. groundwater [Si]) for the Locust Grove site in MD, based on (1) data in Böhlke and Denver (1995) alone, (2) data in Denver et al. (2010) alone, and (3) the combined data from both papers. "n" = number of data points in the regression. In each cell of the last column, the P values apply to the slope and intercept, respectively.

Study	Study Area	n	slope yr/(μM)	intercept (yr)	r²	P
Böhlke and Denver (1995)	Delmarva Peninsula, MD (Chesterville Branch and Morgan Creek)	32	0.3327	-13.5125	0.4853	<0.0001/ 0.0455
Denver et al. (2010)	Delmarva Peninsula, (Locust Grove), MD	13	0.2429	-26.172	0.6605	0.0007/ 0.0271
Böhlke and Denver (1995) and Denver et al. (2010)	Delmarva Peninsula, MD	45	0.1154	5.231	0.2096	0.0016/ 0.2691

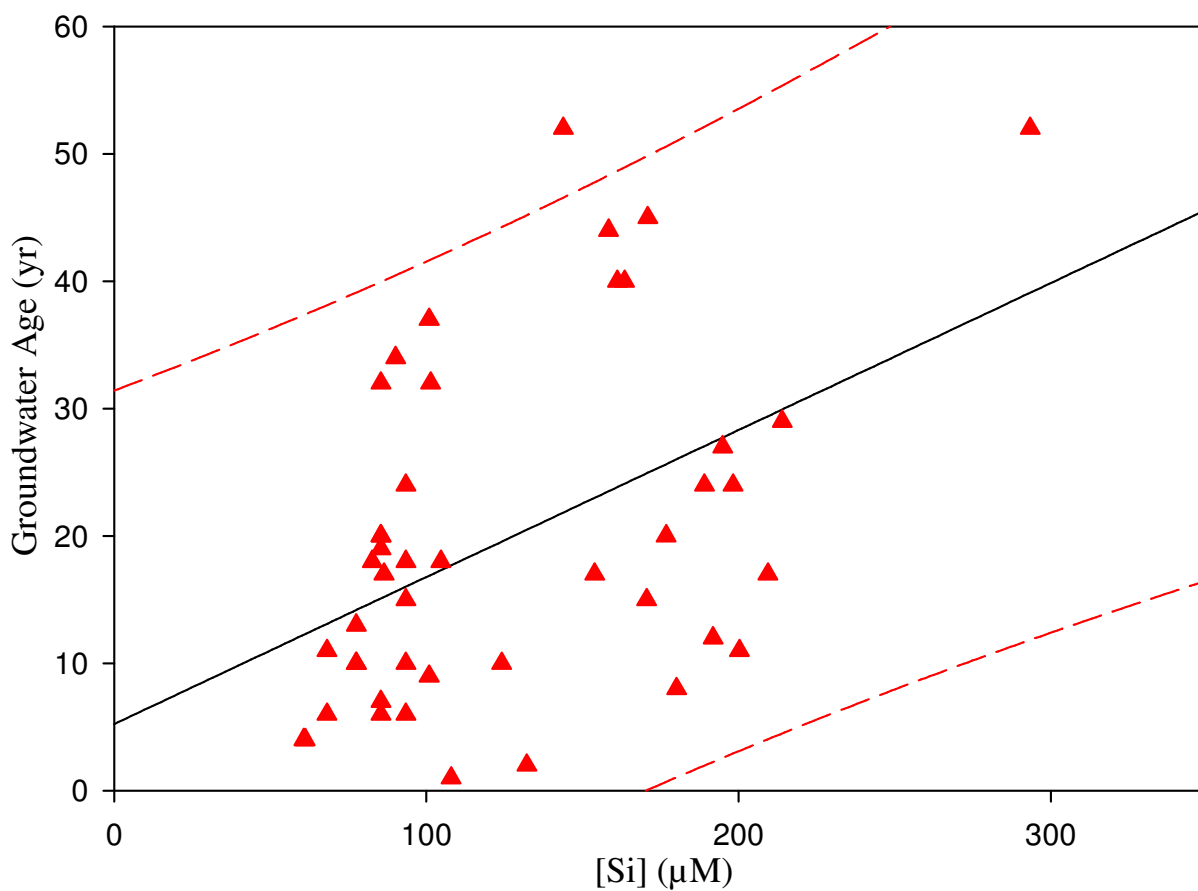


Figure 3.20. Groundwater age vs. groundwater [Si] at the Locust Grove site in MD (For the Chesterville Branch and Morgan Creek), based on combining 45 points from Böhlke and Denver (1995) and Denver et al. (2010). Regression analysis yielded a slope of 0.1154 yr/ μM , an intercept of 5.2306 yr, an r^2 of 0.2096, and p-values of 0.0016 and 0.2691 for slope and intercept, respectively. Red dashed lines are 95% prediction intervals.

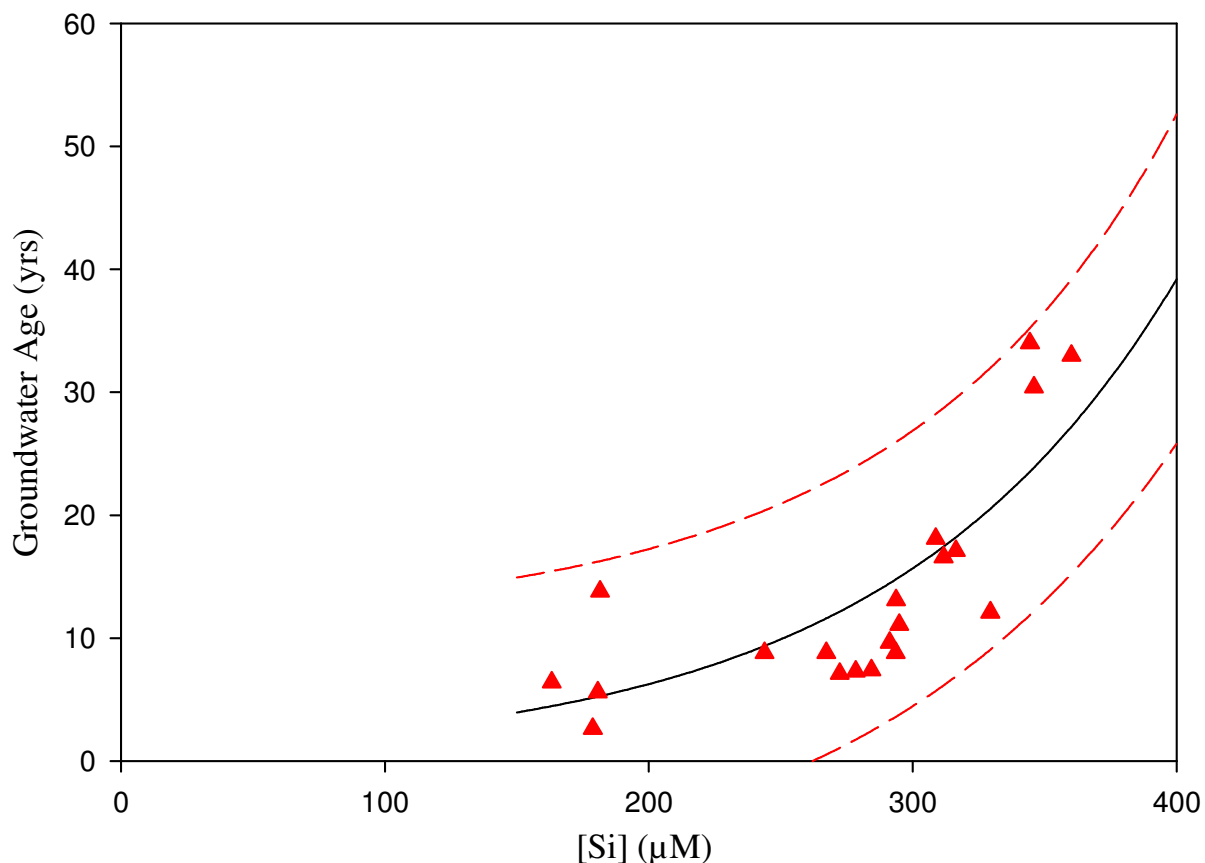


Figure 3.21. Exponential fit ($\text{Age} = \exp(k[\text{Si}])$) to the groundwater age and $[\text{Si}]$ data for the Fairmount site based on 20 points from Denver et al. (2010), with an exponential rate constant k of $0.0092\mu\text{M}^{-1}$, an r^2 of 0.6670, and a p -value of <0.0001 for the k value. Red dashed lines are 95% prediction intervals.

3.8. Rademacher et al. (2001)

3.8.1. Study Site: The study took place in the Sagehen basin, located in the eastern Sierra Basin, California. Samples were collected from Sagehen springs situated in a small, high-elevation catchment with a mean elevation of 2100 meters. The Sagehen basin is covered by glacial till deposits derived from andesite and granodiorite basement rocks, which are exposed at the surface at different locations in and around the site. The granodiorite unit is comprised of 40% plagioclase, 30% quartz, 20% hornblende, and 10% biotite. The

andesite unit consists of 45% plagioclase, with hornblende and augite content varying from 5-25% and 1-25%, respectively. This unit also contains a small amount of glassy groundmass.

3.8.2. Dissolved Solute Sampling and Analysis Method: Sampling for dissolved solutes and age-dating tracers was conducted from the summer of 1997 to the fall of 1999. Samples were collected from 11 springs in the Sagehen Basin from each spring's uppermost discharge zone using a copper sampling tube that was positioned to collect samples at the water-sediment interface. Samples for [Si] analysis were filtered in the field using a 0.4 μm polycarbonate filter and were stored in polyethylene bottles and refrigerated until analysis. Samples for analysis were collected in two bottles, one acidified with concentrated HCl, and one not acidified. [Si] was analyzed via ICP-AES (calculated analytical precision of $\pm 4\%$) and with atomic adsorption techniques (i.e., spectrometry). Both acidified and un-acidified samples were analyzed, and there was no discernable difference detected. Samples were run multiple times, and the data presented in Rademacher et al. (2001) are averages.

3.8.3. Age-dating Method: Samples were collected for the analysis of CFC-11, CFC-12, tritium, and helium isotopes. The samples for helium analysis were collected in 10 ml copper tubes sealed with stainless steel pinch-off clamps, and samples for tritium analysis were stored in glass bottles. For samples collected in 1997, CFCs were collected using a copper tube and a glass syringe, and were then transferred immediately to borosilicate

ampoules which were flame-sealed in the field (leaving headspace for N₂) and were then refrigerated until analysis. 1999 CFC samples were collected in 10 ml copper tubes sealed with stainless steel pinch-off clamps. Samples were also refrigerated until analysis. The ³He accumulation method was used for the measurement of tritium (Surano et al. 1992).

3.8.4. Data Analysis: For this study, the authors noted that the ages determined using the ³H/³He method were consistently 10-15 years younger than the groundwater ages yielded by CFCs. No explanation is provided by Rademacher et al. (2001) for the discrepancy of the ³H/³He determined groundwater ages. There is, however, good agreement for the CFC-11 and CFC-12 determined groundwater ages collected by Rademacher et al. (2001), and there is good agreement for the CFC ages determined from samples collected in 1997 and 1999 as shown in Figure 3 of Rademacher et al. (2001). Rademacher et al. (2001) found that in most cases the higher elevation springs had shorter residence times, with the exception of S13, which had a CFC-determined age of 36 yr, and that is located above younger spring water. S7 was shown to possess excess ⁴He. ⁴He in a sample could be an indicator of deeply circulating groundwater, which except for S7, was not the case for this study. The low ³H+³He in samples S7 and S13 (indicating recharge before the introduction of bomb hydrogen) may be the result of deeply circulating groundwater mixed with shallow groundwater. These samples also had high conductivities, indicating long mineral interaction times. Although not relevant to the determination of groundwater age using CFCs, longer mineral interaction times could result in higher [Si]. The minimum age prediction uncertainty

(Fig. 3.21) was approximately ± 20.7 yr. This regression has the most scatter, the lowest slope, and the lowest r^2 value of all the studies reviewed, perhaps due in part to the fact that springs (usually complex mixtures of groundwater of different age) were sampled rather than wells.

Table 3.12. CFC-11 and CFC-12 groundwater ages and groundwater [Si] for the 1999 sampling event by Rademacher et al. (2001). “Mean GW Age” is the average of the CFC-11 and CFC-12 ages.

Sagehen Spring Number	GW Age (yr), CFC-11	GW Age (yr), CFC-12	Mean GW Age (yr)	[Si] (μM)
S2	23	20	21.5	689
S4	29	31	30	472
S5	31	39	35	438
S6	20	21	20.5	525
S7	31	34	32.5	501
S8	10	10	10	369
S9	26	23	24.5	502
S10	20	23	21.5	303
S11	25	29	27	467
S13	36	38	37	421

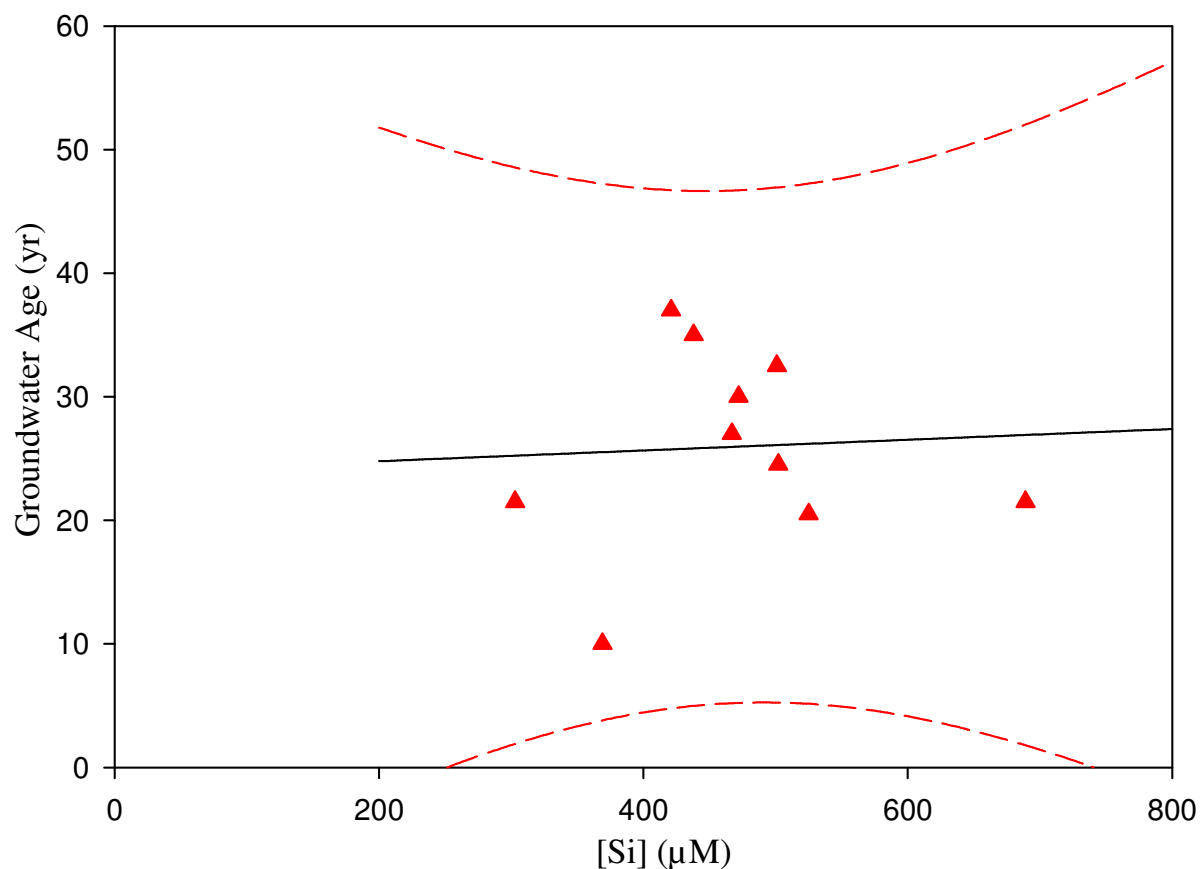


Figure 3.22. Groundwater age vs. groundwater [Si] based on 10 points from the data presented in Rademacher et al. (2001). Regression analysis yielded a slope of 0.0043 yr/ μM , an intercept of 23.9144 yr, an r^2 of 0.0030, and p-values of 0.8802 and 0.1111 for slope and intercept, respectively. Red dashed lines are 95% prediction intervals.

3.9. Lindsey et al. (2003)

3.9.1. Study Site: The study was based on 48 springs in the Chesapeake Bay Watershed (64,000 mi²) and four smaller watersheds in select hydrogeomorphic regions including: coastal plain uplands, piedmont crystalline, valley and ridge carbonate, and valley and ridge siliciclastic. The data summarized here are from the Polecat Creek Watershed in the piedmont crystalline region. The Polecat Creek watershed, located in west-central

Caroline County, Virginia, is approximately 46.9 mi², and the land use is 73.5% forest, 14.2% agriculture, 9.9% urban development, and 2.5% water bodies. Along both sides of the creek is a riparian buffer that extends 350-450 ft. Elevation of the creek ranges from 210-250 ft above sea level. The Polecat Creek watershed is piedmont crystalline to the west, to the east coastal plain deposits are included. The study by Lindsey et al. (2003) focuses on the western part of the watershed. Most groundwater that flows from the watershed into Polecat Creek flows through the surficial aquifer, but some water may flow through a fractured bedrock aquifer. The sample site is underlain by bedrock made up of garnet-biotite gneiss. Bedrock is covered by saprolite (partially weathered rock), the saprolite being a mixture of silt, clay, and some sand. The saprolite is fine-grained and has a low permeability. Because the site is at the eastern edge of the piedmont, saprolite is overlain by coastal plain sediments in the uplands, and by alluvial sediments in the flood plain. Coastal plain sediments consist of fine-to-course-grained sand and gravel in a clay-silt matrix, and can be as thick as 26 ft. Alluvial sediments consist of a mixture of gravel, sand, silt, and clay with a silt and clay matrix, and are typically less than 4 ft thick. The unconfined surficial aquifer at the study site comprises saprolite, coastal plain sediments, and alluvium. The permeability of both the coastal plain sediments and alluvial sediments differ little from that of the saprolite. Groundwater flow at the site reflects natural, unstressed conditions.

3.9.2. Dissolved Solute Sampling and Analysis Method: Well sampling in Polecat Creek took place during 1998-2000, but the primary well sampling period was in April of

1999 (relatively few samples were taken before for preliminary data, and relatively few samples were collected after this period in an effort to complete any gaps in the dataset). The 17 samples used in the regression were collected from a network of 19 wells constructed in a transect along the presumed regional groundwater flow path. Wells were constructed with screens 1.3-5 ft long and 0.010 or 0.020 inch slots for the screens. Wherever possible, wells were constructed to place the bottom of the screen of the deepest well (for well clusters) near the bottom of the surficial aquifer. Water was pumped out of the piezometer using a submersible, gas-driven pump. Before sampling, piezometers were purged 3 well volumes of water or until pH, dissolved oxygen, and specific conductance stabilized. Groundwater samples for lab analysis of [Si] were acidified and passed through a 0.45 μm filter. Samples for [Si] were analyzed at the USGS National Water-Quality Laboratory in Denver, Co, most likely either by the ICP or colorimetric method (not specified in Lindsey et al. 2003).

3.9.3. Age-dating Method: In the Polecat Creek study area samples were age-dated using CFCs, SF₆, and ³H/³He. For each sample point, a 1 L sample was collected for the analysis of SF₆ following the procedures outlined in Busenberg and Plummer (2000). Five replicate unfiltered CFC samples were sealed in glass ampoules for lab analysis for each well, following the procedure outlined by Busenberg and Plummer (1992). In addition, at each well two unfiltered samples for analysis of ³He were sealed in special copper tubes for lab analysis of ³H/³He following the procedure outlined by the USGS Technical Memoranda 97.04 and 97.04S, referenced by Plummer and Mullin (1997). Unfiltered samples were

collected for the analysis of ^3H . Sample size for ^3H was not provided by Lindsey et al. (2003), but samples were likely collected in 500 ml HDPE bottles, as for other studies. Samples for $^3\text{H}/^3\text{He}$ analysis were analyzed by the Lamont-Doherty Earth Observatory of Columbia University, Palisades, NY. Samples for CFCs and SF_6 analysis were analyzed by the USGS National Research Program Isotope Laboratory, Reston, VA.

3.9.4. Data Analysis: As for most groundwater samples collected from the Chesapeake Bay targeted watersheds (targeted in this sense meaning there is groundwater nitrate contamination or other cause for study), CFC-11 was found to be generally depleted at the site relative to CFC-12, presumably because of microbial degradation (Lindsey et al. 2003). The apparent age of groundwater was determined primarily from concentrations of CFC-12, CFC-113, and SF_6 . Data for CFC-11 was used only in water from well 50M2 (in combination with data from CFC-12 and CFC-113). Two tracers were used to determine groundwater age in all wells except for wells 50M3 and 50M5.

Groundwater from the following wells were also determined to be mixtures by Lindsey et al. (2003), and thus were excluded from the age-[Si] regression analysis here: 50M29 (88% young) and 50M30 (64% young). Wells 50M29 and 50M30 were located in the riparian forest buffer, where the area temporarily alternated between being a recharge and a discharge area. This could account for the mixtures of groundwater collected from these wells. Also, three wells stand out as falling well off the piston flow curve on a plot of SF_6 vs.

CFC-12 (Fig. 3.23): 50M4, 50M5, and 50M24. This suggests either a problem with one or both age dates or possible mixing of groundwater of different ages. All three wells have been excluded from the groundwater age-[Si] regression analysis.

Finally, Lindsey et al. (2003) stated that wells 50M21, 50M22, and 50M6 likely included mixtures of modern water and older water. The percentage of younger water, however, is given in Appendix C of Lindsey et al. (2003) as 100% for all three sample sites, and 50M21 and 50M22 both agree well with the piston flow line shown in Fig. 3.24. For this reason they have been included in my regression. 50M6 has a groundwater age provided by only one tracer (CFC-12), but because there is no evident reason to exclude it, 50M6 has also been included in my regression. The minimum age uncertainty for my regression was approximately ± 7.6 yr.

Table 3.13. Polecat Creek groundwater age data and groundwater [Si] for the study by Lindsey et al. (2003). Depths have been calculated as depth below land surface elevation.

Site Name	Depth to bottom of screen (m)	Screen Length (cm)	Recharge date	GW Age (yr)	[Si] (μM)
50M2	12.17	152.40	1968.8	30.5	527.28
50M3	7.66	152.40	1994.0	5.3	152.85
50M6	1.48	147.52	1993.5	5.2	175.30
50M7	14.11	152.40	1972.3	27.1	611.88
50M16	4.94	140.21	1995.5	3.2	104.22
50M17	0.46	353.57	1996.2	3.1	98.95
50M18	4.48	60.96	1988.3	11.1	235.60
50M19	3.51	60.96	1990.3	9.0	168.71
50M21	0.34	60.96	1999.0	0.4	138.02
50M22	2.32	60.96	1999.0	0.4	139.66
50M25	1.10	60.96	1990.9	4.2	209.83
50M26	2.77	60.96	1988.3	5.2	178.00

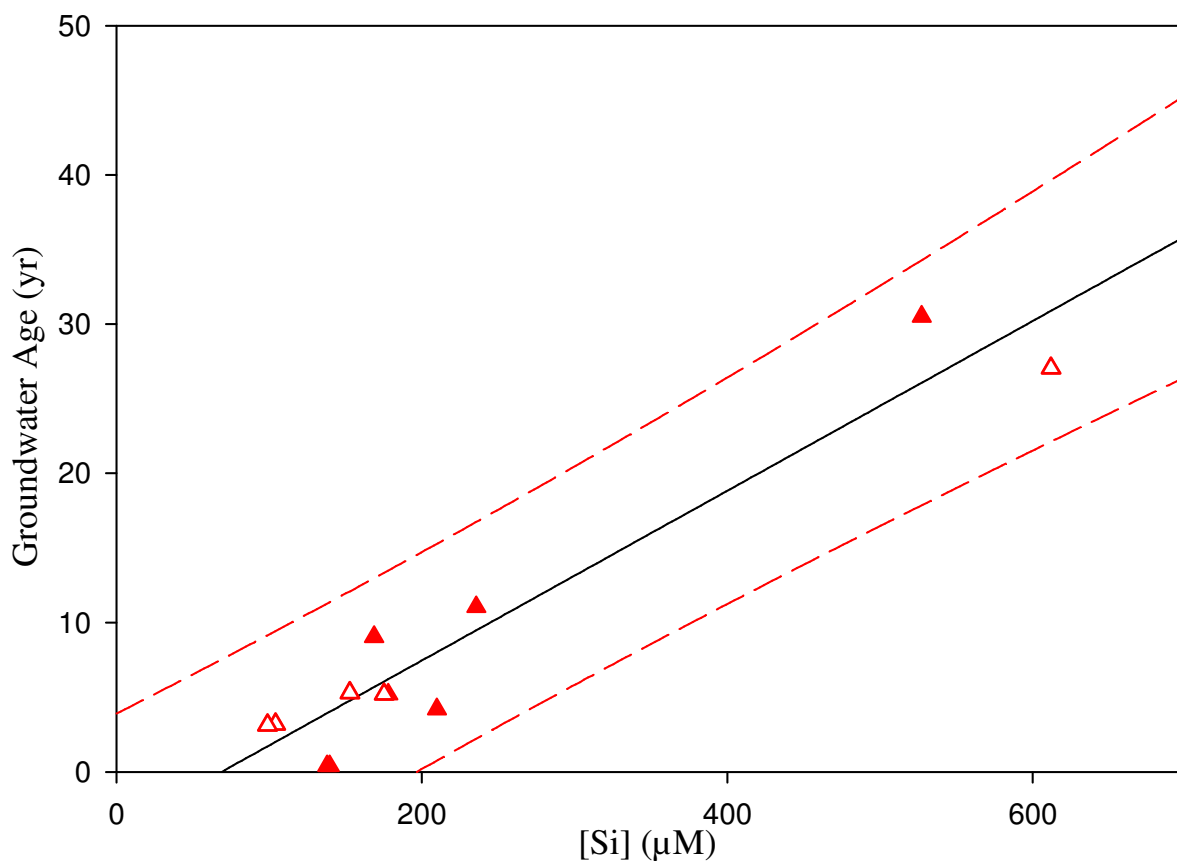


Figure 3.23. Groundwater age vs. groundwater [Si] based on 12 points from Lindsey et al. (2003). Regression analysis yielded a slope of 0.0572 yr/ μM , an intercept of -4.3432 yr, an r^2 of 0.9140, and p-values of <0.0001 and 0.0183 for slope and intercept, respectively. Open triangles indicate data point was taken from a well with screen length ≥ 1 m, and filled triangles indicate data point was taken from a well with screen length < 1 m. Red dashed lines are 95% prediction intervals.

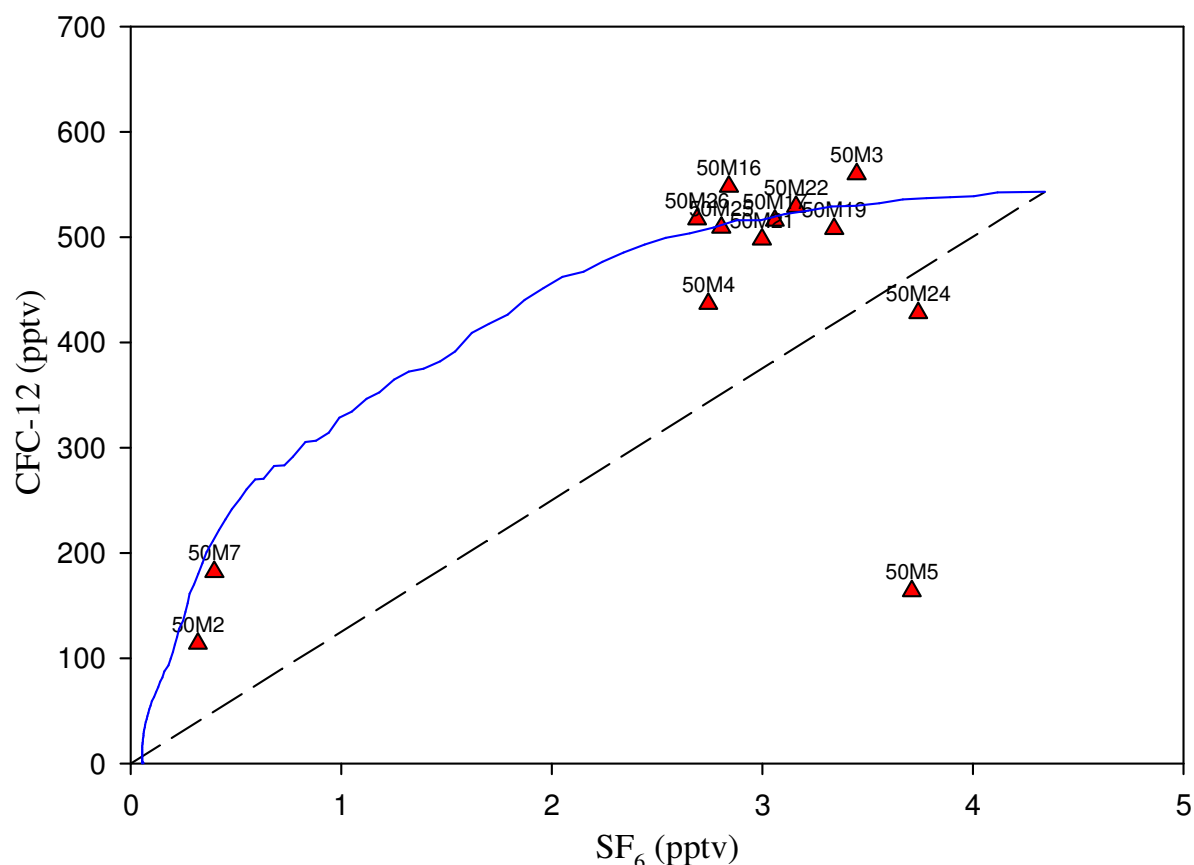


Figure 3.24. Piston flow model (blue line) for CFC-12 and SF₆ constructed from historic atmospheric concentrations. CFC and SF₆ data measured in Niwot Ridge, Co, and analyzed by USGS Chlorofluorocarbons Laboratory, Reston, VA (Busenberg and Plummer 2011). Binary mixing model (dashed line) is also included, but samples of groundwater mixture have not been included in my regression.

3.10. Burns et al. (2003)

3.10.1. Study Site: Study area is the 41 ha Panola Mountain Research Watershed (PMRW), located in the piedmont region of Georgia. The study's focus was on shallow groundwater from the riparian (saprolite) aquifer. The PMRW is underlain by the Panola Granite unit, which intrudes into the Clairmont formation. The Panola Granite is characterized as being a biotite-oligoclase-quartz-microcline granite of Mississippian to

Pennsylvanian age. The primary minerals comprising Panola Granite are plagioclase feldspar (composition is An_{20-25}), quartz, microcline/microperthite, muscovite, and biotite. The Clairmont Formation (present in the lower part of the watershed as pods and lenses) contains varying amounts of amphibolites, granite gneiss, and other rock types of Ordovician age. This unit has mineralogy similar to the Panola Granite unit, with the exception of amphibolites lenses dominated by plagioclase feldspar (An_{32}) and hornblende, and also contains minor amounts of hematite, quartz, and epidote. The dominant secondary minerals present at the site include: hydroxy-interlayered vermiculite, hydrobiotite, gibbsite, goethite, and kaolinite (as well as halloysite). The 0.5 to 1.5 m layer of soil overlying saprolite at the site is predominantly red, clay-rich Ultisols, which grade to Inceptisols in the colluvium, recent alluvium, or eroded areas.

3.10.2. Dissolved Solute Sampling and Analysis: Samples for chemical and age-dating analysis were collected during baseflow conditions March 10th-15th, 1996. Groundwater was collected from 19 wells and 1 borehole using a Bennett pump and/or peristaltic pump. Most wells consisted of 51 mm O.D. PVC casing with screen lengths ranging from 0.3 to 1.52 m, with the exception of well 150, which consisted of 101.6 mm OD PVC pipe that extends from the surface to the bedrock, below which is an open borehole to a depth of 19.8 m below the surface. Average depth to bedrock in the riparian aquifer (where well 150 is located) is 3.57 m. This would imply that well 150 has an open interval length of ~16.2 m. Wells are completed in saprolite, except for well 150, which is completed in Panola

Granite. After each well was purged to flush a minimum of 3 well volumes, samples for chemical analysis were collected into 250 ml polyethylene sample vials. Samples for [Si] were passed through a 0.45 μm cellulose acetate filter, and were acidified prior to analysis to $\text{pH} < 2$ using concentrated HNO_3 . Samples were stored at room temperature until analysis via direct-current plasma emission spectroscopy.

3.10.3. Age-dating Method: The age-dating methods employed in this study were CFCs and $^3\text{H}/^3\text{He}$. Samples for CFCs were collected as described above but with copper and nylon fittings to avoid contamination, and were collected by a system that eliminated air-water contact during sampling before being flame-sealed in borosilicate glass ampoules. Five samples were collected and sealed at each well. CFCs were analyzed by purge and trap gas chromatography (Busenberg and Plummer 1992). Samples for tritium were collected in 500 ml bottles, and samples for ^3He were collected under back-pressure in 10 mm O.D. copper tubes with steel pinch-off clamps. Tritium samples were analyzed at the Lamont-Doherty Earth Observatory Noble Gas Laboratory via quantitatively degassed vacuum extraction. Helium was purified and separated by cryogenic cold trap in the inlet system of the dedicated helium isotope mass spectrometer, and then ^4He concentrations and $^3\text{H}/^3\text{He}$ ratios were measured via mass spectrometer.

3.10.4. Data Analysis: Burns et al. (2003) present [Si] data in their Table 1, CFC data in their Table 2 and $^3\text{H}/^3\text{He}$ derived ages in their Table 3. They state that the $^3\text{H}/^3\text{He}$ and

CFC-12 ages in aerobic samples were reliable, whereas the CFC-11 and CFC-113 ages were not due to microbial degradation. Figure 3 in Burns et al. (2003) shows a relationship between groundwater age and [Si] that uses both CFC-12 and $^3\text{H}/^3\text{He}$ determined ages. The text does not contain any explanation as to what points have been included in Figure 3 of Burns et al. (2003), and which have been excluded, if any. The analytical precision for [Si] was $\pm 5\%$. Analytical precision of the ^4He data is $\pm 0.2\text{-}0.5\%$, and the precision of the $^3\text{H}/^3\text{He}$ data is $\pm 0.2\text{-}1\%$. Four air samples were collected during the study, and their atmospheric CFC concentrations were compared to the North American clean air for 1996, and it was found that values matched closely, except for CFC-11 values which were slightly higher than expected, possibly due to contamination by proximity to the Atlanta metropolitan area.

Two wells (150 and 418) contained measurable amounts of terrigenic helium, and although corrected for, the corrections were considered significant for these two samples by Burns et al. (2003). Samples from both wells have CFC age data that have been used in lieu of the suspect $^3\text{H}/^3\text{He}$ ages for my regression. Wells 322, 323, and 324 contained measurable concentrations of CH_4 , indicating microbial degradation, and for these samples it was assumed by Burns et al. (2003) that differences in CFC-determined ages was due to the preferential degradation of CFC-11. It was determined by Burns et al. (2003) that for samples collected from methanogenic environments all three varieties of CFCs experienced some degree of degradation, and thus the ages are biased high. For this reason $^3\text{H}/^3\text{He}$ determined groundwater age is used in my regression instead for these three wells. The age for well 737

was noted by Burns et al. (2003) as being biased high for CFC-12. All other samples in aerobic environments had CFC-12 determined and $^3\text{H}/^3\text{He}$ determined ages that agreed fairly well. Samples from well 737 were observed to have low dissolved O_2 values, and Burns et al. (2003) speculate that some of the CFC-12 concentration may have been lost in localized anaerobic zones (where biodegradation is more prevalent) in the soil or aquifer, or possibly through sorption to soil organic matter. The $^3\text{H}/^3\text{He}$ was used in my regression for 737 instead.

In general, $^3\text{H}/^3\text{He}$ values from Table 3 of Burns et al. (2003) were used for regression analysis instead of CFC groundwater ages, due to CFC determined ages that were biased high. When available, duplicate $^3\text{H}/^3\text{He}$ age data was averaged and used in our regression. When $^3\text{H}/^3\text{He}$ values were not available for a sample site, the most likely CFC-determined apparent age for each sample (presented in boldface for each sample in Table 2 of Burns et al. 2003) was used for the regression. Where there were multiple boldface values (where Burns et al. 2003 presents most likely apparent ages for more than one CFC tracer), an average was taken. The minimum age prediction uncertainty for Figure 3.24 was approximately ± 4.6 yr.

Table 3.14. Groundwater age data and groundwater [Si] for the study by Burns et al. (2003). Datum for well depth is land surface elevation.

Well	Well Depth to Center of Screen (m)	Screened Length (cm)	GW Age (yr)	[Si] (μM)
130	1.4	152	8.7	246.10
150	19.8	No Screen	27.55	633.53
285	3.6	76	2.2	69.84
316	1.6	152	8	176.26
322	1.1	32	-0.1	139.68
323	1.4	30	6	242.77
324	1.7	30	7.2	262.72
418	0.9	61	10.5	347.53
441	3.4	76	1.35	126.37
479	3.4	76	0.7	167.94
640	2.9	152	0.75	131.36
671.261	2.6	30	-0.4	146.33
671.373	3.7	30	0	146.33
690	2.1	No Data	-0.2	111.41
691	4.3	61	1.4	139.68
696	3.4	61	-0.2	104.76
737	1.1	61	-0.6	64.85
760	1.7	152	0.95	73.16
801	3.3	146	-0.1	161.29
821	na	61	0	91.45

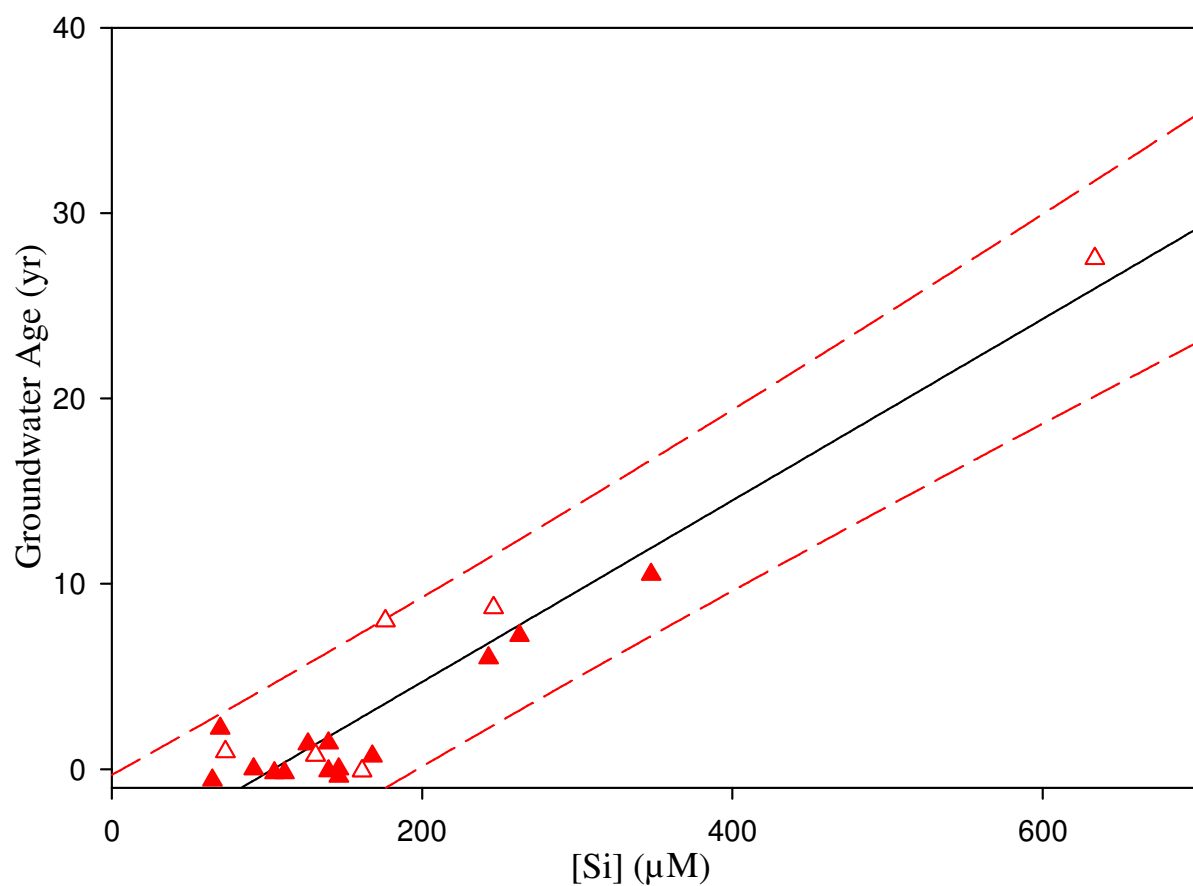


Figure 3.25. Groundwater age vs. groundwater [Si] based on 20 points presented in Burns et al. (2003). Regression analysis yielded a slope of $0.0490 \text{ yr}/\mu\text{M}$, an intercept of -5.0875 yr , an r^2 of 0.8980 , and p-values of <0.0001 for both slope and intercept. Open triangles indicate sample data from wells with screen lengths $\geq 1 \text{ m}$, and filled triangles indicate sample data from wells with screen length $< 1 \text{ m}$. Red dashed lines are 95% prediction intervals.

4. WEST BEAR CREEK STUDY SITE

4.1. Site Location, Land Use, and Previous Research

The study reach is in the West Bear Creek channel (a tributary to Bear Creek) located in Wayne County, North Carolina, 6 km southeast of the town of Goldsboro. West Bear Creek watershed (Figure 4.1-approximate area 61 km²) is situated in the Neuse River Basin, located in the Atlantic Coastal Plain. PVC stakes were driven into the banks every 12.5 m during a previous study (Kennedy et al. 2009a), and the markers indicate distance upstream of the State Road (SR) 1719 bridge over West Bear Creek. Samples for West Bear Creek, NC, 2012 dataset were collected from the meter markers 479 to 537.

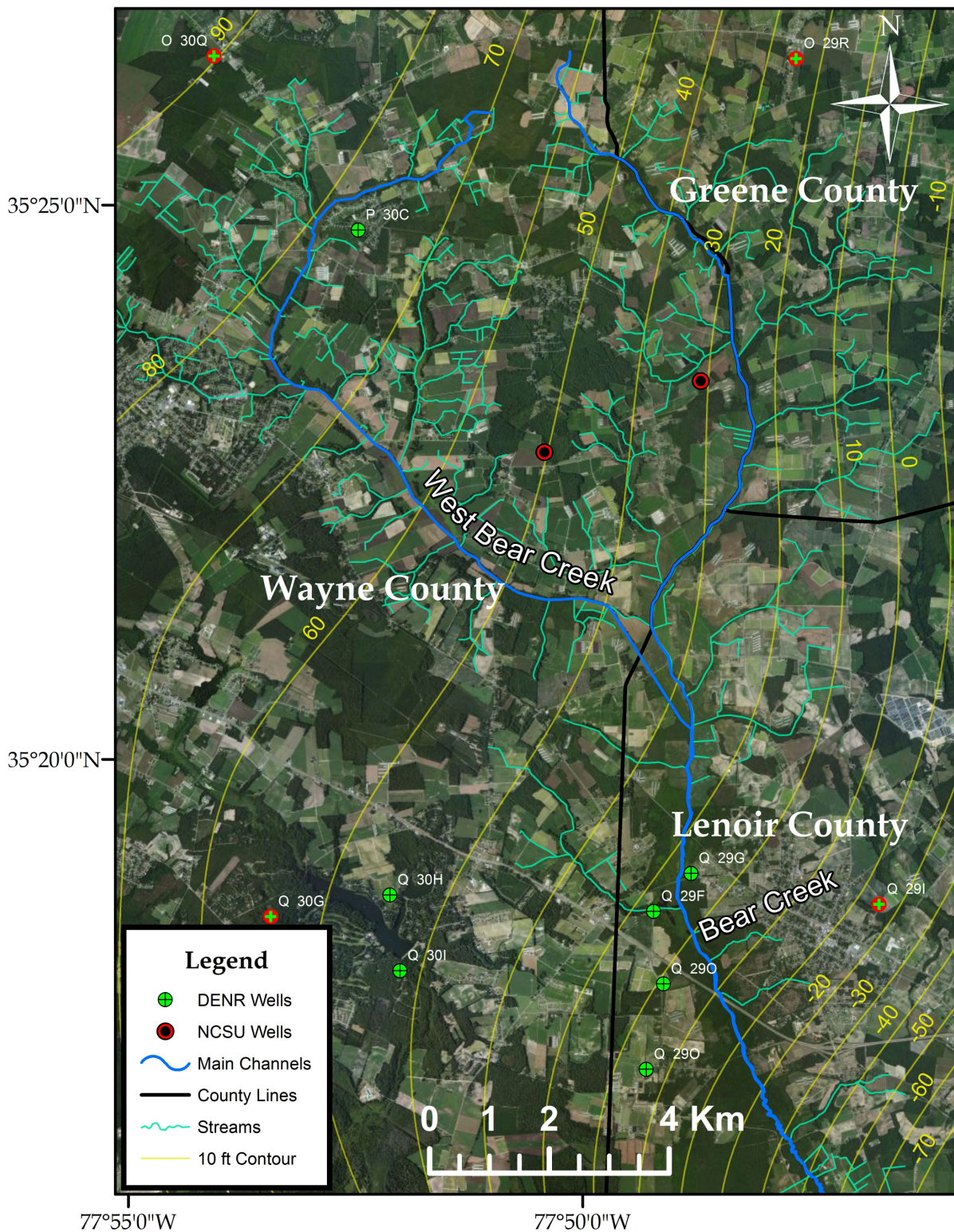
During baseflow conditions the depth of the study channel ranges from 4-103 cm, with an average depth of 35 cm, has a width of approximately 7 m, and a stream discharge ranging from 0.12 to 2.1 m³/s (Kennedy et al. 2009b). The streambed comprises mostly sandy material, except along the banks where silt and clay are prominent, likely due to erosion of the banks which are undercut at the water line and collapse into the stream. The stream is bordered along either side by a wooded riparian buffer that varies in width from 10 m wide along the right bank, to 25 m wide along the left bank (according to measurements made in the field during the study). The channel was dredged and straightened in the 1950s (Kennedy et al. 2009b).

The West Bear Creek watershed is approximately 50% agricultural lands, the rest being residential areas, roads, forest, and open water. For the duration of the study (including reconnaissance and initial visits, a period ranging from February to July of 2012) the main crop grown along the left (west) bank was feed-corn; the crop along the right (east) bank was not determined, but may have been beans. In the past the area has produced cotton, soybeans, cucumbers, wheat, and tobacco (Kennedy et al. 2009a). At one point during the study along the left bank of the channel the corn field had been cleared, and the soil appeared to be covered with a mottled layer of dark material (possibly a post-burn residue), and there were closely-spaced parallel grooves consistent with tilling running the length of the field.

Previous research in this area includes Kennedy et al. (2009a,b) and Kennedy et al. (2007). Kennedy et al. (2009a), from which data was used for the current study (West Bear Creek, NC, 2007), focused on a 75 m reach of the West Bear Creek channel, between the markers 312.5 and 387.5 m. The West Bear Creek, NC, 2007 data was collected over a 2-day period from 21 streambed points: seven 3-point transects with points along the left, right, and center of the channel. Several quantities were measured or calculated at each point: hydraulic head gradient, hydraulic conductivity, seepage rate through the streambed, groundwater age (based on CFCs), extent of denitrification in the groundwater (based on excess N_2), and several other groundwater quality parameters. CFC-12 was used to age date samples from 21 of the 24 points, and CFC-113 was used to obtain age dates from the remaining three samples (two groundwater samples and the streamwater), due to the CFC-12 contamination evident at

these sites. The source of the contamination was indeterminable, but septic tank effluent or illegally dumped refrigerant were considered as possible sources.

Figure 4.1. Map of the area around the West Bear Creek study reach. Map shows location of DENR wells (all wells shown are open boreholes) for which hydrogeologic data is available, new NCSU wells installed just prior to completion of this thesis, water table elevation contours interpolated from DENR groundwater data for 11/01/2012, main channels, and contributing streams. Groundwater contours were interpolated using ArcMap software (spline: tension) from 41 DENR well points distributed throughout Wayne, Green, and Lenoir county. General groundwater flow trends southeast, as can be seen from the 10 foot contour lines shown in yellow. Justification for interpolation method used was based on suggestions from GIS literature (this method typically used for water table modeling) and from comparison with regional topography (interpolated surface and contour intervals indicated groundwater flow eastwards towards the coast, and into streams and low-lying areas). Base map provided by Bing Maps Aerial via ArcMap and county boundary and hydrology data provided by NC Center for Geographic Information & Analysis (2006). All well data presented in the figure and used for spatial interpolation was provided by the NC DENR website.



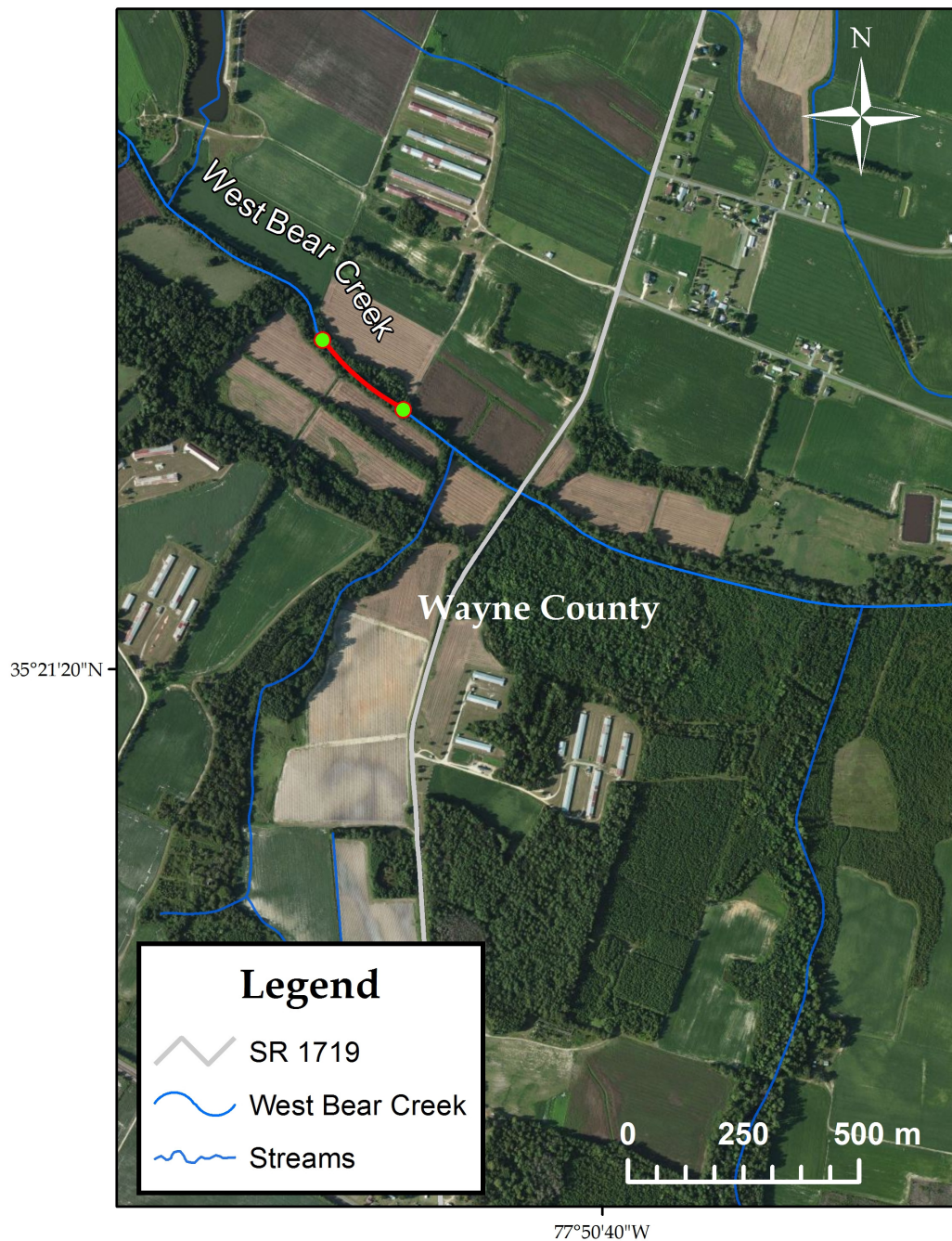


Figure 4.2. Location of West Bear Creek study reach. Red line and green markers show the approximate extent of the reach for both April 2007 sampling (312.5 m - 387.5 m west of SR 1719) and July 2012 sampling (479 m - 537 m west of SR 1719). Base map provided by Bing Maps Aerial via ArcMap and county boundary and hydrology data provided by NC Center for Geographic Information & Analysis (2006).

4.2. Hydrogeology

The geology of the North Carolina Coastal Plain is mostly Pliocene to Quaternary in age and made up of units that were deposited during marine transgression-regression cycles, creating a series of low-relief paleoshorelines and intervening terraces that get progressively younger and step down in elevation as they approach the coastline and into drainage areas (Farrell 2007). Coastal plain deposits have variable mineralogy that include: siliciclastic grains comprised of quartz, feldspar, fragments of igneous, metamorphic, and sedimentary rocks, bioclastic grains (such as carbonate grains or allochems), glauconite, phosphate, and organic debris (Farrell 2007).

The surficial aquifer is laterally continuous throughout the North Carolina coastal plain in that it does not pinch out to the west as underlying aquifers do. It is unconfined, and is also referred to as the water table aquifer. It is primarily made up of Quaternary age sediments, but can also include parts of older formations depending on the age of underlying sediments and the stratigraphic position of the uppermost confining unit (Lautier 2001). Water is recharged into the surficial aquifer as precipitation (and in some areas to a far lesser extent as irrigation) in the interstream areas. Factors such as precipitation rate, soil type and infiltration capacity, water table position relative to land surface, slope of the land surface, and evapotranspiration rate control the rate of recharge for this aquifer (Lautier 2001). The majority of water that enters the surficial aquifer flows laterally from recharge to discharge areas. Less than two inches per year of water flows vertically downward to recharge shallow

confined aquifers, and less than 0.5 inches per year to deeper aquifers (Lautier 2001). It is assumed that most of the recharge to the Cretaceous aged aquifers occurs predominantly in the western portion of the coastal plain deposits where they are close to the surface and covered only by the surficial aquifer (Lautier 2001).

The surficial aquifer is made up of sediments of Holocene and Pleistocene age (Lautier 2001). In the inner coastal plain (Gellici and Lautier 2010), the surficial aquifer consists of sand, sandy clay, clay, and some scattered gravel units. The infiltration capacity of the surficial aquifer can be relatively high, with vertical saturated permeabilities ranging from 0.2 to 20 inches per hour (Tant et al. 1974), and recharge rates range from 4-20 inches per year (Heath 1994, 1997). The thickness of the surficial aquifer varies from 4 to 224 ft (1-60m), with the maximum thickness occurring in Craven, Carteret, and Onslow Counties (Lautier 2001). On a regional basis, the lithology of the inner Coastal Plain surficial aquifer is generally composed of coarse and poorly-sorted sand, sandy-clay, and some scattered gravel units, characteristic of shallow fluvial sediments (Gellici and Lautier 2010).

The Black Creek formation in the study area includes the Black Creek Confining unit (the top of which defines the bottom of the surficial aquifer) and the Black Creek aquifer. Regionally, the Black Creek Confining Unit is defined as a thick layer of clay and silt with variable amounts of sand. Aquifer tests conducted in the coastal plain have indicated that there is little to no leakage across this unit. Most of the recharge into the Black Creek aquifer

occurs through the surficial aquifer where confining units are absent (Lautier 2001). The Black Creek aquifer is described regionally as Upper Cretaceous-aged deposits (although it can include permeable beds that are from younger or older formations) that dip gradually to the southeast (Lautier 2001). The lithology of the aquifer is described as alternating beds of gray (and sometimes calcareous) glauconitic sand and black to grayish clay. Permeable sediments in the aquifer are well-connected and sand bodies within the aquifer are often interbedded with numerous thin clay layers. The Black Creek Aquifer has a transmissivity that varies between 290 to 1,700 ft²/day (Lautier 2002, 2006), and the hydraulic conductivity varies from 2 to 7.35 ft/day, according to well tests done in the area (Lautier 2001). The Black Creek Aquifer is heavily used for public, industrial, and agricultural supplies in the North Carolina Central Coastal Plain (Gellici and Lautier 2010).

The Upper Cape Fear Confining Unit consists of beds of clay and silt, with variable amounts of sand in the upper portion of the unit. In areas where the unit is directly overlain by Quaternary age sediments (such as at the West Bear Creek site, well O 30Q), clays and silts in the lower part of the Quaternary unit are considered part of the confining unit. The thickness of the confining unit is typically 50 to 100 feet. The Upper Cape Fear Aquifer is primarily of Cretaceous age, and in some cases can include the Middendorf formation and sands layers near the bottom of the Black Creek Formation. Sediments of the Cape Fear Formation are considered to be nonmarine, and were likely deposited in a fluvial-deltaic environment (Gellici and Lautier 2010). Transmissivities for the aquifer have been reported

to range from 25 to 440 ft²/day, according to aquifer tests (Lautier 2002), and the thickness of the aquifer can range from 10 to 665 ft. The lithology of the Upper Cape Fear aquifer is described as consisting of alternating layers of clay and fine to course-grained, poorly sorted, gray to red sand. Gravel beds, conglomerates, iron-oxides such as siderite, marcasite, and pyrite are present in the unit. Sediments of this formation are nonmarine in origin, and are interpreted as having been deposited in a fluvial-deltaic environment (Gellici and Lautier 2010).

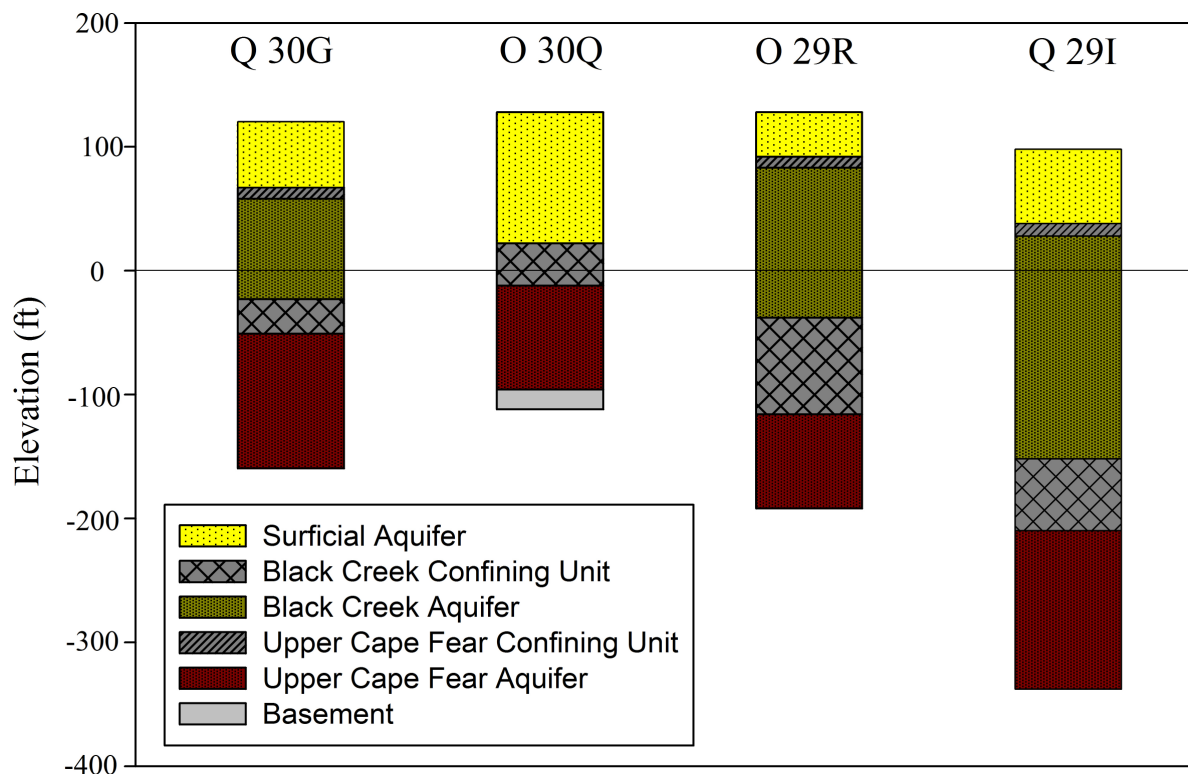


Figure 4.3. Stratigraphy of the four boreholes shown in Figure 4.1 (red circles with green crosses), based on hydrogeologic data available from the NC DENR website (<http://www.ncwater.org/>). Elevation datum is sea level (NGVD 29).

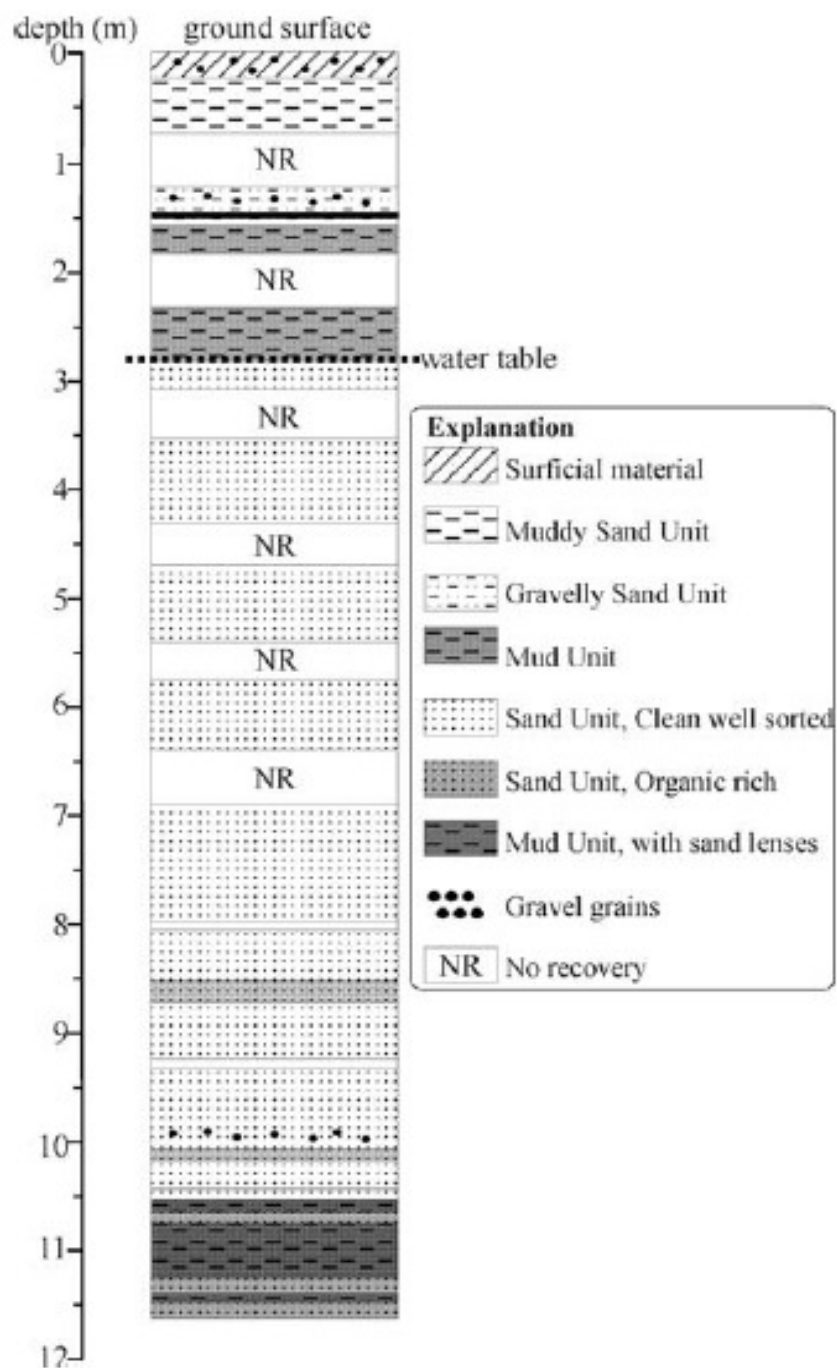


Figure 4.4. Stratigraphic column constructed from geoprobe core, collected from the grassy road on the left (north) side of West Bear Creek at the 350m marker, i.e., 350 m upstream of State Road 1719 (Kennedy et al. 2009b).

The stratigraphy immediately adjacent to West Bear Creek (the study reach for data set 1) was described in Kennedy et al. (2009b), interpreted from a core that was obtained during the study (Figure 4.4). From the geoprobe core, surficial sediments consisted of sand and gravel with interbedded layers of mud and organic matter. These sediments were underlain by 7.8 meters of permeable sand layers interpreted to be the surficial aquifer that feeds into West Bear Creek. Below the surficial aquifer (which extended to a depth of 10.6 m at that point) was a mud unit interpreted to be the top of the Black Creek Confining Unit (Kennedy et al. 2009b). The streambed material was also sieved during this study, presumably to provide insight on the permeability of the top 35 cm. The results indicated streambed material that was 94% sand by mass, with a range in grain-size of 0.05-2.0mm. Most of the sand could be classified as medium to coarse-grained. There were also small amounts of clay, silt, gravel, and organic matter. Kennedy et al. (2009b) used USDA soils data to estimate that soils in the West Bear Creek watershed were 81% Ultisols and 13% Inceptisols.

5. METHODS

5.1. Sample Collection Methods, West Bear Creek, April 2007 and July 2012 Sampling

5.1.1. Sample Collection Strategy: In April 2007, a total of 23 groundwater samples were collected for the West Bear Creek (2007/2012) dataset from a 75 m reach upstream of the North Beston Road (also known as NC State Road 1719) bridge over West Bear Creek. The study reach was situated between the meter markers 312.5 and 387.5, markers placed there by Kennedy et al. (2009a). Twenty one samples of groundwater from beneath the streambed were collected over a 2-day period from seven 3-point transects across the stream, spaced 12.5 m apart. The 3 sampling points on each transect spanned a width of about 5 m across the stream, somewhat less than the full channel width at waterline of about 7 m (Kennedy et al. 2009b). Samples were collected to represent groundwater of different ages and groundwater recharged on different sides of the watershed (both north and south of West Bear Creek). In addition, groundwater samples were collected from two shallow wells along the banks of the channel, situated at 325 m and 401 m.

In July 2012, a total of 39 samples were collected for the West Bear Creek (July 2012) dataset from a 58 m reach upstream of the reach for the West Bear Creek (2007/2012) dataset. The study reach was situated between the meter markers 479 and 537. Samples were collected over a 3-day period from eight 5-point transects (one transect contained a point where water could not be produced) spaced approximately 6-7 m apart along the channel.

However, results are presented here for only 10 of the 39 (data analysis for the others was still underway at the time of completion of this thesis).

5.1.2. [Si] Sample Field Collection Method: For the April 2007 dataset water samples for the analysis of [Si] were collected from between 35-40 cm beneath the streambed using the stainless steel piezomanometer with copper sampling line and a 5 cm screened interval, as described in Kennedy et al. (2009a). As noted by Kennedy et al. (2009b), water collected at this depth was predominately discharging groundwater with little to no stream water mixed in by hyporheic flow. Samples for [Si] analysis were pulled from the piezomanometer with a 60 ml plastic syringe, filtered in the field to 0.7- μm (nominal-used to remove solid particles, while still allowing water to be pulled through uninhibited) with pre-combusted Whatman GF/F filters and GF/D filters in series, and collected in 20-mL high density polyethylene (HDPE) liquid scintillation vials (Kennedy et al. (2009a, b). Each sampling point was purged of 370 to 700 ml before sample collection in order to achieve stability in pH, temperature, and specific conductance. Sampling and collection methods are described in Kennedy et al. (2009a, b).

Groundwater samples for the July 2012 dataset were collected similarly to those for April 2007, using a similar steel and copper piezomanometer for 2 of the 8 transects (487 m and 522 m) and a PVC piezomanometer for the other 6 transects. Groundwater samples were extracted from between 31-36 cm beneath the streambed using a 60 ml plastic syringe which

was used to purge each sampling site between 400 to 600 ml, and to collect the samples.

Samples were pushed through a 0.45 micron Millipore MCE membrane filter attached to the syringe.

Samples were not acidified, as Si can precipitate in acidic solutions, nor frozen, which can lower [Si] by 20 to 40% (Standard Methods for the Examination of Water & Wastewater, 2012, p. 4-165 & 4-166). Samples were stored in a cooler in the field until their transport to a refrigerator (temperature held between ~4-6°C) 2-14 hours later. Recommended storage temperature for Si samples is 4°C (Standard Methods for the Examination of Water & Wastewater, 2012, p. 4-165 & 4-166).

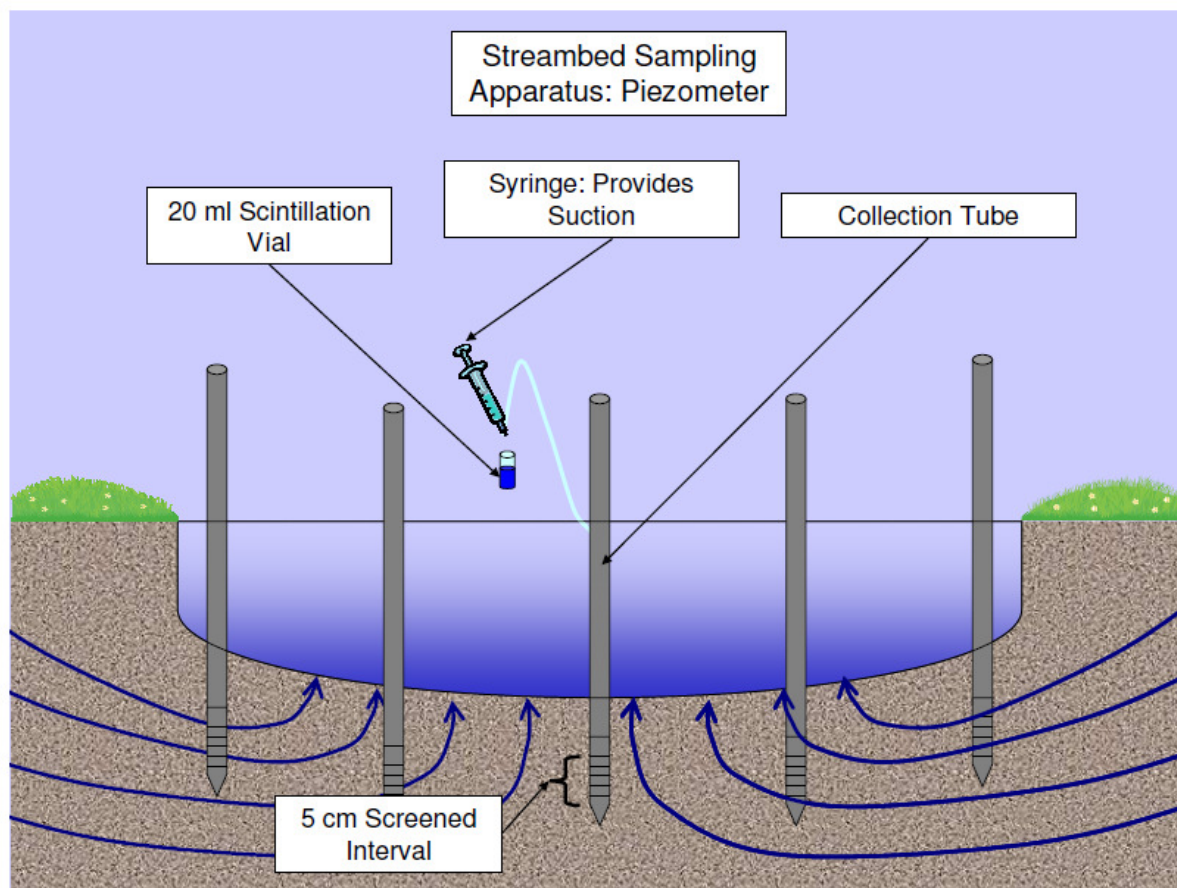


Figure 5.1. Simplified sketch (not to scale) of collection of streambed groundwater with a piezomanometer, for analysis of [Si] for a 5-point transect (West Bear Creek July 2012 dataset). Collection of other samples for age-dating tracers required additional equipment and sample containers (see text).

5.1.3. CFC and SF₆ Field Collection Method: For the West Bear Creek (2007/2012) dataset the age-dating method employed for all sample points was CFCs. Samples for CFC analysis for datasets 1 and 2 were collected in 125 ml glass bottles following the procedure outlined by the USGS Reston CFC laboratory (<http://water.usgs.gov/lab/chlorofluorocarbons>). Details are given in Kennedy et al. (2009a).

For the West Bear Creek (July 2012) dataset samples were collected for CFC and SF₆ analysis to determine groundwater age (Cook & Solomon 1997) for a subset of the sample points (the two transects at 487 m and 522 m). The collection method for CFCs followed the sampling procedure outlined by Kennedy et al. (2009a). For each sampling point, four sampling bottles were used to collect samples for CFC analysis. Groundwater was collected using a battery-powered peristaltic pump with a short section of Viton tubing in the pump head. The Viton (a flexible tubing that reduces the likelihood of contamination, Cook et al. 2006) was attached to the copper sampling line of the steel piezomanometer, and another short piece of copper tubing at the outlet of the pump was inserted into the bottles during sampling.

For each sample point the start time was written on each of the four sample bottles for CFC samples and the 1 L bottle used for the SF₆ sample. Flow from the pump was adjusted to be as high as possible without producing bubbles from the outlet, and was typically 50-100 ml/min. The “overflow” method of sample collection (Kennedy et al. 2009a) was used for all CFC and SF₆ samples. The collection procedure for SF₆ was very similar to the method described above, except the purge volume was larger, and the sample bottle (1 L amber coated glass container) was larger. The samples for SF₆ and CFCs were stored at room temperature or below until being driven to the USGS CFC Laboratory in Reston, VA (<http://water.usgs.gov/lab/chlorofluorocarbons/lab>).

5.2. Lab Methods and Analysis

5.2.1. [Si] Analysis of April 2007 Samples: [Si] analyses on April 2007 samples were completed at the Korea Institute of Geoscience and Mineral Resources by Dong-Chan Koh in 2012. The instrument used was a PerkinElmer ICP-OES 7300 DV. Si standards were prepared with a stock standard of 1000 ppm as Si in 2% HNO₃, and working standards of 20 ppm, 2 ppm, 0.2 ppm as Si were used. Construction of calibration curves included linear curve fitting with 4 points including 3 working standards and 1 blank, and the r^2 was > 0.999 , and the signal acquisition had an average of three readings per run. Typical precision as a coefficient of variation was $< 2 \%$ (email correspondence with Koh, November, 2012).

5.2.2. [Si] Analysis of July 2012 Samples: Groundwater samples and [Si] standards for the July 2012 dataset were analyzed at the Center for Applied Aquatic Ecology using the Flow Injection Analysis procedure for Molybdate-Reactive Silicate, referred to as method 4500-SiO₂F by Standard Methods for the Examination of Water and Wastewater (2012).

Standards of 4 different Si concentrations (5 mg SiO₂/L, 10 mg SiO₂/L, 15 mg SiO₂/L, and 20 mg SiO₂/L) were made and sent to the lab as a quality control check. These values would then be compared to “true” values calculated by me using the concentrations I measured out in the lab (Table 5.1). Several grams of Na₂SiF₆ salt were placed in an aluminum foil container and baked at 60-70°C for 16-20 hours. The oven was turned off and the samples were allowed to cool. All beakers and materials used were washed with soap and

warm water, rinsed three times using Deionized (DI) water, and allowed to air dry. Two 300 ml glass beakers were used to bring ~600 ml of DI water to ambient room temperature, i.e. ~20°C. A 40 ml glass beaker was used to weigh out 0.6716 g of dried Na₂SiF₆ on a covered analytical balance. The contents of the beaker were transferred to a 500 ml volumetric flask using DI water. Room temperature at the time was 20.9°C, and the temperature of the DI water was 21.0°C. The beaker was rinsed 20-25 times with DI water, each time pouring the rinse into the flask. The mouth of the flask was closed using Parafilm, and the flask was inverted 3 times. The flask was left to settle for 10-15 minutes. After this period the flask was visually checked for any Na₂SiF₆ that had not completely dissolved. The flask was then filled to the 500 ml mark (still using the same 40 ml beaker, to insure complete transference of Si salt) and allowed to stand for several minutes. A clean 500 ml HDPE bottle was rinsed 3 times (including the cap) with the Si stock solution (200 mg Si/L) from the volumetric flask. The remainder of the solution (~460 ml) was transferred to the 500 ml HDPE bottle. Total contact time of any water used in this process with glassware was not greater than ~3 hours, and so Si contamination from glassware is unlikely. The four standards mentioned above were then prepared by dilutions of the stock solution with DI water. The standards were assigned fictional stream transect IDs and submitted as samples (to insure a blind test) to The Center for Applied Aquatic Ecology (CAAE) at NCSU for analysis. Figure 5.2 shows the relationship between the calculated concentrations of the standards (True [Si]), and the concentrations determined by CAAE.

Table 5.1. Values for lab determined and calculated (true) [Si] for the four standards discussed in the text.

Sample ID	Lab [Si] (μM)	Lab [Si] (μM)	True [Si] (μM)
	12/14/2012	2/1/2013	
WBC543LP	40.03	37.98	38.46
WBC543CP	78.05	77.29	77.38
WBC543RP	117.39	115.17	116.51
WBC543RBP	156.71	154.07	154.64

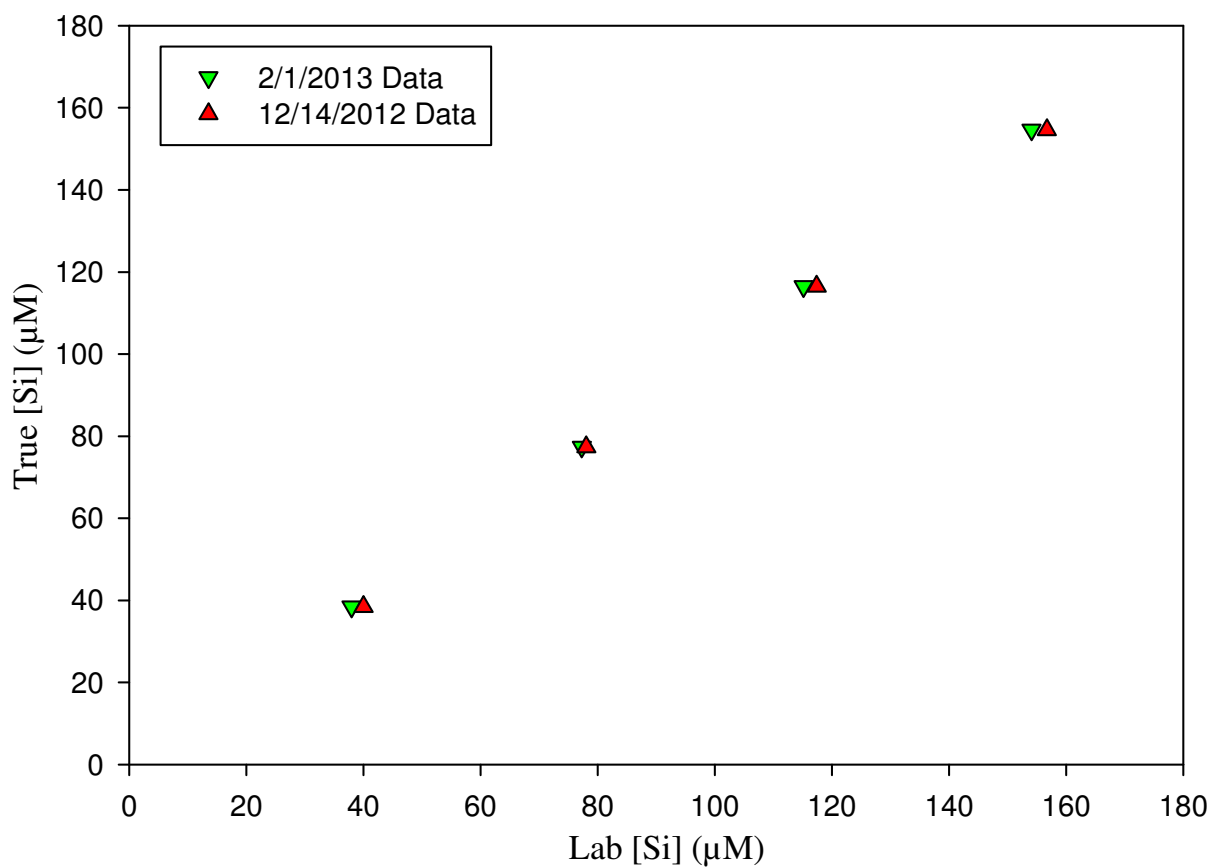


Figure 5.2. Calculated true values of [Si] vs. lab-determined values of [Si] from 12/14/2012 (regular triangles) and 2/1/2013 (inverted triangles). Regression analysis of values from 12/14/2012 yielded an r^2 of 0.9999, a slope of 0.9954, and a p value of <0.0001 . Regression analysis of values from 2/1/2013 yielded an r^2 of 0.9999, a slope of 1.0038, and a p value of <0.0001 .

5.2.3. Lab Analysis of CFCs and SF₆: The samples for CFC analysis for both West Bear Creek datasets were analyzed at the USGS Reston Chlorofluorocarbon Laboratory in Reston, VA, following the procedure described in Kennedy et al. (2009b). Samples for CFC analysis were analyzed using the method and equipment outlined by the International Atomic Energy Agency (Busenberg and Plummer 2006). The method for analysis of SF₆ was very similar to that of CFCs (Busenberg and Plummer 2006).

6. WEST BEAR CREEK RESULTS

6.1. West Bear Creek, April 2007 Samples

6.1.1. Study Site: This study involved sampling groundwater beneath a portion of the West Bear Creek channel, which is part of the Neuse River basin in the highly agricultural coastal plain of North Carolina. The study reach was 75 m long, with an average width of approximately 7 m. Study site description and methods are in chapters 4 and 5 respectively.

6.1.2. Data Analysis: CFC-determined apparent ages presented in the study are the result of averaging the ages from all replicate samples collected at each site. The estimated recharge temperature for the samples ranged between 16.5 and 19.4°C (as evidenced by disparate [Ar] values), and the recharge elevation was 31 m. Historic atmospheric concentrations were assumed to be equal to the measured and reconstructed values for Niwot Ridge, Colorado, prior to 1970 (Elkins 1989; Plummer et al. 2006). Variation between replicate CFC samples was 0 to 23%, with an average of 4%.

Most of the samples collected for analysis were relatively unaffected by degradation or sorption in the aquifer. Five sampling points, however, showed differences of >3 years between some of the replicates: 325L, 325R, 337L, 362.5L, and 362.5R. For site 325R, mixing of groundwaters of different ages (perhaps as a result of extracting approximately 5 L from the streambed sampling point) may have contributed to the differences in ages for the 3 replicates, the third sample taken providing an age that was approximately two times older

than the first two. The third sample was excluded from the average. Three of the 24 sampling points had CFC-12 contamination, and their recharge dates were based on CFC-113 concentration instead: 387.5L, 325RW, and SW. CFC-12 was used to age date samples from the other 21 sampling points. The source of the CFC-12 contamination was indeterminable, but septic tank effluent or illegally dumped refrigerant were considered as possible sources. The groundwater age-[Si] data in Table 6.1 are plotted in Figure 6.1.

Table 6.1. West Bear Creek data set showing groundwater age data collected by Kennedy et al. (2009a) in 2007, and [Si] values determined by Koh at KIGAM in 2012. Groundwater samples were collected through the screened interval from a depth of 35-40 cm below the streambed.

Site ID	Screen Length (cm)	Recharge Date	GW Age (yrs)	[Si] (μM)
312.5L	5	1983	24	175.1
312.5C	5	1974	34	176.9
312.5R	5	1968	39	202.0
325L	5	1966	41	218.6
325C	5	1963	44	249.7
325R	5	1987	20	188.3
337.5L	5	1976	32	177.4
337.5C	5	1970	37	215.2
337.5R	5	1976	32	194.7
350L	5	1988	19	97.2
350C	5	1962	45	190.7
350R	5	1982	26	173.2
362.5L	5	1983	25	161.7
362.5C	5	1963	45	241.6
362.5R	5	1977	30	204.5
375L	5	1986	21	68.0
375C	5	1976	32	206.7
375R	5	1994	13	260.1
387.5L	5	1991	16	149.8
387.5C	5	1987	20	185.2
387.5R	5	1947	60	301.7
325LW	5	1990	17	150.9
325RW	5	1980	28	187.2

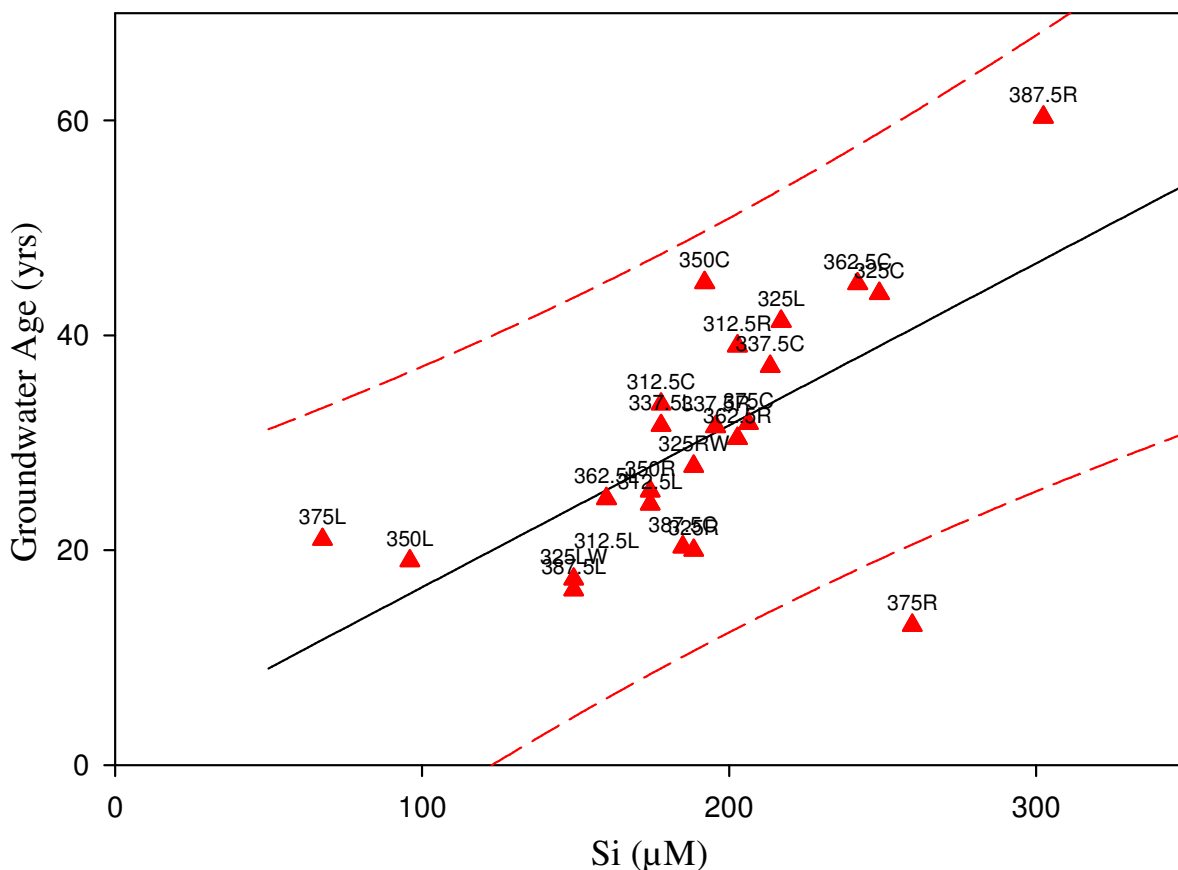


Figure 6.1. Groundwater age vs. [Si] based on 23 samples collected in 2007 from beneath the streambed of West Bear Creek (CFC ages from Kennedy et al. (2009a), and [Si] analysis done in 2012 as discussed in Chapter 5). Regression analysis yielded a slope of 0.1470 yr/ μM , an intercept of 2.4717 yr, an r^2 of 0.3987, and p-values of 0.0012 and 0.7523 for the slope and intercept, respectively.

6.2. West Bear Creek, July 2012 Samples

CFC-11 and CFC-113 determined groundwater ages have been included in my report (Fig. 6.3 and 6.4), but samples collected from West Bear Creek in July 2012 showed evidence of local contamination with respect to CFC-12 (the source(s) of which have not been determined). For this reason CFC-12 determined groundwater ages have not been included in my report. In the near future $^3\text{H}/^3\text{He}$ groundwater ages will be available to allow

regression of age vs. [Si] on a total of 39 data points, but as of the time of completion of this thesis those analyses were not complete at the University of Utah.

Regressions of age vs. [Si] for SF₆, CFC-11, and CFC-113 show slopes ranging from 0.073 to 0.21 yr/ μ M (Figs. 6.2-6.4). I explored different approaches to combining these July 2012 data with each other and with the April 2007 West Bear Creek data, to settle on one final regression for West Bear Creek groundwater. Figure 6.5 shows all July 2012 data from West Bear Creek combined in a single regression. Figure 6.6 shows all July 2012 data from West Bear Creek combined with the April 2007 data from West Bear Creek. CFC-113 age data vs. [Si] data from West Bear Creek (July 2012) produced the regression with the highest r^2 value (0.7474), and to avoid any concerns over “double counting” any of the July 2012 sampling, it seems best to simply use the July 2012 CFC-113 data (Table 6.3) together with the April 2007 data to create a final preferred version of age vs. [Si] for West Bear Creek (Fig. 6.7). This regression was used for the additional West Bear Creek analysis presented in Chapter 7.

Table 6.2. West Bear Creek data set showing SF₆ determined groundwater age and [Si] data collected in July 2012. Groundwater samples were collected through the screened interval from a depth of 31-36 cm below the streambed.

Site Name	Screen Interval (cm)	GW Age (yrs)	[Si] (μM)
WBC487RBP	5	20.54	227.84
WBC487RP	5	26.04	152.42
WBC487CP	5	32.04	207.17
WBC487LP	5	30.04	167.68
WBC487LBP	5	10.04	187.02
WBC522RBP	5	30.55	170.61
WBC522RP	5	38.05	304.10
WBC522CP	5	32.05	184.10
WBC522LP	5	28.05	167.96
WBC522LBP	5	18.05	134.10

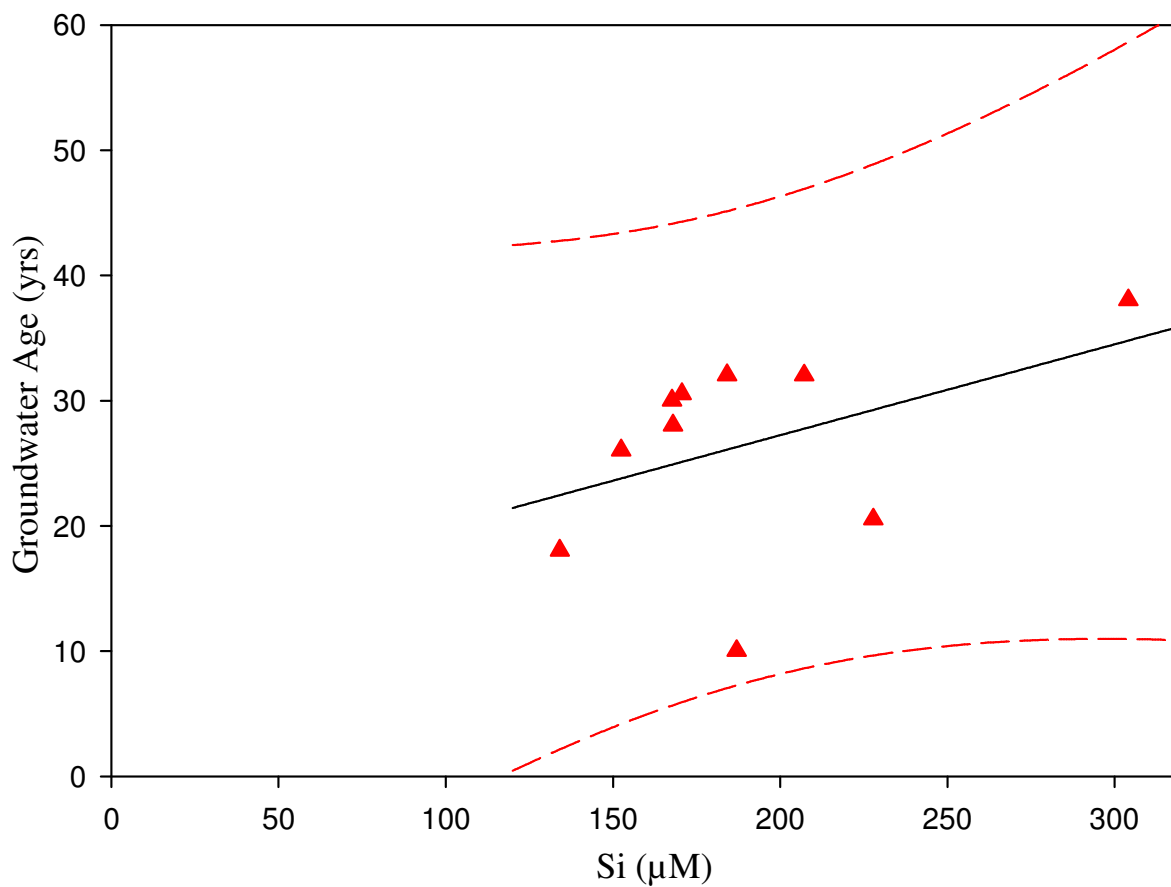


Figure 6.2. SF₆ determined groundwater age vs. [Si] based on 10 samples collected in July of 2012 from beneath the streambed of West Bear Creek. Regression analysis yielded a slope of 0.0726 yr/µM, an intercept of 12.7329 yr, an r² of 0.1804, and p-values of 0.2212 and 0.2683 for the slope and intercept, respectively.

Table 6.3. West Bear Creek data set showing CFC-11 and CFC-113 determined groundwater age and [Si] data collected in July 2012. Groundwater samples were collected through the screened interval from a depth of 31-36 cm below the streambed.

Site Name	Screen Interval (cm)	GW Age [CFC-11] (yrs)	GW Age [CFC-113] (yrs)	[Si] (μM)
WBC487RBP	5	34.04	25.54	227.84
WBC487RP	5	33.71	25.21	152.42
WBC487CP	5	51.04	39.54	207.17
WBC487LP	5	28.88	25.54	167.68
WBC487LBP	5	24.54	23.04	187.02
WBC522RBP	5	43.05	30.21	170.61
WBC522RP	5	55.55	59.55	304.10
WBC522CP	5	44.05	32.21	184.10
WBC522LP	5	39.80	29.30	167.96
WBC522LBP	5	22.05	17.38	134.10

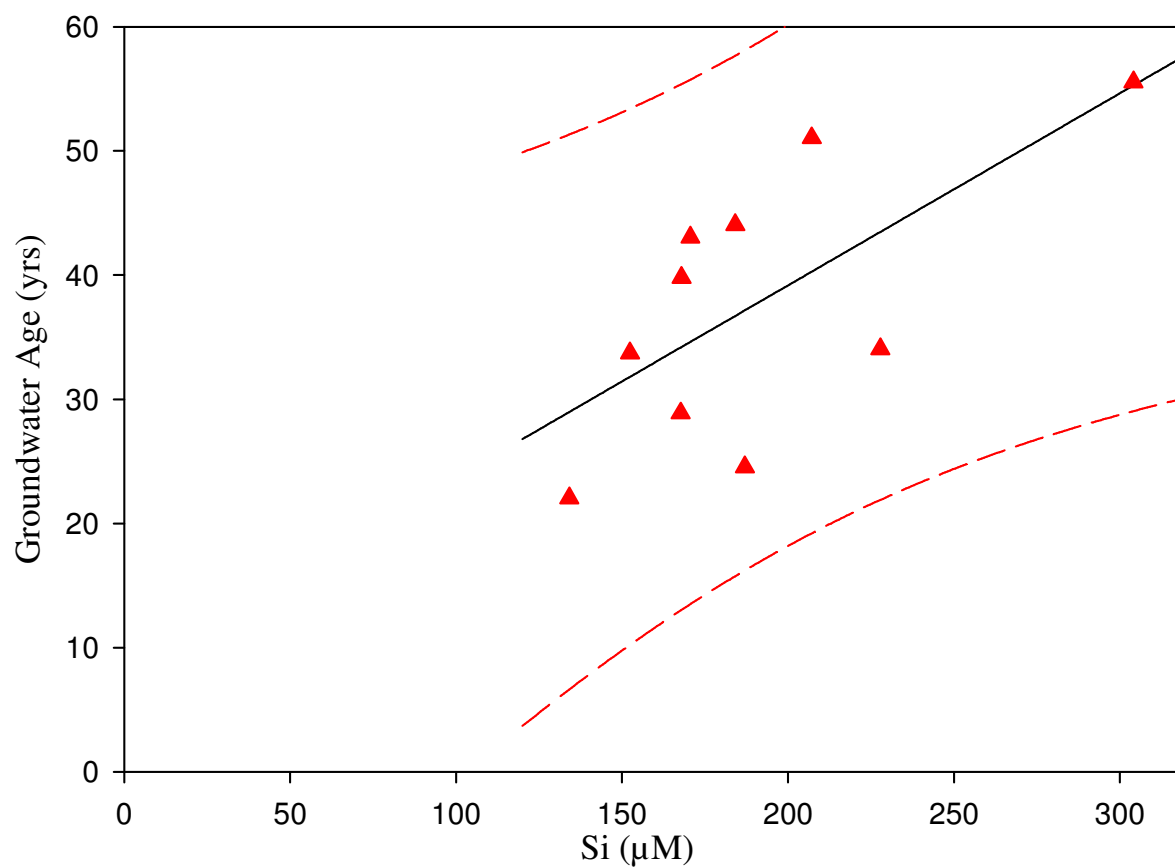


Figure 6.3. CFC-11 determined groundwater age vs. [Si] based on 10 samples collected in July of 2012 from beneath the streambed of West Bear Creek. Regression analysis yielded a slope of $0.1547 \text{ yr}/\mu\text{M}$, an intercept of 8.2230 yr , an r^2 of 0.4523 , and p-values of 0.0331 and 0.5049 for the slope and intercept, respectively. Red dashed lines are 95% prediction intervals.

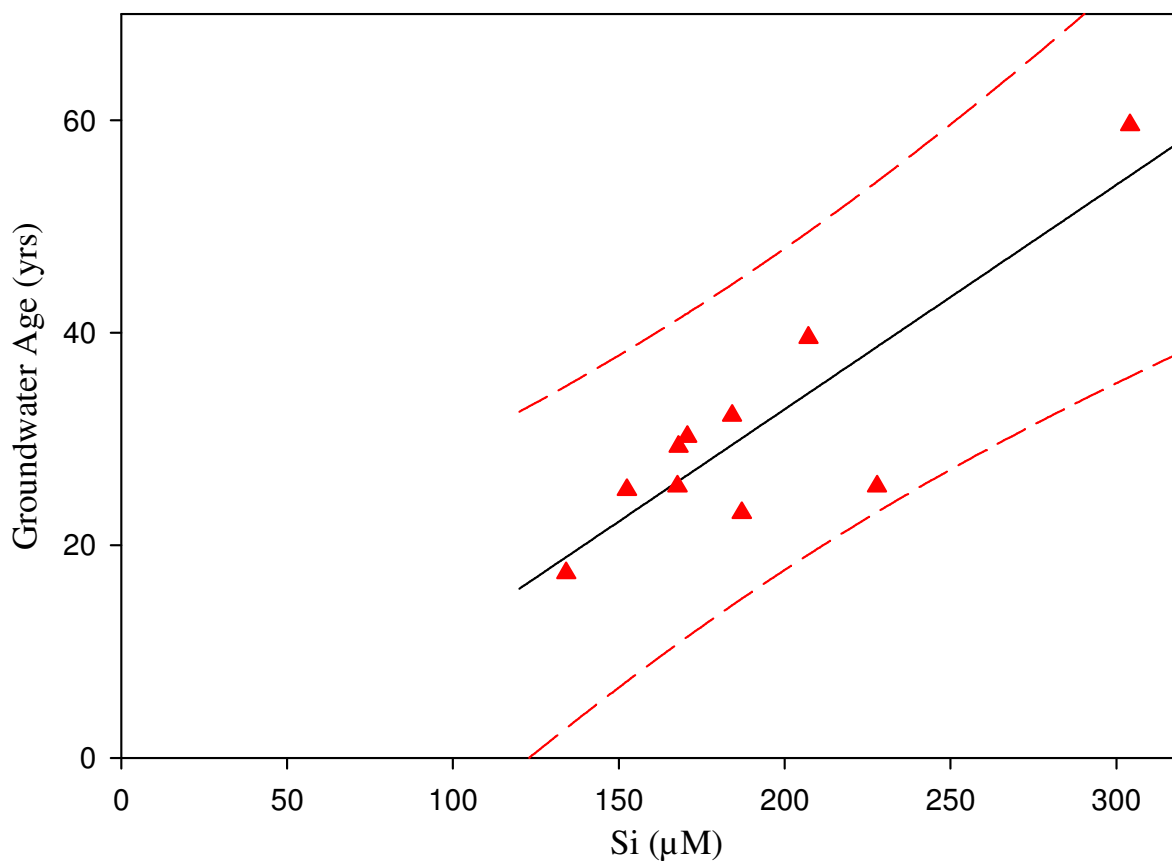


Figure 6.4. CFC-113 determined groundwater age vs. [Si] based on 10 samples collected in July of 2012 from beneath the streambed of West Bear Creek. Regression analysis yielded a slope of $0.2112 \text{ yr}/\mu\text{M}$, an intercept of -9.4324 yr , an r^2 of 0.7474 , and p-values of 0.0012 and 0.2989 for the slope and intercept, respectively. Red dashed lines are 95% prediction intervals.

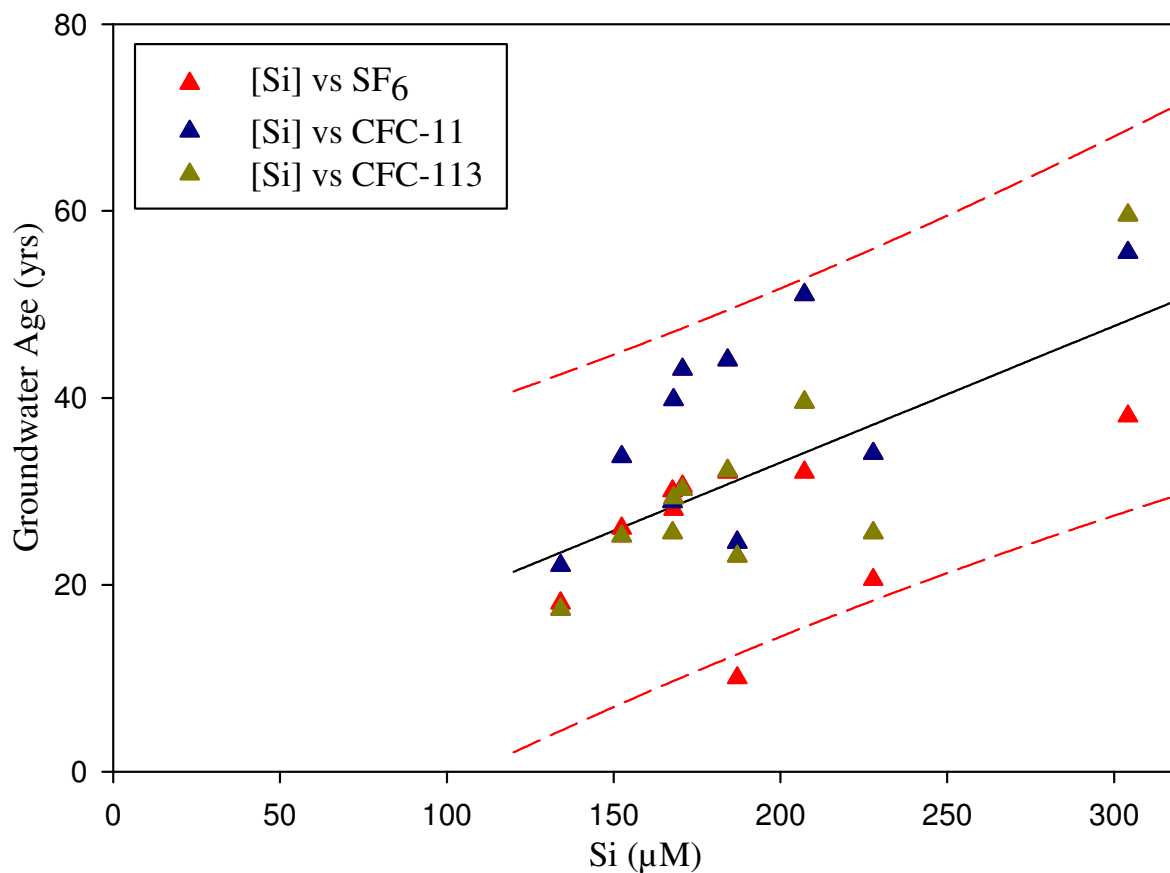


Figure 6.5. CFC-11, CFC-113, and SF₆ determined groundwater age vs. [Si] for samples collected from 10 points in July of 2012 from beneath the West Bear Creek streambed (same ten sampling points for all three age tracers). Regression analysis yielded a slope of 0.1462 yr/µM, an intercept of 3.8412 yr, an r^2 of 0.3720, and p-values of 0.0003 and 0.5887 for the slope and intercept, respectively.

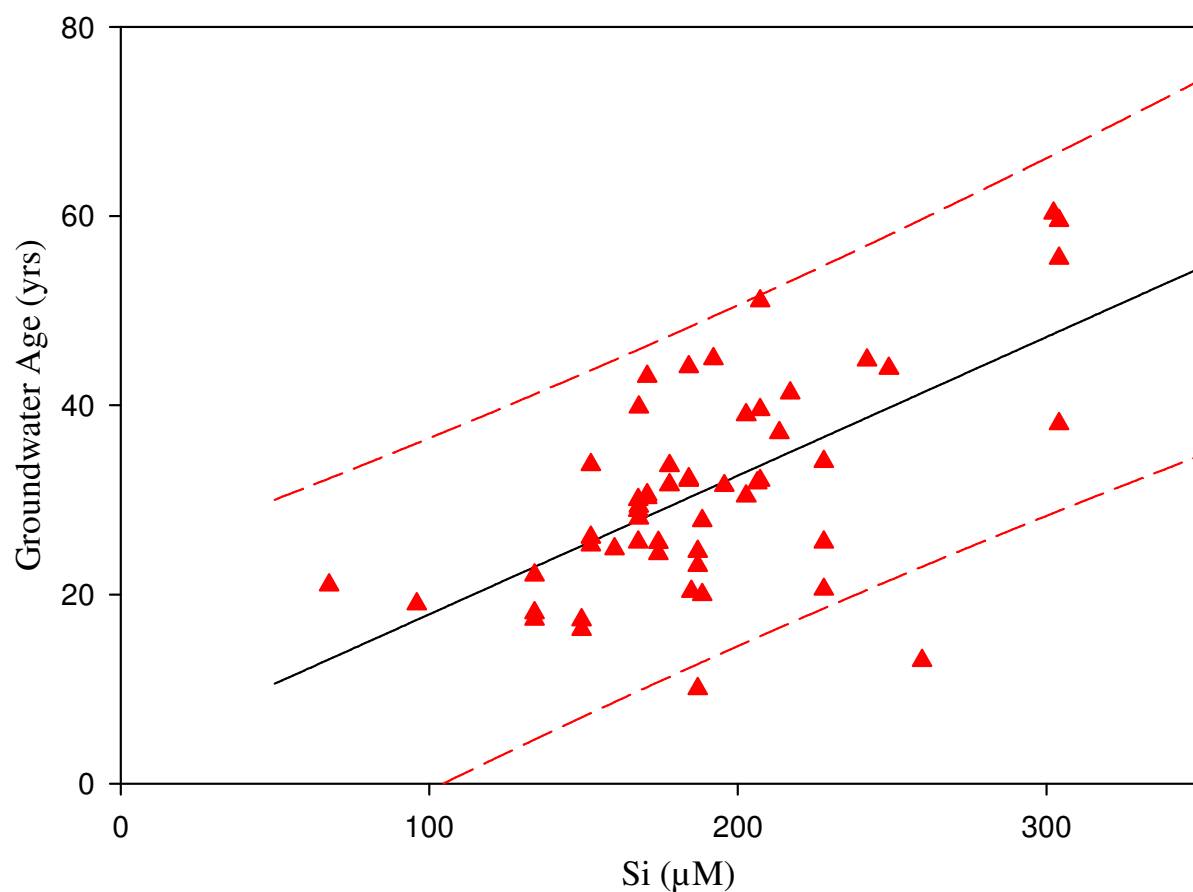


Figure 6.6. Groundwater age vs. [Si] for West Bear Creek based on 23 samples collected in April 2007 combined with all July 2012 data (CFC-11, CFC-113, and SF₆) from Figure 6.5. Regression analysis yielded a slope of 0.1466 yr/µM, an intercept of 3.2352 yr, an r² of 0.3830 and p-values of <0.0001 and 0.5289 for the slope and intercept, respectively.

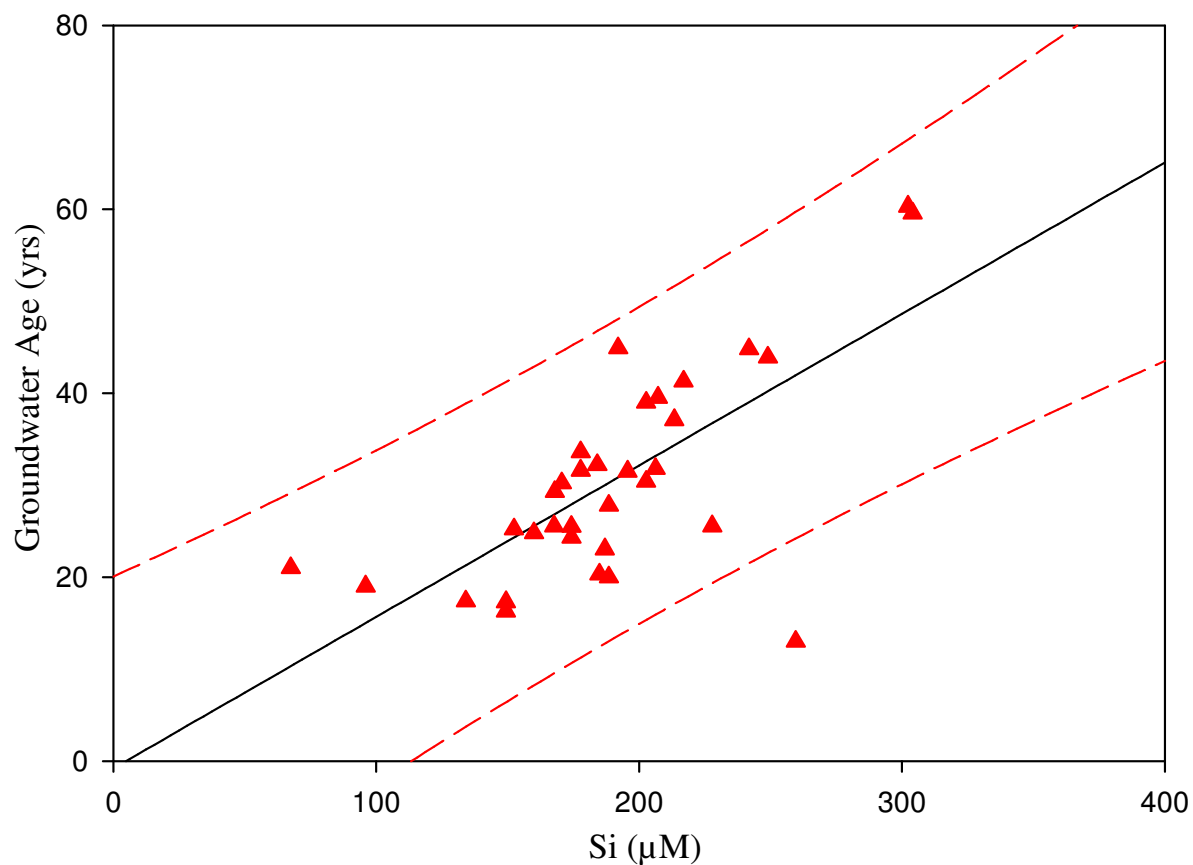


Figure 6.7. Groundwater age vs. [Si] for West Bear Creek based on 23 samples collected in April 2007 combined with CFC-113 determined groundwater age and [Si] for 10 samples collected in July 2012. Regression analysis yielded a slope of 0.1647 yr/ μM , an intercept of -0.7991 yr, an r^2 of 0.4868 and p-values of <0.0001 and 0.8941 for the slope and intercept, respectively.

7. ANALYSIS OF AGE-[SI] RELATIONSHIPS IN GROUNDWATER

7.1. Sources of Dissolved Silica in Groundwater

The source of Si in the groundwater in all of the observed study areas, and in any aquifer system in general, is a function of the geologic units through which the groundwater passes (i.e., fractured bedrock or clastic deposits), the mineral constituency of those units, the grain-size classification, and to a lesser extent, the pH of the groundwater (Schott et al. 2009). Mineralogy seems to have a strong control on the [Si] of groundwater. In the study performed by Burns et al. (2003) it was determined that plagioclase had the highest weathering rate at the Panola Mountain Research Watershed (PMRW), GA (~6.4 $\mu\text{M}/\text{yr}$). In Burns et al. (2003), NETPATH geochemical mass balance modeling was used to show that the dominant weathering reaction in the chemical evolution of groundwater chemistry was plagioclase (An_{23}) feldspar weathering to kaolinite, similar to previous findings of other weathering studies performed in springs in the Sierra Nevada (Rademacher et al. 2001). Velbel & Price (2007) also state that in silicate-dominated natural hydrologic systems, plagioclase dissolution is typically the most important weathering reaction. The dissolution of potassium feldspar, biotite, and to some extent amphibolite (all of which are silicate minerals) was somewhat important for the chemical evolution of groundwater at PMRW but far less so than the weathering of plagioclase (Table 6 in Burns et al. 2003). It is also important to note that for the study conducted by Burns et al. (2003), the models show that the inclusion of well 150, which was finished in granite, had the effect of doubling the weathering rate of plagioclase. For scenario 1 of the mass-balance model well 150 was

included, and the plagioclase weathering rate was 6.3-7.2 $\mu\text{M}/\text{yr}$. For scenario 2, which was run with well 150 excluded, the plagioclase weathering rate became 3.7 $\mu\text{M}/\text{yr}$. This led Burns et al. (2003) to conclude that weathering rates in bedrock fractures may be more rapid than in saprolite (partially weathered bedrock).

When considering granites, which are a source of Si, the two minerals most closely associated with the increase of [Si] with increasing groundwater age are plagioclase and quartz. The dissolution rate of minerals in a geologic unit (clastic or comprised of weathered bedrock) is directly related to the exposed surface area, and within granitic rock the two mineral species that have the greatest degree of connected pore spaces are plagioclase and quartz, which possess two distinct types of porosity networks (quartz crystals possess microfractures, and plagioclase crystals possess dissolution voids (Sardini et al. 1997)). In addition, it has been noted in other studies that plagioclase is easily altered (Sardini et al. 1997).

7.2. Relationships Between Groundwater [Si] and Groundwater Age

This section provides an overview of groundwater age-[Si] relationships presented in Chapters 3 and 6. Table 7.1 shows the regression statistics for individual data sets and for four combined data sets:

- all West Bear Creek data presented in Chapter 6 (Fig. 6.7)
- Lizzie site data in Tesoriero et al. (2005) and in Denver et al. (2010) (Fig. 3.19)

- data from Böhlke and Denver (1995) for both Morgan Creek and Chesterville Branch in the Locust Grove MD area (Fig. 3.9), and
- Locust Grove data from both Böhlke and Denver (1995) and Denver et al. (2010) (Fig. 3.20).

The combined regressions allow for the creation of new statistics based on a higher number of sample points. [Si] acquisition rates and r^2 values for all the studies listed in Table 7.1 are represented in Figure 7.2, which shows the acquisition rate of [Si] over time (i.e., the amount of [Si] acquired per year, which has been calculated for each study using the inverse of the slope to give the rate of increase of [Si] in units of $\mu\text{M}/\text{yr}$).

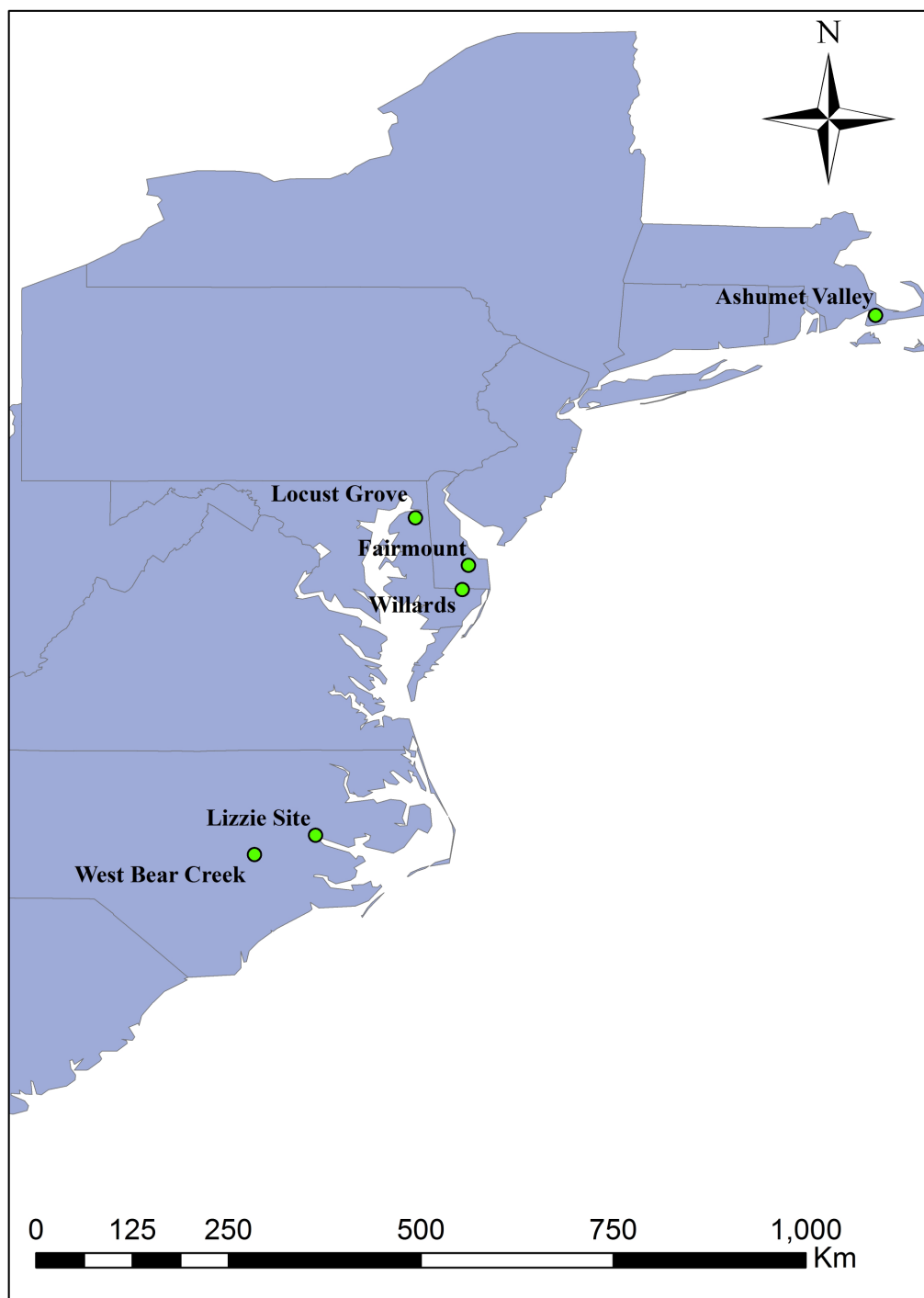


Figure 7.1. Approximate positions for the six studies located in the coastal plain, as determined from GIS data and relative positions from the published figures presented in the original publications for the studies shown.

Table 7.1. Regression results (groundwater age vs. groundwater [Si]) for published studies. “n” = number of data points in the regression. In each cell of the last column, the P values apply to the slope and intercept, respectively.

#	Study	Study Area	n	Geology/Geologic Formations	slope (yr/ μ M)	intercept (yr)	r ²	P
1	West Bear Creek (April 2007 and July 2012) ^A	Bear Creek sub-basin of the Neuse River, NC	33	Surficial siliciclastic aquifer, underlain by the Black Creek formation	0.1647	-0.799	0.4868	<0.0001/ 0.8941
2	Kenoyer and Bowser (1992)	Crystal Lake, Vilas County, WI	6	Glacial sediments overlie Precambrian bedrock comprised of gneisses, amphibolite, schists, granites, monzonites, mafic metavolcanics, and quartzose and feldspathic sandstones	0.0186	0.566	0.9555	0.0005/ 0.0219
3	Tesoriero et al. (2005) and Denver et al. (2010) ^B	Lizzie site in the Contentnea Creek sub-basin of the Neuse River, NC	24	Yorktown aquifer material overlain by sandy-clayey silt	0.1385	-4.013	0.6842	<0.0001/ 0.2440
4	Böhlke and Denver (1995) ^C	Delmarva Peninsula, MD (Chesterville Branch and Morgan Creek, both in Locust Grove)	32	Permeable sand and gravel units of the fluvial Pensauken Formation and the marine glauconitic Aquia Formation	0.3327	-13.5125	0.4853	<0.0001/ 0.0455

Table 7.1 Continued

5	Böhlke and Denver (1995) and Denver et al. (2010) ^D	Delmarva Peninsula, MD (all Locust Grove data)	45	Permeable sand and gravel units of the fluvial Pensauken Formation and the marine glauconitic Aquia Formation	0.1154	5.231	0.2096	0.0016/ 0.2691
6	Shapiro et al. (1999) and Savoie et al. (1998) ^E	Ashumet Valley, Falmouth, MA	62/ 40	Carbonate-free silicate Pleistocene sediments (90% quartz) deposited during last glacial regression	0.0995/ 0.1278	-1.422/ -2.259	0.3357/ 0.6751	(<0.0001/ 0.6742)/ (<0.0001/ 0.3887)
7	Denver et al. (2010) ^F	Fairmount, DE/ Locust Grove (Chesterville Branch only) MD/ Willards, MD	20/ 13/ 9	Fair-mount study site consists primarily of permeable sand and gravel of the Beaverdam Formation, underlain by the sandy strata of the Bethany Formation. Willards site comprised of Beaverdam sand overlain by 3-8 m the clay, silt, peat, and sand of the Omar Formation, which is overlain by 3-8 m of the Parsonsburg Sand, and sandy unit with interspersed clay, silt, and organic matter.	0.1074/ 0.2429/ 0.0440	-16.170/ -26.172/ 0.520	0.4863/ 0.6605/ 0.6077	(0.0006/ 0.0414) /(0.0007/ 0.0271) /(0.0132/ 0.8474)
8	Rademacher et al. (2001)	Sagehen Basin, Nevada County, CA-eastern Sierra Nevada	10	Glacial till deposits derived from a combination of andesite and granodiorite basement rocks	0.00430	23.914	0.0030	0.8802/ 0.1111

Table 7.1 Continued

9	Lindsey et al. (2003)	Polecat Creek, VA Piedmont	12	Piedmont Crystalline consisting primarily of garnet- biotite gneiss	0.0572	-4.3432	0.9140	<0.0001/ 0.0183
10	Burns et al. (2003)	Panola Mountain, Piedmont, GA	20	Panola Granite intruded into the Clairmont Formation	0.0490	-5.088	0.8980	<0.0001/ <0.0001

A: Results in this row are for a single regression based on all West Bear Creek NC data from samples collected in April 2007 and July 2012 (see Chapter 6).

B: Results in this row are reported for one regression for data from Tesoriero et al. (2005) and Denver et al. (2010): Lizzie site.

C: Results in this row are reported for one regression based on all the Locust Grove data in Böhlke and Denver (1995), from the two different Locust Grove watersheds: Chesterville Branch (n=18) and Morgan Creek (n=14).

D: Results in this row are reported for one regression based on all Locust Grove data in Böhlke and Denver (1995) and in Denver et al. (2010).

E: Results in this row are reported for two regressions, one for all the data points from Ashumet valley (n=62), and one for only the data points for wells downgradient of Ashumet pond (n=40).

F: Results in this row are reported for 3 different regressions for three different watersheds: Fairmount (n=20), Locust Grove (Chesterville Branch only, n=13), and Willards (n=9), respectively.

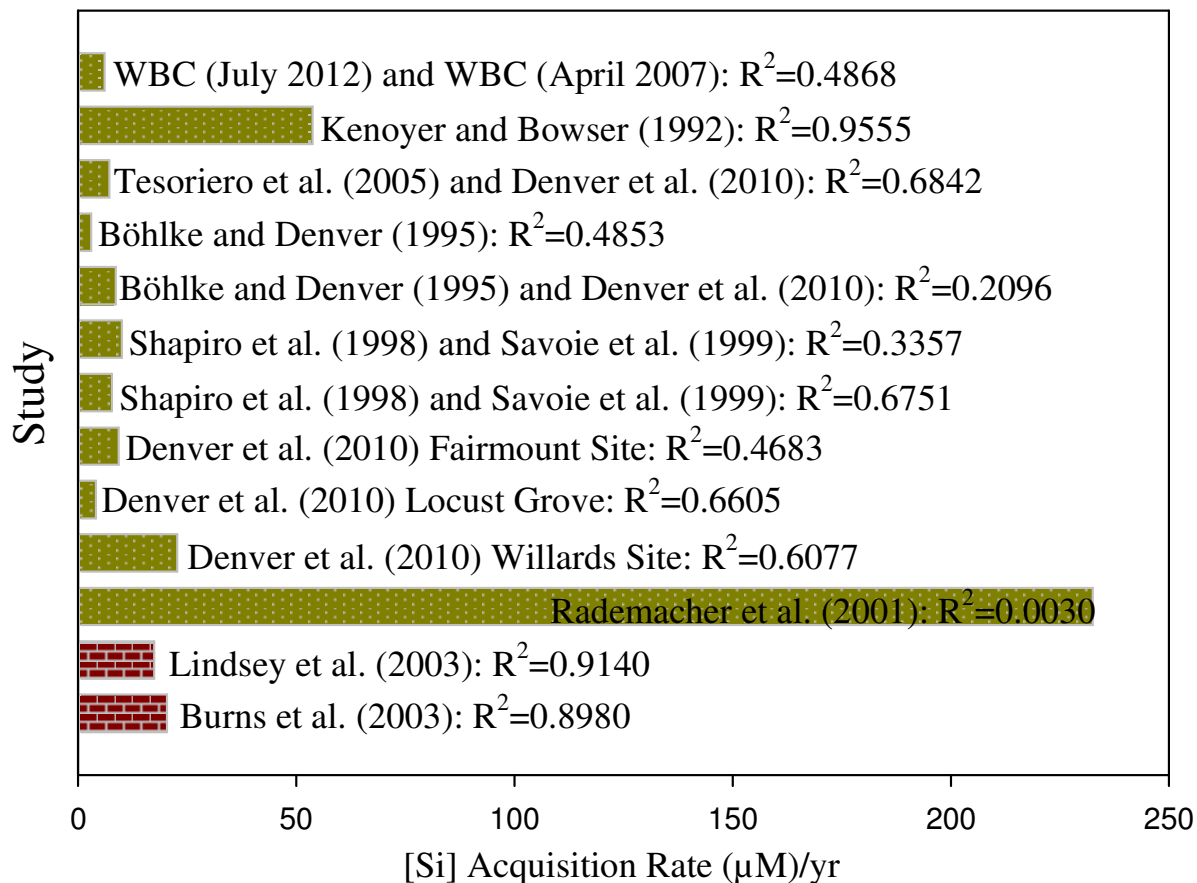


Figure 7.2. [Si] acquisition rate (inverse of regression slope) for 13 age-[Si] regressions from 10 studies. Red bars represent studies conducted in areas with crystalline bedrock, and yellow bars represent studies conducted in areas with clastic aquifers. Each bar represents a row in Table 7.1.

Besides the two studies conducted by Lindsey et al. (2003) and Tesoriero et al. (2005), the above mentioned studies do not state explicitly that [Si] can be used as an age-dating proxy for groundwater age, although the study by Burns et al. (2003) notes a strong positive correlation ($r^2=0.87-0.90$, $p < 0.001$) between apparent riparian groundwater age and [Si]. Also, Denver et al. (2010) state that differences in [Si] could be useful for understanding

the relative age of groundwater at a local scale but the variability between the sites they investigated indicate that [Si] would not be a good indicator of groundwater age at the regional scale.

It is evident from the slopes and r^2 values from my regression analysis of the studies in Table 7.1 that there is an increase of [Si] with increasing groundwater age. This relationship is better correlated for some studies than others. This is due to a variety of differences in the environments of the studies, including hydrogeology, mineralogy, and to some extent the climate of the sites. For the studies in Table 7.1 (containing the combined regression results for studies with common locations) the slopes of the data range from 0.004-0.333 yr/ μM (with an average of 0.108 yr/ μM and standard deviation of 0.080 yr/ μM), and the r^2 values range from 0.003-0.956 (with an average value of 0.570 and a standard deviation of 0.268). The remainder of this chapter focuses on the regression results presented in Table 7.1.

The Locust Grove (Chesterville Branch plus Morgan Creek) data ($n = 32$) from Böhlke and Denver (1995) has a slope of 0.333 yr/ μM and the r^2 is 0.485. However, when these data are combined with the Locust Grove data (Chesterville Branch only) from Denver et al. (2010) ($n = 45$), the regression slope becomes 0.115 yr/ μM and the r^2 is 0.210, resulting in the lowest r^2 value for the studies conducted in the coastal plain. With the combined regression the slope becomes closer to the slope values for North Carolina (0.164 yr/ μM at the West Bear Creek location, and 0.138 yr/ μM at the Lizzie Site), though the reason it does

so (the clustering of Denver et al. 2010 points below the regression trend defined by the Böhlke and Denver 1995 points alone) does not necessarily suggest the full combined regression (Böhlke and Denver 1995 plus Denver et al. 2010) is the “best” one for this site (it raises the question of whether the sample sets in the two papers are drawn from the same underlying “population” or not, even though they are collected in the same Locust Grove geographic area). Several factors seem relevant to this. First, while both studies involved sample collection in the Locust Grove area, the Denver et al. (2010) samples were collected only from wells in the upstream portion of Chesterville Branch while the Böhlke and Denver (1995) samples span a larger range of Chesterville Branch (several km downstream) and also include the adjacent Morgan Creek. Second, the median well depth reported in Denver et al. (2010) for their samples is 11.6 m, and the median well depth I calculated for all of the wells sampled by Böhlke and Denver (1995) is 2.8 m (sampling different groundwater at different depths may explain part of the differences in age-[Si] between the two studies). In addition, some of the data in Böhlke and Denver (1995) represent discharging groundwater collected from beneath the streambed using minipiezometers, whereas all the data in Denver et al. (2010) represent samples collected from wells. It may also be pertinent to note that the sampling events for the two studies were separated by approximately 7 yr. Based on these factors and the regression results it is not completely clear whether it is best to consider all the Locust Grove data from the two studies together in one regression, and so a combined regression (row 5, Table 7.1) and separate regressions (rows 4 and 7, Table 7.1) are considered for Locust Grove in this chapter.

The slope of 0.138 yr/ μ M for the Lizzie site ($r^2 = 0.684$, $n = 24$) is similar to the slope of 0.165 yr/ μ M for West Bear Creek ($r^2 = 0.487$, $n = 33$). These study sites are 30-40 km distant from each other (the Lizzie Research station is to the NE of the WBC study site) and have similar rates of [Si] acquisition in groundwater, suggesting that in at least some cases it might be reasonable to extrapolate an age-[Si] regression over some distance (tens of km) in the Atlantic coastal plain to get an approximate indication of age from [Si]. This is a positive sign regarding the possible use of groundwater [Si] as a proxy for groundwater age.

In the discussion that follows, I make comparisons among the six coastal plain sites to assess the variation in age-[Si] relationships and [Si] acquisition rates (Fig. 7.2) by location. Figure 7.3 shows a range of age-[Si] relationships exist for the studies conducted in the coastal plain, with differences large or small over both short (tens of km) or long (hundreds of km) distances. For example, Lizzie, NC (row 3, Table 7.1) and West Bear Creek, NC (row 1, Table 7.1) are relatively close together (30-40 km), and very similar in age-[Si], with similar slopes (0.139 and 0.164 yr/ μ M, respectively) and ages within 4-10 year of each other for a given [Si] (Figure 7.3). Two lines from more distant sites have slopes close to those of the NC sites: those for Fairmount, DE which has a slope of 0.107 yr/ μ M and Ashumet Valley, MA (for the points downgradient of Ashumet pond) which has a slope of 0.123 yr/ μ M. This Ashumet Valley line plots almost on top of the Lizzie NC line (Figure 7.3), and the Ashumet Valley study site is approximately 920 km NE of Lizzie, NC and West Bear Creek, NC. Fairmount, DE (row 7, Table 7.1) is approximately 400 km from both Lizzie, NC

and West Bear Creek, NC. These four coastal plain sites represent two sites 10s of km from each other with similar age-[Si] relationships, and two sites that are 100s of km distant but with similar age-[Si] relationships to those of the NC sites. Willards, MD (row 7, Table 7.1), with a slope of $0.044 \text{ yr}/\mu\text{M}$, is approximately 60 km south of Fairmount, DE (row 7, Table 7.1), and has a very different age-[Si] relationship with a faster growth in [Si] with time (Figure 7.3). This represents an example of two sites within 10s of km of each other that do not have similar rates of [Si] acquisition. Overall, these examples show the rate for [Si] acquisition and age-[Si] relationship can be similar or different for sites close together (10s of km) or for sites far apart (100s of km) in the coastal plain.

In general, regressions for the coastal plain show that variation in the age-[Si] relationship may be large or small over distances of tens of km or hundreds. The results of my study indicate that geological and mineralogical properties of a study area are the controlling factors for the rate of [Si] acquisition, and that geographical location does not appear to be a controlling factor for the rate of [Si] acquisition. There seems to be potential for using [Si] as an indicator of groundwater age within an area of similar geology that has been "calibrated" through an observed age-[Si] relationship, and perhaps even outside that calibration area if hydrogeological conditions are similar. If the [Si] method for determining groundwater age were used for a location in the coastal plain other than the areas considered in this report (NC, DE, MD, MA) it would be relevant to explore the variability in groundwater age for a particular [Si], in order to predict what the expected variation in

groundwater age would be. Using Figure 7.3, I have estimated that for a [Si] value of 50 μM the approximate range in estimated groundwater age among coastal plain sites is 2.4-11.2 yr, and for a value of 250 μM the approximate range is 10.6-69.8 yr (over the range of [Si] from 0 to 400 μM , the mean range in estimated groundwater age among all the regressions in Figure 7.3 is approximately 34.4 yr). The Locust Grove, MD site (row 4, Table 7.1) has the line of highest slope, and the Willards, MD site (row 7, Table 7.1) has the line of lowest slope in Figure 7.3. Overall, Figure 7.3 shows that the expected range in groundwater ages increases with increasing [Si].

Two studies that correlate well with each other but are spaced far apart are the two piedmont studies at Panola Mountain, GA (row 11, Table 7.1) and Polecat Creek, VA (row 10, Table 7.1). Both sites are underlain by crystalline bedrock that weathers to form the soil and aquifer material through which groundwater flows. At Panola the crystalline bedrock is predominately Panola Granite, a biotite-oligoclase-quartz microcline granite, containing the primary minerals plagioclase feldspar, quartz, microcline-microperthite, biotite, and muscovite. Dominant secondary minerals include kaolinite, hydroxyl-interlayered vermiculite, hydrobiotite, gibbsite, and goethite. As stated in section 7.1, it was determined that at this site the dissolution of plagioclase was the dominant weathering reaction. Plagioclase weathers in the soils and saprolite to form kaolinite. In comparison biotite, which weathers rapidly, was shown to weather to vermiculite (Burns et al. 2003). The Polecat Creek site is also underlain by saprolite with crystalline bedrock below (garnet-biotite gneiss),

though there was no detailed discussion in Lindsey et al. (2003) of mineralogy, mineral weathering, or the production of secondary minerals at this site.

The study by Kenoyer and Bowser (1992) is an interesting case, in that the relationship between [Si] and groundwater age is for a much shorter timescale (0-4 yr) than that for the other studies. This study produced a relatively low slope of 0.019 yr/ μM , and an r^2 of 0.956, for the study site in Crystal Lake, WI. The closest slope value from the other studies presented in Table 7.1 is that of Rademacher et al. (2001), which has the lowest r^2 value of any study. Although the method used for the determination of groundwater age is fundamentally different for these two studies (Rademacher et al. 2001 collected water discharging from springs for CFC-analysis, and Kenoyer and Bowser 1992 used physical measurements to determine groundwater age along a flowpath), it is interesting to note that both studies were conducted in study sites with surficial aquifers composed of glacial till. For Kenoyer and Bowser (1992), the r^2 value is high but the dataset is limited ($n=6$) and the age estimates had a high level of uncertainty (40%, as reported by Kenoyer and Bowser 1992), as can be seen from Figure 7 in Kenoyer and Bowser (1992). The study conducted in Ashumet Valley, MA (row 6, Table 7.1), is also in glacial sediments, but the slope for the data for the entire dataset ($n=62$) for this study is 0.099 yr/ μM with an r^2 of 0.336. The slope for this study is roughly an order of magnitude greater than that of the other two studies which collected samples from glacial aquifer material.

The study displaying the lowest slope ($0.0043 \text{ yr}/\mu\text{M}$) and the lowest r^2 (0.003) was Rademacher et al. (2001), located in the Sagehen Valley, CA. For this study, samples were collected from springs at the sediment-water interface. All samples from other studies were collected either from wells or from below the stream bed along a transect, following sampling processes which are designed to collect groundwater of distinct ages. Since springs are points where groundwater flowlines are converging and discharging, collecting groundwater at a spring results in samples that generally comprise waters that vary widely in age. For this reason samples collected from springs cannot be assigned a singular age, confounding regression of age vs. [Si] or other chemical parameters.

It is evident that a linear trend with a positive slope generally exists between groundwater age and [Si]. An obvious question concerns the predictive power of these relationships, i.e., what is the uncertainty associated with collecting a single groundwater sample, measuring its [Si], and using that value with an age-[Si] regression to estimate the age of the groundwater in the sample? Among the data sets summarized in this thesis, there is a fairly wide range of uncertainty associated with estimating groundwater age from groundwater [Si]. Figure 7.4 is a plot of this uncertainty, as a function of [Si], based on the 95% prediction intervals for age-[Si] regressions presented earlier (Table 7.1).

The three studies with the lowest age uncertainty are the two conducted in areas of crystalline Piedmont bedrock, Lindsey et al. (2003) and Burns et al. (2003) ($\pm 5\text{-}9 \text{ yr}$), as well

as the study by Kenoyer and Bowser (1992) (± 1 yr) in which groundwater age was estimated with a numerical model rather than age-dating tracers. The two regressions with the highest prediction uncertainty are those from the studies by Rademacher et al. (2001) (focusing on spring samples representing mixtures of groundwater ages; ± 21 -30 yr), and the Locust Grove MD regression based on data from both Böhlke and Denver (1995) and Denver et al. (2010) (± 25 -29 yr); these are rows 8 and 5, respectively, in Table 7.1. Prediction uncertainty for the rest of the studies falls into the range of ± 10 -20 years.

Some potential advantages of using [Si] as an age-dating proxy, where applicable, are that it is relatively inexpensive and simple to collect. Only 3-10 ml of filtered groundwater are needed for analysis, so collection materials are limited to the 0.45 μm filter, the 20 ml scintillation vial, and the piezomanometer-system used to collect the sample. In addition, there are multiple analysis procedures that are relatively inexpensive per sample (~\$3 for the ICP-AES method, and ~\$8 for the colorimetric method), and the sample storage procedure is simple, as they do not need to be acidified or frozen, but rather only need to be kept at a temperature of 4°C.

The main disadvantage to estimation of groundwater age from [Si] is the larger uncertainty, relative to the lower uncertainty that is often achievable with direct use of a “primary” age dating tracer (CFCs, SF₆, or ³H/³He). Uncertainty in age from direct use of these primary age dating tracers is generally in the range of ± 2 -3 yr (Plummer et al. 2006;

Ekwurzel et al. 1994), in some cases as low as ± 0.4 -1.2 yr (Plummer et al. 2003). At up to \$1000 or more for analytical costs alone, use of the primary age dating tracers is at least 100x more expensive than estimation of age from [Si]. With a better understanding of the tradeoff between increased cost and reduced uncertainty, groundwater scientists and managers may be able to make a more informed decision regarding data collection for individual projects (e.g., is ± 10 -20 yr adequate to answer a question at hand, or is ± 3 yr needed, and within reach financially?). Of course, estimation of age from [Si] still assumes that an age-[Si] regression is available for the groundwater system of interest, and if not available from past work it would have to be created, or “borrowed” from a location with related geology. Of the 11 different locations examined in this study, 9 had hydrogeologic environments comprised of clastic aquifers, and two had hydrogeologic environments comprised of saprolite aquifers weathered from crystalline bedrock in the piedmont area. For the piedmont sites, age-[Si] regressions had higher r^2 and less variability between sites, but then only two piedmont sites with age-[Si] data could be identified. Results suggest that the potential for the use of [Si] as proxy for groundwater age is higher in the piedmont than in the coastal plain, but it is not known whether that conclusion would be supported if age-[Si] data were available for a greater number of piedmont sites, similar to the number of coastal plain sites.

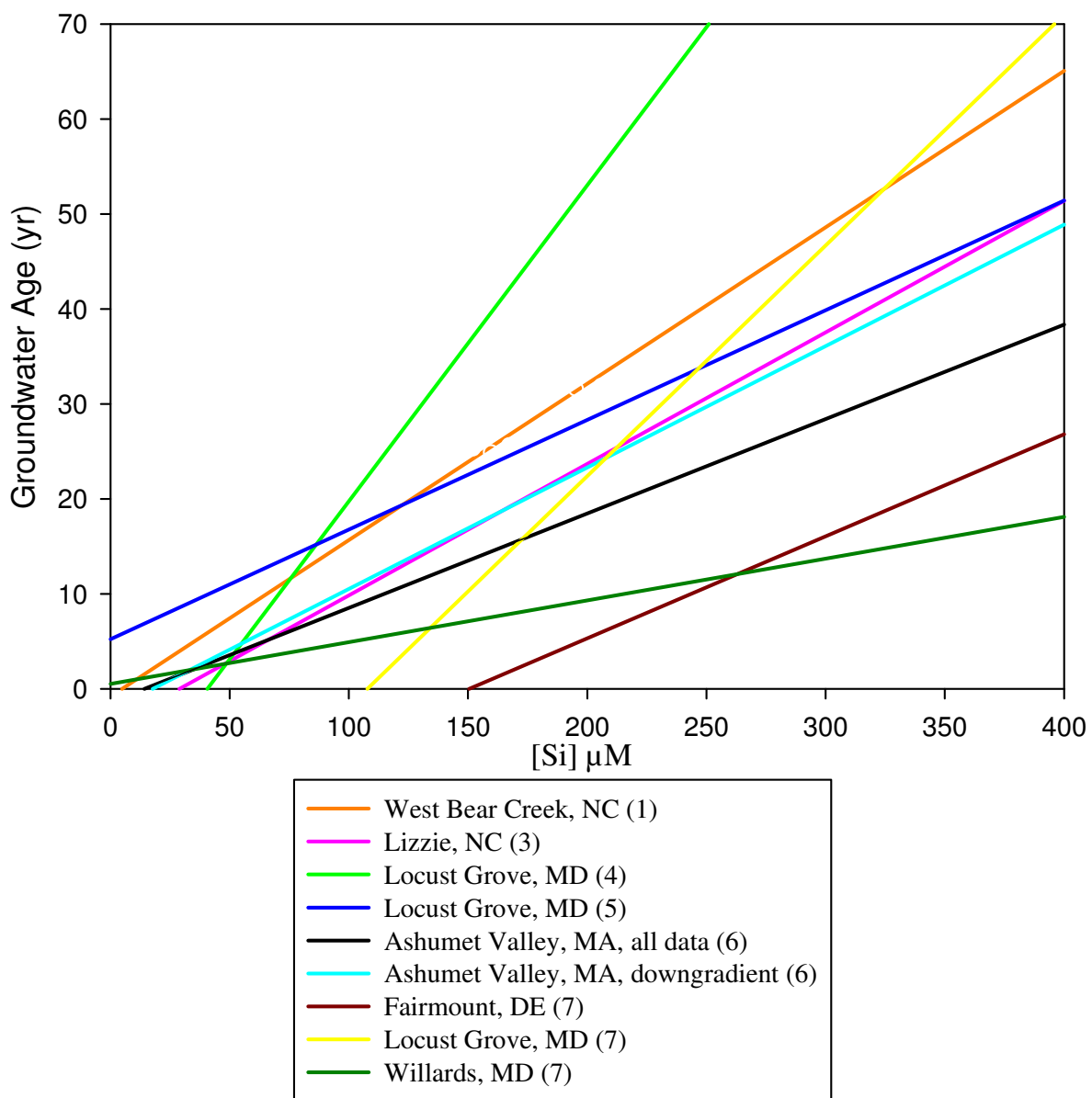


Figure 7.3. Coastal plain regressions from Table 7.1. In the legend, numbers in parentheses after site names refer to row numbers in Table 7.1.

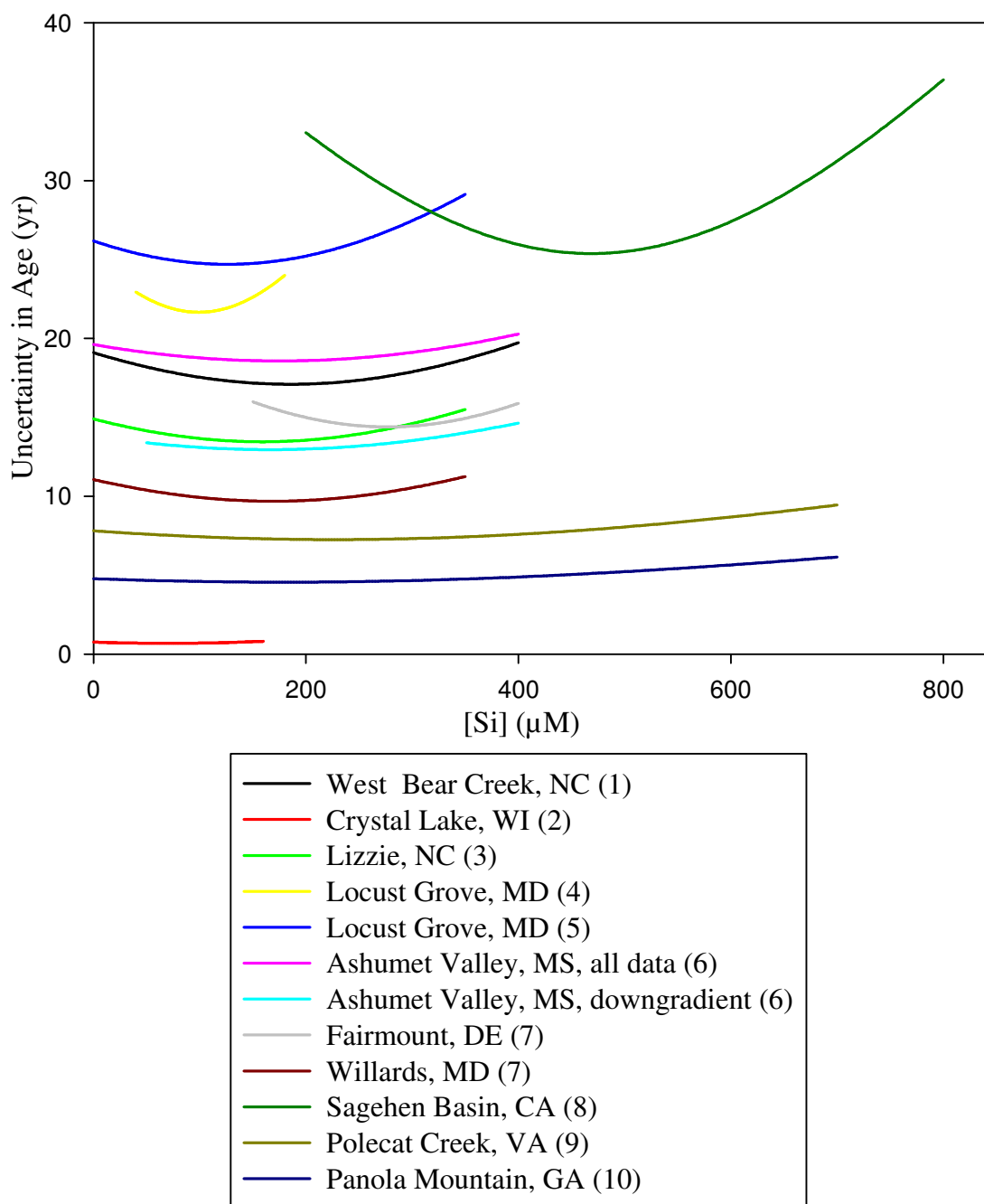


Figure 7.4. The uncertainty in groundwater age prediction based on the age- $[Si]$ regressions in Table 7.1. “Uncertainty in age” plotted above is half of the vertical distance between the regression 95% prediction limits, i.e., if on a given regression the 95% prediction limits were 20 years apart at a $[Si]$ of 200 μM , then that particular regression is able to predict age to ± 10 years at $[Si]$ of 200 μM , and that result is plotted above as 10 years, at $[Si] = 200 \mu M$, for that regression.

7.3. Comparison of Lab-based and Field-based [Si] Kinetics

In order to determine a meaningful relationship between the concentration of [Si] and the age of the groundwater, the rate at which [Si] is being added to the groundwater system should be known. Several studies have already been conducted looking at lab-based (Scanlon et al. 2001; Brantley and Mellot 2000) and field-based (Velbel & Price 2007, Day and Nightingale 1984) dissolution rates for a variety of silicate minerals and geologic units. Field-based dissolution rates are commonly conducted by calculating natural weathering rates based on solute fluxes measured from watershed discharge, infiltrating soil pore water, or along groundwater flow paths (White and Brantley 2003). It has been observed that often the lab-based and field-based mineral dissolution rates can differ by orders of magnitude (a phenomenon which has been covered extensively by White and Brantley 2003). For example, Velbel (1985) found in his study of garnet and plagioclase dissolution that the lab-determined dissolution rate was one to two orders of magnitude greater than the field-determined dissolution rate under similar hydrogeochemical conditions. In addition, Brantley and Mellot (2000) sought to quantify the porosity in samples of primary silicate minerals ground in the lab and natural samples to help explain the discrepancy between field and laboratory-based estimates of silicate weathering rates. Brantley and Mellot (2000) concluded that porosity had a significant effect on the laboratory measurements of reactive surface area, and that further research remained on how to accurately estimate this parameter in the laboratory for use in extrapolation to the field.

Probable reasons for disparate mineral dissolution rates include: grain size (lab samples are typically ground, altering grain-size and making it more heterogeneous), contact time with infiltrating water (lab studies typically have water continually running through a sample column, which does not allow for the possibility of stagnant or very slow moving water to come into chemical equilibrium, reducing dissolution rate, as can happen in natural environments), and the formation of secondary minerals (kaolinite, smectite, etc.) which can remove [Si] from the groundwater system. In addition, Scanlon et al. (2001) notes that dissolution rates of silicates in the field experience seasonal variations as the position of the water table changes, changing the availability of silicate minerals for weathering in the regolith and bedrock, and changes in the position of the water table also affect residence times. Scanlon et al. (2001) also found in their study that concentrations of [Si] increased rapidly after the initial water contact with soil (for the laboratory study) but after one to two days the concentrations changed very gradually. Scanlon et al. (2001) cite Buttle and Peters (1997) who suggest that the observed rapid reactions are a result of laboratory conditions where samples are repacked, and do not reflect natural soil (or regolith) material which contains structural voids (i.e., macropores).

An example of the effect of grinding lab samples is outlined by the study conducted by Brantley & Mellot (2000) wherein the authors cite several studies that show the specific surface area (SSA, m^2 of surface area per g of solid) of naturally weathered silicate minerals tends to be greater than laboratory-ground samples. Brantley and Mellot (2000) found that it

was not possible to reproduce measurements of SSA for course-grained ground primary silicate minerals, possibly due to complications in the gas adsorption technique used to measure SSA, healing of microcracks, and impurities (entrainment of fine, second phase minerals). Brantley and Mellot (2000) state that for plagioclase, hornblende, olivine, and diopside, lab-based dissolution rates up to five orders of magnitude higher than field-based dissolution rates have been observed (White and Brantley 1995), and that differences in SSA for lab-based and field-based silicate measurements have been used to explain the discrepancy between field-based and lab-based dissolution rates (Anbeek 1992a, 1992b, 1993; Anbeek et al. 1994), owing to the fact that surface area created during natural weathering is relatively non-reactive while the surfaces created in laboratory ground samples are reactive. Brantley and Mellot (2000) estimate that for primary silicate minerals, field samples have 20 times the surface area of laboratory samples. In a related study, Day and Nightingale (1984) state that the rate at which Si goes into solution is related to the particle surface over which the water passes, the mechanism of dissolution being simultaneous hydrations and de-polymerization.

White and Brantley (2003) performed column studies using freshly prepared Panola Granite, producing ambient plagioclase weathering rates that decreased over 6 years to a final rate of $7.0 \times 10^{-14} \text{ mol m}^{-2} \text{ s}^{-1}$. White and Brantley (2003) note that a calculated field weathering rate of plagioclase in a Panola weathering profile from White et al. (2001) was $2.8 \times 10^{-16} \text{ mol m}^{-2} \text{ s}^{-1}$, more than two orders of magnitude slower than the 2003 lab value for

fresh Panola granite. White and Brantley (2003) used relatively large grain sizes of similar dimension in their lab study to produce high porosities and relatively homogeneous flow in the column bed. The column used was obtained from a Panola Granite weathering profile, and was classified as a biotite-muscovite-oligoclase-quartz-microcline granodiorite. Fresh and weathered granite samples were processed through a steel jaw crusher and a disc mill to obtain a grain size fraction of <2 mm. Fines and most of the clays were removed. After 6.2 years, surface area of the fresh granite increased by a factor of 3.5, while the surface area of the weathered granite increased by a factor of 1.2. A corresponding plagioclase reaction rate for partially kaolinized Panola Granite, after reaching steady-state weathering after 2 months, was $2.1 \times 10^{-15} \text{ mol m}^{-2} \text{ s}^{-1}$. Both rates are orders of magnitude faster than field-based weathering rates measured for a weathering profile in the Panola Granite.

Factors responsible for the differences between lab-based and field-based mineral dissolution rates include progressive depletion of energetically reactive surfaces, difficulties in normalization of rates by surface area, and accumulation of leached layers and secondary precipitates (White and Brantley 2003). In addition, White and Brantley (2003) state that controls such as low permeability, high mineral/fluid ratios and increased solute concentrations (which produce weathering reactions close to thermodynamic equilibrium under field conditions compared to highly unsaturated lab conditions) explain the time-dependent difference in field and lab-based studies. Uncertainties in natural weathering rates included estimating the fluid residence times and flow paths, surface areas of complex

mineral assemblages, variations in climate, solute composition, and biological activity. White and Brantley (2003) state that experimental weathering rates for a specific silicate mineral are commonly two to four orders of magnitude faster than field-derived rates (White et al. 2006, Brantley 1992, Schnoor 1990).

Table 7.2 shows dissolution rates for Ab-plagioclase, calculated from the regression slopes in Table 7.1, and Figure 7.7 compares field dissolution rates (White and Brantley 2003), lab dissolution rates (White and Brantley 2003), and plagioclase dissolution rates derived from Table 7.2. Lab-based dissolution rates are typically derived from column studies (passive gravity flow systems which allow water to flow through aquifer material from the field that has been ground in the lab), bed reactors, batch reactors, and flow reactors (White and Brantley 2003). In addition, grain size and SSA are usually known for lab-based studies (as they are typically ground to match a specific grain size). Laboratory methods listed above measure the number of moles of mineral released into solution per square meter of surface area per second by measuring the dissolved cations present in the effluent over time. Field-based studies are approached by measuring the water discharge for a given watershed, the soil infiltration rate, or the groundwater flow along a flow path, in conjunction with dissolved solute content measured in water samples (White and Brantley 2003). Both the lab-based methods and field-based methods can be used to determine the amount of [Si] in groundwater over time by using the mineral dissolution rates of particular minerals and the chemical dissolution equations predicting the number of moles of [Si] released per mole of

mineral being reacted (for example, one mole of plagioclase (An_{23}) is predicted by Kenoyer and Bowser (1995) to produce 5.32 moles of dissolved Si when weathered to kaolinite).

Table 7.2 and Figure 7.7 shows the results of converting age-[Si] regression slopes in $yr/\mu M$ into the same units ($mol\ Si\ m^{-2}s^{-1}$) used for 41 studies of plagioclase dissolution rates in Table 4 of White and Brantley (2003). An exhaustive search of the scientific literature only yielded 8 studies (Table 7.1) that contained both groundwater [Si] and groundwater age data. However, mineral dissolution studies are common in the scientific literature, and as Table 7.2 shows, they could be used to estimate the amount of [Si] in groundwater in relation to groundwater age, and thus could be used to calibrate an age-dating technique based on [Si].

Several parameters were required to make the conversion from $yr/\mu M$ to $mol\ Si\ m^{-2}s^{-1}$ for the regressions listed in Table 7.1, including porosity (Θ) which is unitless, particle density (ρ_s) with units of g/cm^3 or kg/L , bulk density (ρ_b) with units of g/cm^3 or kg/L , and Specific Surface Area (SSA) with units of m^2/g :

$$\left(\frac{\mu mol Si}{L_{pores} \cdot yr} \right) \left(\frac{L_{pores}}{L_{bulk}} \right) \left(\frac{L_{bulk}}{kg_{bulk}} \right) \left(\frac{kg_{bulk}}{m^2_{bulk}} \right) \left(\frac{mol}{10^6 \mu mol} \right) \left(\frac{yr}{3.154 \times 10^6 s} \right) = \frac{mol Si}{m^2 s} \quad (1)$$

The first term in equation (1) (which shows only the units and not the values for the first 4 terms in parentheses) is the [Si] accumulation rate, which is calculated as the inverse of the slope units produced by my regressions. Liters of pore water (L_{pores}) is used because the Si entering groundwater by mineral weathering is, by definition, entering the water-saturated

pore space. The second term in equation 1 is the inverse of the porosity; the third term is the inverse of the bulk density; the fourth term is the inverse of the SSA. The last two terms are unit conversions.

In order to relate moles of Si accumulating in the pore water (i.e., groundwater) to moles of weathering mineral (i.e., weathering rates of White and Brantley) values for particle density and porosity are needed to calculate the bulk density (equation 2), and the particle density and grain size are needed to calculate the SSA (equation 3). In my calculations I used assumed values for the particle density and porosity unless one or both of these values were available from other published studies conducted in the same area or in areas of similar geology within a few 100 km, in which case those values were used instead (Table 7.2). For most of the results presented in Table 7.2, a particle density of 2.62 g/cm^3 and a porosity of 0.30 were assumed (which are reasonable values for silicate aquifer material). For other studies I used more site-specific information, e.g., the study by Burns et al. (2003) reported values for SSA, bulk density, and porosity for their study area, and Lindsey et al. (2003) had a value for SSA reported by White and Brantley (2003) as representative of their study site, a bulk density value reported by White (2005) as representative of their study site, and a porosity value reported by Cooper et al. (1998) as representative of their study site. In addition, a value for porosity representative of the Fairmount site in Denver et al. (2010) was reported by Mackey et al. (2000). For all other studies presented in Table 7.2, my assumed

general values for porosity (0.3) and particle density (2.62 g/cm^3) were used to calculate the dissolution rate.

For Locust Grove, MD and for the Willards, MD sites, an estimate of grain size is available from Penn et al. (2013). The study by Penn et al. (2013) collected samples for grain size analysis near the village of Oyster, VA, and was used here because it was reasonably close (about 200 km south) to the Locust Grove site; sediment samples were collected from the unsaturated portions of the Wachapreague Formation, which is the surficial unit for that area. For Ashumet Valley, MA, an estimate of grain size (D_{50}) is available from Bau et al. (2004). The study by Bau et al. (2004) was also conducted in the Cape Cod aquifer at Ashumet valley. For Fairmount, DE an estimate of grain size (D_{50}) is available from Mackey et al. (2000). The study by Mackey et al. (2000) was conducted in the unconfined (i.e., surficial) aquifer at the Dover Air Force Base in DE, approximately 100 km north of Fairmount. For the Sagehen Basin, CA, an estimate of grain size is available from White et al. (1996) for silicates in soils near Merced in the Central Valley of California. Merced, CA is approximately 200 km to the SW of the Rademacher et al. (2001) site, and samples for grain size were collected from a soil sequence.

I calculated bulk density using the following equation:

$$\rho_b = \rho_s(1 - \Theta) \quad (2)$$

Some studies contained information on SSA, but most did not, and so the SSA had to be calculated using median grain size, D_{50} and the equation for the specific surface area of a sphere (Santamarina et al. 2002) where r is half the particle diameter:

$$SSA = 3/(rp_s) \quad (3)$$

Grain-size distributions for the West Bear Creek and Lizzie study sites were derived from a 60 ft core collected on March 9th 2013 near West Bear Creek. Samples were collected at 8 different depths along the core to represent the range of grain size of the surficial aquifer (Table 7.3). The samples for grain-size analysis were analyzed at the Department of Marine, Earth, and Atmospheric Sciences using a Beckman-Coulter LS 13-320 Laser Particle Size Analyzer. Results for two samples representing depths of 16.4 and 48.2 ft are shown in Figs. 7.5 and 7.6, respectively. To obtain an estimate of SSA of the entire core, I used the grain size for each sample to calculate an individual SSA assuming a particle density of 2.62 g/cm^3 and a porosity of 0.30. After I calculated a SSA for each sample, I took the average SSA of all samples and used this to calculate the dissolution rate in units of $\text{mol Si m}^{-2}\text{s}^{-1}$.

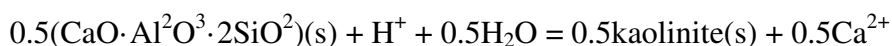
The calculations I performed using equation 1 give moles of Si released into solution per unit time. The published mineral weathering rates (e.g., White and Brantley 2003), however, are typically reported for moles of mineral weathering per unit time, and in order to relate one to the other (so that I can compare my Si release rates to the published mineral weathering rates reported in White and Brantley 2003) a conversion factor based on the stoichiometry of the weathering reactions is needed. This is because the moles of Si released

per mole of mineral weathered depend on the composition of the mineral and on the formation of secondary minerals. The following reactions are relevant to dissolved [Si] in groundwater, and one example for each type of reaction (Morel and Herring 1993) is given for albite and anorthite:

- albite (Ab) weathered to Na montmorillonite: 0.35 mole albite weathered per mole of dissolved Si produced
- albite (Ab) weathered to kaolinite: 0.25 mole albite weathered per mole of dissolved Si produced:



- anorthite (An) weathered to Ca montmorillonite: -0.875 mole anorthite weathered per mole of dissolved Si produced (Si uptake)
- anorthite (An) weathered to kaolinite: no dissolved Si produced by this reaction:



The chemical equation for the dissolution of anorthite to kaolinite shows that no Si is produced by this reaction, and the reaction that produces montmorillonite takes up Si. The chemical dissolution reactions for albite show that for one mole of Si released, 0.25-0.35 moles of albite are weathered. By multiplying the right-hand side of equation 1 by these albite factors (or by the average, 0.3, which is the value I used for my Ab calculations), I have calculated the mineral weathering rate in moles of albite for the [Si] acquisition rates that I have produced. This is not to say that all the dissolved Si in groundwater at the sites

analyzed in this thesis is from weathering of albite, but rather to allow a simple order-of-magnitude comparison of Si release from the field data in this thesis and other lab and field weathering studies (White and Brantley 2003), using a representative feldspar weathering reaction that is a known source of dissolved Si in the environment. Kenoyer and Bowser (1992) state the weathering of An_{23} (plagioclase that is 23% anorthite, 77% albite) into kaolinite requires 0.19 moles of An_{23} weathered for one mole of dissolved Si produced. To produce weathering rates with the units of moles of mineral weathered (albite) per m^2 of mineral surface area per second (the same units used by White and Brantley 2003), I multiplied my results from equation 1 above by 0.3 moles of albite weathered per mole of dissolved Si released; the results of this are reported in the last column of Table 7.2. Figure 7.7 shows the comparison of lab-based and field-based dissolution rates from White and Brantley (2003) and the dissolution rates I calculated for plagioclase for the two different compositions mentioned above. In general, we can see from Figure 7.7 that my calculated mineral dissolution rates are typically 1-4 orders of magnitude less than the lab-determined dissolution rates in White and Brantley (2003).

The equations I used to calculate the dissolution rates assume that all of the solids in the porous medium are producing dissolved Si equally, which of course is typically not the case. Instead of using liters of bulk volume per kg of bulk solid, it would be more relevant for the comparison of dissolution rates to focus only on solids that are actually producing dissolved Si. This would require knowing the liters of bulk volume per kg of Si-producing

solids, which was information that was not available for my study. Using the mass of Si-producing solids in equation 1 instead of the bulk mass of solids would increase the weathering rate computed (e.g., if most of the dissolved Si is produced by 10% of the solids, accounting for that in equation 1 would increase the weathering rate by a factor of 10). This of course is not the only uncertainty in this rough, ballpark conversion of age-[Si] regression slopes to approximate mineral weathering rates.

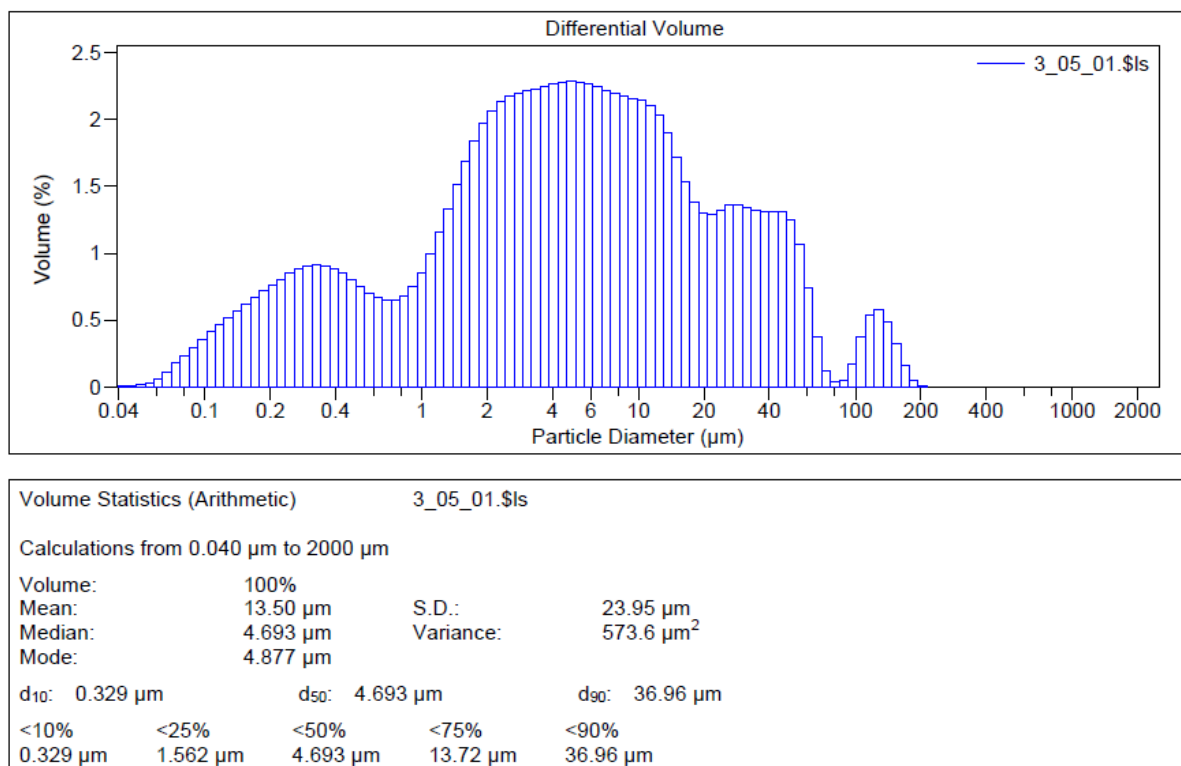


Figure 7.5. Grain-size distribution for sample Wayne-2013-01-E, representing a depth of approximately 16.5 ft below the land surface.

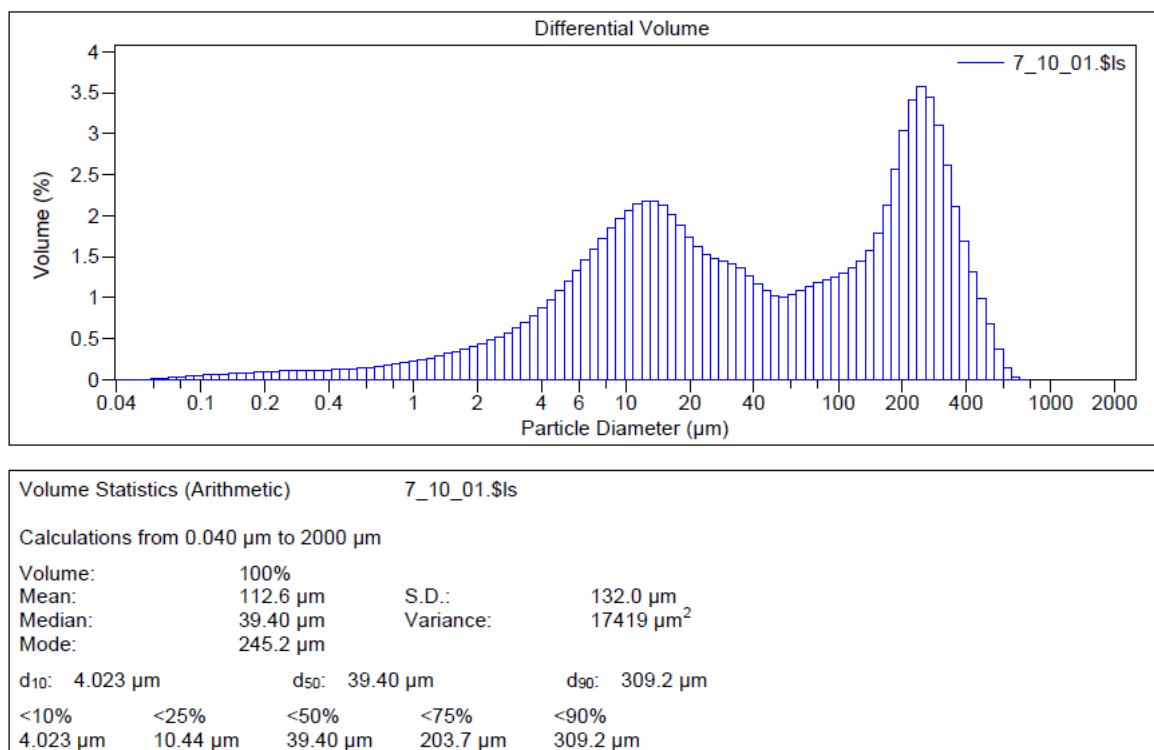


Figure 7.6. Grain-size distribution for sample Wayne-2013-01-J, representing a depth of approximately 48.3 ft below the land surface.

Table 7.2. Mineral weathering rates in the units commonly reported in the scientific literature ($\text{mol}\cdot\text{m}^{-2}\cdot\text{s}^{-1}$), as estimated from [Si] accumulation rates ($\mu\text{M}/\text{yr}$, inverse of the slopes of the age-[Si] regressions); see text for details. The dissolution rates in the last column are plotted in Figure 7.7. Unless otherwise noted below, porosity was assumed to be 0.30, bulk density was calculated using an assumed particle density of $2.62\text{ g}/\text{cm}^3$, and SSA was calculated using the assumed particle density. Grain size is the median grain size (D_{50}) for all studies except those marked with subscript C, which are mean grain sizes.

Study	[Si] Accumulation Rate ($\mu\text{M}/\text{yr}$)	Bulk Density (g/cm^3) and Porosity	D_{50} (nm) and SSA (m^2/g)	Ab Dissolution Rate $\text{mol m}^{-2}\text{s}^{-1}$
West Bear Creek, NC	6.072	1.83 and 0.30	7.9-159.9 ^A and 0.190	4.97×10^{-17}
Crystal Lake, WI (Kenoyer & Bowser 1992)	53.763	1.83 and 0.30	1-100 and 0.120 ^B	6.97×10^{-16}
Lizzie, NC (Tesoriero et al. 2005 and Denver et al. 2010)	7.220	1.83 and 0.30	7.9-159.9 ^A and 0.190	5.92×10^{-17}
Locust Grove, MD (Böhlke and Denver 1995)	3.006	1.83 and 0.30	150 ^C and 0.015	3.06×10^{-16}
Locust Grove, MD (Böhlke and Denver 1995) and Denver et al. 2010)	8.666	1.83 and 0.30	150 ^C and 0.015	8.83×10^{-16}
Ashumet Valley, MS (Shapiro et al. 1998 & Savoie et al. 1999) -Downgradient-	7.825	1.83 and 0.30	500 ^D and 0.005	2.66×10^{-15}

Table 7.2 Continued

Ashumet Valley, MS (Shapiro et al. 1998 & Savoie et al. 1999) -All Points-	10.050	1.83 and 0.30	500 ^D and 0.005	3.42x10 ⁻¹⁵
Fairmount, DE (Denver et al. 2010)	9.311	1.83 and 0.35E	520 ^E and 0.004	4.13x10 ⁻¹⁵
Locust Grove, MD (Denver et al. 2010)	4.117	1.83 and 0.30	150 ^C and 0.015	4.20x10 ⁻¹⁶
Willards, MD (Denver et al. 2010)	22.727	1.83 and 0.30	150 ^C and 0.015	2.32x10 ⁻¹⁵
Sagehen Basin, CA (Rademacher et al. 2001)	232.558	1.83 and 0.30	4-2000 ^F and 1.52 ^F	2.38x10 ⁻¹⁶
Polecat Creek, VA (Lindsey et al. 2003)	17.482	1.49 and 0.40	NA and 1.000 ^G	4.46x10 ⁻¹⁷
Panola Mountain, GA (Burns et al. 2003)	20.408	1.40 and 0.50	NA and 1.000 ^H	6.93x10 ⁻¹⁷

A: Grain size was measured in 8 core samples from the surficial aquifer near West Bear Creek, see text for details.

B: SSA reported by White and Brantley (2003) for the Crystal Lake Aquifer at Crystal Lake, WI, the study site of Kenoyer and Bowser (1992).

C: Grain size reported by Penn et al. (2013). Mean particle size was provided in Penn et al. (2013) as 100-200 nm, a value of 150 nm was used with assumed particle density (2.62g/cm³) to calculate the SSA. The study by Penn et al. (2013) collected samples for grain size analysis near the village of Oyster, VA, and was used here because it was reasonably close (about 200 km south) to the Locust Grove site. Sediment samples were collected from the unsaturated portions of the Wachapreague Formation, which is the surficial unit for that area.

D: D₅₀ from Bau et al. (2004) was used with assumed particle density (2.62g/cm³) to calculate SSA. The study by Bau et al. (2004) was also conducted in the Cape Cod aquifer at Ashumet valley.

E: D₅₀ reported by Mackey et al. (2000) was used with assumed particle density (2.62g/cm³) to calculate SSA. The study by Mackey et al. (2000) was conducted in the unconfined (i.e., surficial) aquifer at the Dover Air Force Base in DE, approximately 100 km north of Fairmount.

F: Range of grain sizes and SSA reported by White et al. (1996) for silicates in soils near Merced in the Central Valley of California. Merced, CA is approximately 200 km to the SW of the Rademacher et al. (2001) site, and samples for grain size were collected from a soil sequence.

G: Bulk density and porosity of saprolite reported by White (2005) and Cooper et al. (1988). The thesis study by White (2005) was conducted in the Virginia Blue Ridge Physiographic Province, approximately 300 km SE of Polecat Creek, and the study by Cooper et al. (1998) was conducted in Loudoun County, VA approximately 100 km to the north of Polecat Creek. SSA reported for solids in saprolite for Davis Run, VA by White et al. (2001), which is similar to the hydrologic environment at Polecat Creek.

H: Bulk density, porosity, and SSA for weathered saprolite reported by Burns et al. (2003).

Table 7.3. Grain size results from the core collected near West Bear Creek in Wayne County, NC. Total depth refers to the depth below ground surface.

Core Name	Sample Number	Depth from top of run (ft)	Total depth (ft)	Median Grain Size (D50)
Wayne-2013-01-B	1	3.0 to 3.2	7.0 to 7.2	7.91
Wayne-2013-01C/D	2	3.9 to 4.1	12.9 to 13.1	11.96
Wayne-2013-01-E	3	2.4 to 2.6	16.4 to 16.6	4.69
Wayne-2013-01-F	4	1.1 to 1.3	20.1 to 30.1	159.90
Wayne-2013-01-G	5	2.8 to 3.1	29.8 to 30.1	7.66
Wayne-2013-01-H	6	0.6 to 0.8	37.6 to 37.8	16.22
Wayne-2013-01-J	7	1.2 to 1.4	48.2 to 48.4	39.40
Wayne-2013-01-K	8	1.4 to 1.6	53.4 to 53.6	62.56

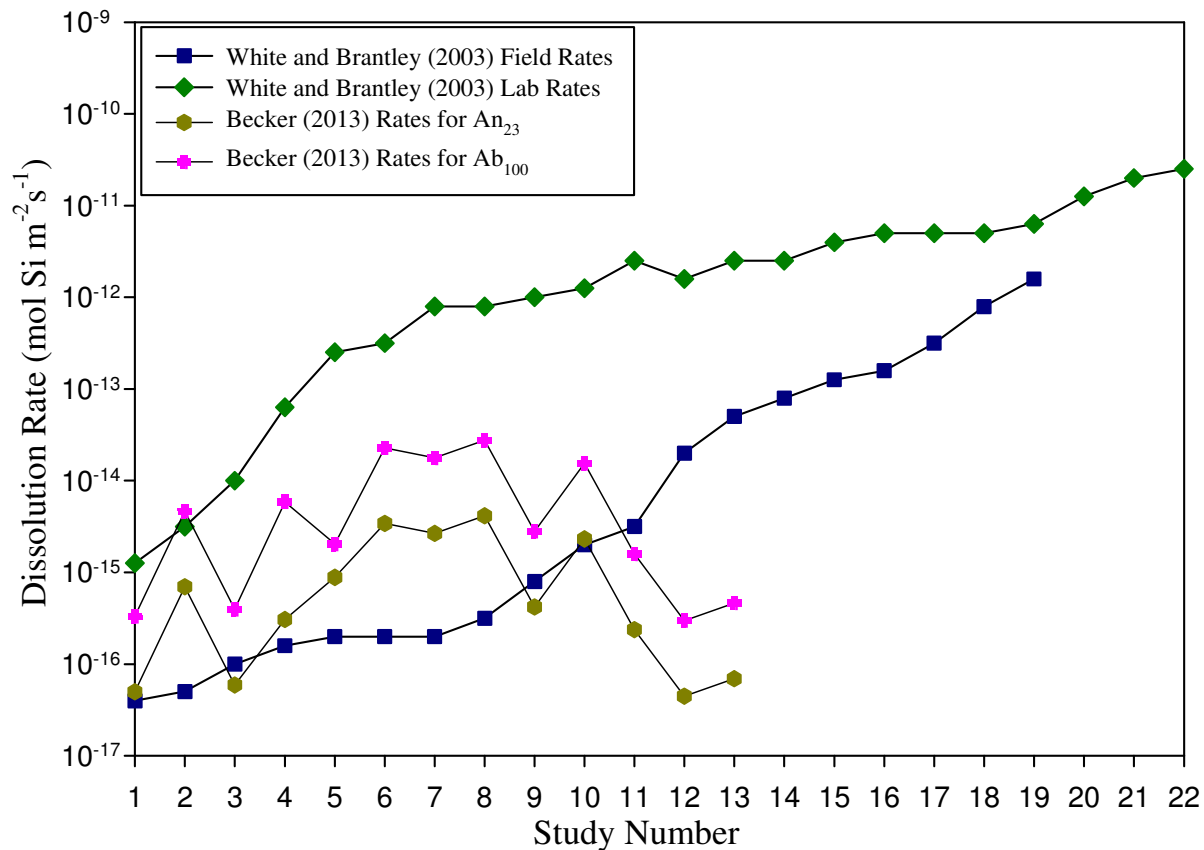


Figure 7.7. Mineral dissolution rates for the studies reported in Table 4 in White and Brantley (2003), and rates from Table 7.2 of this report (see text for details). Studies are plotted in order of their occurrence in these two tables. The field-based and lab-based studies from White and Brantley (2003) are presented in a single table (their Table 4), but for my purpose have been separated into two datasets, each plotted above in order of occurrence within Table 4. For example, the lab-based study plotted above as number 3 is listed in Table 4 of White and Brantley (2003) as study 14, but it is the third occurrence of a lab-based study in Table 4 of White and Brantley (2003). The lab-based studies and the field-based studies from White and Brantley (2003) are two separate and different groups of studies. The two "Becker" plots on the graph represent the same studies (those from Table 7.2) but with different assumptions about the mineral producing the dissolved Si in groundwater: An_{23} (which is the same as Ab_{77}), and Ab_{100} .

7.4. Effect of Biological Activity on [Si]

Although outside the scope of this study, the effect of vegetation and biological activity on [Si] should be mentioned. A study by Derry et al. (2005) provides evidence that vegetation can uptake and sequester measurable amounts of Si from the soil zone. They also mention that biological activity has the ability to enhance mineral dissolution rates, thus increasing the rate which Si is added to the groundwater system. An additional study by Velbel and Price (2007) shows in Table 4 of their report that a biomass term in their mineral dissolution equations that accounts for vegetation in a natural environment has an effect on the weathering rates of plagioclase, almandine garnet, and biotite, increasing the weathering rate with respect to all three minerals. It was observed in Taylor and Velbel (1991) that the exclusion of the biological term underestimated weathering rates by approximately four orders of magnitude. Taylor and Velbel (1991) also note that biotite is much more susceptible (in contrast to plagioclase) to increases in weathering rate due to vegetation because of the biological influence on potassium biogeochemistry.

As evidenced by these studies, vegetation could have an effect on the relationship of increasing [Si] with increasing groundwater age. This effect is most likely limited to the unsaturated portion of the unconfined aquifer (the root zone), where it may affect the intercept on plots of groundwater age vs. groundwater [Si] (i.e., the [Si] of groundwater of zero age at the time of recharge). In areas where the water table is well into the root zone in

the presence of plants with significant Si uptake, the effect of biological activity on age-[Si] relationships may be more complex.

7.5. Summary and Conclusions

Relatively few studies have evaluated the use of increasing [Si] with increasing groundwater age as an age-dating proxy. In my study I evaluated the use of [Si] as an age-dating proxy by performing a critical review on 11 published data sets that contained both groundwater age and [Si] in addition to new data from the West Bear Creek watershed in the coastal plain of North Carolina. The data from these studies was used to build a series of regressions of age vs. [Si] for 10 different locations (6 in the Atlantic coastal plain, 2 in the piedmont, and 2 elsewhere in the US) which I suggest can be used to estimate groundwater age from groundwater [Si] for these locations. Results from my regression analysis indicate an increase in [Si] with increasing groundwater age for all of the studies considered in my thesis. This correlation between increasing [Si] with increasing groundwater age should have a variety of uses in the field of hydrology, such as an initial screening process to identify areas of interest for more in-depth study, or for use in survey work when an inexpensive method that can be used to evaluate a large area is needed. The 95% prediction uncertainty using [Si] to estimate groundwater age was determined for each study location, and for all study areas ranged in value from ± 0.7 to ± 25.8 yr, with a calculated average of ± 14.5 yr (calculated using the mean for each study). For studies conducted in the coastal plain the predicted range in age uncertainty is ± 10.2 - 25.8 yr with an average of ± 17.2 yr.

When considering whether it could be possible to use existing regressions to predict the rate of [Si] acquisition for areas that had not been calibrated within the coastal plain, it was found that variation in the age-[Si] relationship may be large or small over distances of tens of km or hundreds. This implies that the geological and mineralogical properties of a study site are the controlling factors on the rate of [Si] acquisition, and that geographical location is likely not in itself a strong controlling factor. It may be possible to estimate age from [Si] at an unstudied site using an age-[Si] regression from a site with similar geology. For West Bear Creek, a reasonable regression was created using only ten data points with CFC-113 and [Si] data.

The low sampling and analytical costs of [Si] (about 100x less than currently-used age dating tracers) and the ease and speed with which samples can be collected in comparison to currently-used gaseous age-dating tracers make it an attractive method for the initial assessment of groundwater age, if the relationship between [Si] and groundwater age for a particular area can be determined. The [Si] method for estimating groundwater age could be useful for studies that would benefit from a large number of approximate ages (uncertainty of ± 10 -20 yr for the coastal plain, less for the piedmont).

Figure 7.4 summarizes the predictive power of all the studies considered in my thesis, and from this figure it is evident that areas in piedmont geology (Burns et al. 2003 and Lindsey et al. 2003) have a lower predicted age uncertainty than areas in the coastal plain

(± 4.6 - 9.2 years in the piedmont, compared to ± 10 - 20 years typically in the coastal plain).

However, only two piedmont sites with age-[Si] data could be identified and studied, so it is not clear if this would hold true if/when additional piedmont data are available. Both piedmont areas are comprised of hydrologic units composed of saprolite and fractured bedrock. For all of the studies considered in my thesis the rate of [Si] acquisition ranges from 3.0 - 232.6 $\mu\text{M}/\text{yr}$. For studies conducted in the coastal plain the range in [Si] acquisition rate is 3.0 - 22.7 $\mu\text{M}/\text{yr}$. Using Figure 7.3, estimates of the predicted groundwater ages for areas in the coastal plain can be made, for a given [Si]. For example, for a [Si] of 150 μM , the range of groundwater age predicted by the age-[Si] regressions in Table 7.1 is approximately 0.3 - 36.7 yr. Future work relating simple indices (e.g., mineralogy, grain size, formation/presence of certain secondary minerals such as kaolinite) to age-[Si] relationships may allow for the range in age uncertainty of the [Si] method to be reduced for calibrated areas, as well as helping to extend this method to new, unstudied areas within the piedmont and/or coastal plain.

REFERENCES

American Public Health Association, American Water Works Association, & Water Environment Federation. 2012. Standard Methods for the Examination of Water & Wastewater, 21st edition. Port City Press, Baltimore, Maryland.

Anbeek, C. 1992a. Surface roughness for minerals and implications for dissolution studies. *Geochimica et Cosmochimica Acta* 56: 1461-1469.

Anbeek, C. 1992b. The dependence of dissolution rates on grain size for some fresh and weathered feldspars. *Geochimica et Cosmochimica Acta*. 56: 3957-3970.

Anbeek, C. 1993. The effect of natural weathering on dissolution rates. *Geochimica et Cosmochimica Acta* 57: 4963-4975.

Anbeek, C., van Breemen, N., Meijer, E.L., van der Plas, L. 1994. The dissolution of naturally weathered feldspar and quartz. *Geochimica et Cosmochimica Acta* 58: 4601-4614.

Bau, M., Alexander, B., Chesley, J.T., Dulski, P., Brantley, S.L. 2004. Mineral dissolution in the Cape Cod aquifer, Massachusetts, USA: I. Reaction stoichiometry and impact of accessory feldspar and glauconite on strontium isotopes, solute concentrations, and REY distribution. *Geochimica et Cosmochimica Acta*, v. 68 no. 6 p. 1199-1216, doi: 10.1016/j.gca.2003.08.015.

Bauer, S., Fukla, C., and Schäfer, W. A multi-tracer study in a shallow aquifer using age dating tracers 3H, 85K, CFC-113, and SF6, -indication for retarded transport of CFC-113. *Journal of Hydrology* 248: 14-34.

Bethke, C. M., and Johnson, T.M., 2008. Groundwater Age and Groundwater Age Dating. *Annual Review of Earth and Planetary Sciences* 36: 121-52, doi: 10.1146/annurev.earth.36.031207.124210.

Böhlke, J. K., and Denver, J.M. 1995. Combined use of Groundwater Dating, Chemical, and Isotopic Analyses to Resolve the History and Fate of Nitrate Contamination in Two Agricultural Watersheds, Atlantic Coastal Plain, Maryland. *Water Resources Research* 31(9): 2319-2339, doi: 10.1029/95WR01584.

Böhlke, J.K., O'Connell, M.E., and Prestegard, K.L. 2007. Ground water stratification and delivery of nitrate to an incised stream under varying flow conditions. *Journal of Environmental Quality* 36: 664-680.

Brantley, S.L., and Mellott, N.P. 2000. Surface area and porosity of primary silicate minerals. *American Mineralogist*. 85: 1767-1783.

Burns, D. A., Plummer, N.L., McDonnell, J.J., Busenberg, E., Casile, G.C., Kendall, C., Hooper, R.P., Freer, J.E., Peters, N.E., Beven, K., Schlosser, P. 2003. The Geochemical Evolution of Riparian Ground Water in a Forested Piedmont Catchment. *Ground Water* 41(7): 913-925, doi: 10.1111/j.1745-6584.2003.tb02434.x

Busenberg, E. and Plummer, L.N. 1992. Use of Chlorofluorocarbons (CCl_3F and CCl_2F_2) as Hydrologic Tracers and Age-Dating Tools: The Alluvium and Terrace System of Central Oklahoma. *Water Resources Research* 28(9): 2257-2283, doi: 10.1029/92WR01263.

Busenberg, E. and Plummer, L.N. 2000. Dating young groundwater with sulfur hexafluoride: Natural and anthropogenic sources of sulfur hexafluoride. *Water Resources Research* 36(10): 3011-3030, doi: 10.1029/2000WR900151.

Busenberg, E., Plummer, L. N., 2006. Potential use of other atmospheric gases in *Use of Chlorofluorocarbons in Hydrology: A Guidebook*, chap. 10, pp. 183-190, Int. At. Agency, Vienna.

Busenberg, E., and N. L. Plummer. 2011. Compilation of data on the CFC and SF6 concentrations in North American air. Spreadsheet prepared at and available from the USGS Chlorofluorocarbon Laboratory in Reston, VA, based on data from: (1) AFEAS, www.afeas.org, (2) NOAA, www.esrl.noaa.gov/gmd/, gaw.kishou.go.jp/cgi-

bin/wdcgg/accessdata.cgi?index=NWR440N00-NOAA&select=inventory, and (3)
Georgia Tech, agage.eas.gatech.edu/data.htm.

Busenberg, E., Plummer, L. N., Cook, P.G., Solomon, D.K., Han, L.F., Gröning, M., and Oster, H. 2006. Sampling and analytical methods in *Use of Chlorofluorocarbons in Hydrology: A Guidebook*, chap. 12, pp. 199-220, Int. At. Agency, Vienna.

Cherry, A. J. 2000. A multi-tracer estimation of groundwater recharge in a glaciofluvial aquifer in southeastern Manitoba. *University of Ottawa, Canada*.

Cook, P.G., and Böhlke, J-K. 2000. Determining Timescales for Groundwater Flow and Solute Transport in *Environmental Tracers in Subsurface Hydrology*, chap.1, pp. 1-30, Kluwer Academic Publishers. CSIRO Land and Water, Glen Osmond, Australia.

Cook, P.G. & Solomon, D.K. 1995. Transport of atmospheric trace gases to the water table: Implications for groundwater dating with chlorofluorocarbons and krypton 85. *Water Resources Research* 31: 263-270, doi: 10.1029/94WR02232.

Cook, P.G., Plummer, L.N., Solomon, D.K., Busenberg, Han, L.E. 2006. Effects and processes that can modify apparent age in *Use of Chlorofluorocarbons in Hydrology: A Guidebook*, chap. 4, pp. 31-58, Int. At. Agency, Vienna.

Cook P.G. and Solomon D.K. 1997. Recent advances in dating young groundwater: chlorofluorocarbons, $^3\text{H}/^3\text{He}$, and ^{85}Kr . *Journal of Hydrology* 191: 245-265, doi: 10.1016/S0022-1694(96)03051-X.

Cooper, B-B. 1988. Hydrogeologic Characterization of an Existing Solid Waste Disposal Site: A Case Study in Complying with Recent Environmental Regulations. *The Department of Natural Resources, Loudoun County, Virginia*.

Day, B.A. and Nightingale, H. I. 1984. Relationships Between Ground-Water Silica, Total Dissolved Solids, and Specific Electrical Conductivity. *Groundwater* 22(1): 80-85.

Denver, J.M., Tesoriero, A.J., Barbaro, J.R. 2010. Trends and Transformations of Nutrients and Pesticides in a Coastal Plain Aquifer System, United States. *Journal of Environmental Quality* 30: 154-167, doi: 10.2134/jeq2009.0107.

Derry, L.A., Kurtz, A.C., Ziegler, K., Chadwick, O.A. 2005. Biological control of terrestrial silica cycling and export fluxes to watersheds. *Letters to Nature* 433: 728-731.

Dunkle, S.A., Plummer, L.N., Busenberg, E., Phillips, P.J., Denver, J.M., Hamilton, P.A., Michel, R.L., Coplen, T.B. 1993. Chlorofluorocarbons (CCl₃F and CCl₂F) as dating tools and hydrologic tracers in shallow groundwater of the Delmarva Peninsula, Atlantic coastal plain, United States. *Water Resources Research* 29: 3837-3860.

Ekwrudel, B., Schlosser, P., Smethie, W., Plummer, L., Busenberg, E., Michel, R., Weppernig, R., Stute, M. 1994. Dating of shallow groundwater: Comparison of the transient tracers ³H/³He, chlorofluorocarbons, and ⁸⁵Kr. *Water Resources Research* 30(6), doi: 10.1029/94WR00156.

Elkins, J.W. 1989. Geophysical monitoring for climatic change. *Summary Rep. 1998*, 17, NOAA, Boulder Colo.

Farrell, K.M. 2002. Contentnea Creek Geologic Framework to Support Ground-Water – Model Upscaling. *Report to the Planning Section Division of Water Quality North Carolina Department of Environmental and Natural Resources*, FY-01 Contract No. EWO2018.

Farrell, K.M. 2007. Shallow Aquifers and Confining Units in the Neuse River Basin, Surry to Suffolk Scarp. *Fiscal Year2003 Grant*, NC-DENR Contract Number EW04035.

Fritz, B. and Noguera, C. 2009. Mineral Precipitation Kinetics in *Thermodynamics and Kinetics of Water-Rock Interaction*, chap. 8, pp. 371-432, The Mineralogical Society of America, Chantilly, Virginia.

Garrels, R.M., Mackenzie, F.T., 1967. Origin of the chemical compositions of some springs and lakes. In: Stumm, W. (Ed), *Equilibrium Concepts in Natural Water Systems*, Advances in Chemistry Series, 67. *American Chemical Society*, p. 222-242.

Gellici, J.A. Lautier, J.C. 2010. Hydrogeologic Framework of the Atlantic Coastal Plain, North and South Carolina in *Groundwater Availability in the Atlantic Coastal Plain of North and South Carolina* chap. B, pp. 64-92. U.S. Department of the Interior, and the U.S. Geological Survey, Professional Paper 1773.

Han, L.E., Gröning, M., Plummer, L.N., Solomon, D.K. 2006. Comparison of the CFC technique with other techniques (^3H , $^3\text{H}/^3\text{He}$, ^{85}Kr) in *Use of Chlorofluorocarbons in Hydrology: A Guidebook*, chap.11, pp. 191-198, Int. At. Agency, Vienna.

Heath, R.C. 1994. Ground-Water Recharge in North Carolina: Unpublished report prepared for the NC-DWQ Groundwater Section, 44 p.

Heath, R.C. 1997. Aquifer Sensitivity Map of Brunswick County, North Carolina, unpublished report for the Brunswick County Planning Department, 21 p.

Kazemi, G.A., Lehr, J.H., and Perrochet, P. 2006. *Groundwater Age*. Wiley-Interscience. Hoboken, New Jersey.

Katz, B.G. 2004. Sources of nitrate contamination and age of water in large karstic springs in Florida. *Environmental Geology* 46: 689-706.

Kennedy, C.D. and Genereux, D.P. 2007. ^{14}C Groundwater age and the importance of chemical fluxes across aquifer boundaries in confined Cretaceous aquifers of North Carolina, USA. *Radiocarbon* 49 (3): 1191-1203.

Kennedy, C. D., Genereux, D. P., Corbett, D. R., & Mitasova, H. 2009a. Relationships among groundwater age, denitrification, and the coupled groundwater and nitrogen fluxes through a streambed. *Water Resources* 45, W09402, doi: 10.1029/2008WR007400.

Kennedy, C. D., Genereux, D. P., Corbett, D. R., & Mitasova, H. 2009b. Spatial and temporal dynamics of coupled groundwater and nitrogen fluxes through a streambed in an agricultural watershed. *Water Resources Research* 45, W09401, doi: 10.1029/2008WR007397.

Kenoyer, G.J., and Bowser, C.J. 1992. Groundwater Chemical Evolution in a Sandy Silicate Aquifer in Northern Wisconsin 1. Patterns and Rates of Change. *Water Resources Research* 28(2): 579-589, doi: 91WR02302.

Kittrick, J.A. 1970. Precipitation of kaolinite at 25°C and 1 ATM. *Clays and Clay Minerals* 18: 261-267.

Koterba, M.T., Wilde, F.D., and Lapham, W.W. 1995. Ground-water data collection protocols and procedures for the National Water Quality Assessment program: Collection and documentation of water-quality samples and related data. U.S. *Geological Survey Open-File Rep.* 95-399. USGS, Washington, DC.

Iler, R.K. 1979. *The Chemistry of Silica: Solubility, Polymerization, Colloid and Surface Properties, and Biochemistry*. Wiley-Interscience. New York.

International Atomic Energy Agency. 2006. *Use of Chlorofluorocarbons in Hydrology: A Guidebook*. IAEA. Vienna.

Lautier, J.C. 2001. Hydrogeologic Framework and Ground Water Conditions in the North Carolina Northwestern Coastal Plain. *Division of Water Resources, NC Department of Environment and Natural Resources*, 38 p.

Lautier, J.C. 2002. Hydrogeologic framework and groundwater conditions in the North Carolina central Coastal Plain: *North Carolina Department of Environment, Health, and Natural Resources, North Carolina Division of Water Resources*, 38 p.

Lautier, J.C. 2006. Hydrogeologic framework and groundwater conditions in the North Carolina central Coastal Plain: *North Carolina Department of Environment, Health, and Natural Resources, North Carolina Division of Water Resources*, 31 p.

Lindsey, B. D., Phillips, S.W., Donnelly, C.A., Speiran, G.K., Plummer, L.N., Böhlke, J., Focazio, M.J., Burton, W.C., Busenberg, E. 2003. Residence Times and Nitrate Transport in Ground Water Discharging to Streams in the Chesapeake Bay Watershed. *Water-Resources Investigations Report*, 03-4035.

Mackay, D.M., Wilson, R.D., Brown, M.J., Ball, W.P., Xia, G., Durfee, D.P. 2000. A controlled field evaluation of continuous vs. pulsed pump-and-treat remediation of a VOC-contaminated aquifer; site characterization, experimental setup, and overview of results. *Journal of Contaminant Hydrology* 41: 81-131.

Morel, F.M.M., and Hering, J. G. 1993. *Principles and Applications of Aquatic Chemistry*. John Wiley and Sons, Inc., New York, 588 pages.

Penn, R.L., Zhu, C., Xu, H., Veblen, D.R. 2013. Iron oxide coatings on sand grains from the Atlantic coastal plain: High-resolution transmission electron microscopy characterization. *Geology* 2001 (29): 843-846, doi: 10.1130/0091-7613(2001)029<0843:IOCOSG>2.0.CO; 2.

Plummer, L.N., and Busenberg, E. 2000. Chlorofluorocarbons in *Environmental Tracers in Subsurface Hydrology*, chap. 15, pp. 441-478, Kluwer Academic Publishers, Boston.

Plummer, L.N., Böhlke, J.K., and Busenberg, E. 2003. Approaches for ground-water dating. *U.S. Geological Survey Water-Resources Investigations Report* 03-4035: 12-24.

Plummer, L.N., Busenberg, E., Böhlke, J.K., Nelms, D.L., Michel, R.L., Schlosser, P. 2001. Groundwater residence times in Shenandoah National Park, Blue Ridge Mountains, Virginia, USA: a multi-tracer approach. *Chemical Geology* 179: 93-111, ISSN 0009-2541, 10.1016/S0009-2541(01)00317-5.

Plummer, L.N., Busenberg, E., Cook, P.G. 2006. Principles of Chlorofluorocarbon Dating in *Use of Chlorofluorocarbons in Hydrology: A Guidebook*, chap.3, pp. 17-30, Int. At. Agency, Vienna.

Plummer, L.N., Busenberg, E. 2006. Chlorofluorocarbons in the atmosphere in *Use of Chlorofluorocarbons in Hydrology: A Guidebook*, chap. 2, pp. 9-16, Int. At. Agency, Vienna.

Plummer, L.N., and Mullin, A.H. 1997. Collection, processing, and analysis of ground-water samples for tritium/helium-3 dating: *U.S. Geological Survey National Water Quality Laboratory Technical Memorandum 97.04S*, accessed December 7, 2011.

Plummer, L.N., Prestemon, E.C., and Parkhurst, D.L. 1991. An interactive code (NETPATH) for modeling NET geochemical reactions along flow PATH. *U.S. Geological Survey Water Resources Investigative Report 91-4078*.

Poreda, R.J., Cerling, T.E., and Salomon, D.K. 1998. Tritium and Helium isotopes as hydrologic tracers in a shallow unconfined aquifer. *Journal of Hydrology* 103: 1-9, doi: 10.1016/0022-1694(88)90002-9.

Puckett, L.J., Cowdery, T.K., McMahon, P.B., Tornes, L.H., Stoner, J.D. 2002. Using chemical, hydrologic, and age dating analysis to delineate redox processes and flow paths in the riparian zone of a glacial outwash aquifer-stream system. *Water Resources Research* 38(8): 1134, doi: 10.1029/2001WR000396.

Rademacher, L. K., Clark, J.F., Hudson, G.B., Erman, D.C., Erman, N.A. 2001. Chemical Evolution of Shallow Groundwater as Recorded by Springs, Sagehen Basin; Nevada County, California. *Chemical Geology* 179: 37-51, ISSN: 0009-2541.

Rademacher, L.K., Clark, J.F., and Hudson, G.B. 2002. Temporal changes in stable isotope composition of spring waters: Implications for recent changes in climate and atmospheric circulation. *Geology* 30: 139-142. doi: 10.1130/0091-7613.

Santamarina, J.C., Klein, K.A., Wang, Y.H., Prencke, E. 2002. Specific surface: determination and relevance. *NRC Canada*.

Sardini, P., Ledesert, B., and Touchard, G. 1997. Quantification of microscopic porous networks by image analysis and measurements of permeability in the Soultz-Sous-Forets

granite (Alsace, France) in *Fluid Flow and Transport in Rocks: Mechanisms and Effects*, chap. 10, pp. 171-189, Chapman & Hall, London.

Savoie, J., LeBlanc, D.R., Coppola, S.P., Hess, K.M. 1998. Water-Quality Data and Methods of Analysis for Samples Collected Near a Plume of Sewage-Contaminated Ground Water, Ashumet Valley, Cape Cod, Massachusetts, 1993-94. *U.S. Geological Survey Water-Resources Investigations Report 97-4269*, 208p.

Scanlon, T. M., Raffensperger, J.P., Hornberger, G.M. 2001. Modeling transport of dissolved silica in a forested headwater catchments: Implications for defining the hydrochemical response of observed flow pathways. *Water Resources Research* 37(4): 1071-1082.

Schott, J., Pokrovsky, O. S., and Oelkers, E.H. 2009. The Link Between Mineral Dissolution/Precipitation Kinetics and Solution Chemistry in *Thermodynamics and Kinetics of Water-Rock Interaction*, chap. 6, pp. 207-253, The Mineralogical Society of America, Chantilly, Virginia.

Schnoor, J.L. 1990. Kinetics of chemical weathering a comparison of laboratory and field rates in Strum, W. (Ed.), *Aquatic Chemical Kinetics* pp. 475-594, Wiley, New York.

Shapiro, S. D., LeBlanc, D., Schlosser, P., Ludin, A. 1999. Characterizing a Sewage Plume Using the ^3H - ^3H Dating Technique. *Ground Water* 37(6): 861-878.

SigmaPlot® 10 User's Manual. 2006. *Systat Software, Inc.* Point Richmond, CA.

Solomon, K.D., Cook, P.G., and Plummer, L.N. 2006. Models of groundwater ages and residence times, in *Use of Chlorofluorocarbons in Hydrology: A Guidebook*, chap. 6, pp. 73-88, Int. At. Agency, Vienna.

Solomon, K.D., and Cook, P.G. 2000. ^3H and ^3He in *Environmental Tracers in Subsurface Hydrology*, chap. 13, pp. 387-424, Kluwer Academic Publishers, Boston.

Solomon, K.D., Poreda, R.J., Schiff, S.L., Cherry, J.A. 1992. Tritium and Helium 3 as Groundwater Age Tracers in the Borden Aquifer. *Water Resources Research* 28(3): 741-755, doi: 0043-1397/92/91WR-02689.

Stolp, B.J., Solomon, D.K., Suckow, A., Vitvar, T., Rank, D., Aggarwal, P.K., Han, L.F. 2010. Age dating base flow at springs and gaining streams using helium-3 and tritium: Fischa-Dagnitz system, southern Vienna Basin, Austria. *Water Resources Research* 46: W07503.

Stoner, J.D., Cowdery, T.K., and Puckett, L.J. 1997. Ground-water Age Dating and Other Tools Used to Assess Land-use Effects on Water Quality. *U.S. Department of the Interior and U.S. Geological Survey Water-Resources Investigations Report* 97-4150.

Stute, M., and Schlosser, P. 2000. Atmospheric Noble Gases in *Environmental Tracers in Subsurface Hydrology*, chap. 11, pp. 349-377, Kluwer Academic Publishers. CSIRO Land and Water, Glen Osmond, Australia.

Surano, K.A., Hudson, G.B., Failor, R.A. 1992. Helium-3 mass spectrometry for low level-tritium analysis of environmental samples. *Journal of Radioanalytical Nuclear Chemistry* 161: 443-453.

Szabo, Z., Rice, D.E., Plummer, L.N., Busenberg, E., Drenkard, S., Schlosser, P. 1996. Age dating of shallow groundwater with chlorofluorocarbons, tritium/helium 3, and flow path analysis, southern New Jersey coastal plain. *Water Resources Research*. 32(4): 1023–1038, doi: 10.1029/96WR00068.

Taylor, A.S., and Velbel, M.A. 1991. Geochemical mass balances and weathering rates in forested watersheds of the southern Blue Ridge II. Effects of botanical uptake terms. *Geoderma* 51: 29-50.

Tant, P.L., Bryd, H.J., and Horton, R.E. 1974. General Soil Map of North Carolina: U.S. Soil Conservation Service 1:1,000,000 scale map.

Tesoriero, A.J., Liebscher, H., and Cox, S.E. 2000. Mechanism and rate of denitrification in an agricultural watershed: Electron and mass balance along groundwater flow paths. *Water Resources Research* 36(6): 1545–1559, doi: 10.1029/2000WR900035.

Tesoriero, A. J., Spruill, T.B., Mew Jr., H.E., Farrell, K.M., Harden, S.L. 2005. Nitrogen transport and transformations in a coastal plain watershed: Influence of geomorphology on flow paths and residence times. *Water Resources Research* 41, W02008, doi: 10.1029/2003WR002953.

Velbel, M. A. 1985. Geochemical Mass Balances and Weathering Rates in Forested Watersheds of the Southern Blue Ridge. *American Journal of Science* 285: 904-930.
Velbel, M.A., Price, P.R. 2007. Solute geochemical mass-balances and mineral weathering rates in small watersheds: Methodology, recent advances, and future directions. *Applied Geochemistry* 22: 1682-1700, doi: 10.1016/j.apgeochem.2007.03.029.

White, B.A. 2005. Physical Investigation of Field Scale Groundwater Recharge Processes in the Virginia Blue Ridge Physiographic Province. *Masters Thesis*. Virginia Polytechnic Institute and State University, Blacksburg, Virginia.

White, A.F., Blum, A.E., Schulz, M.A., Bullen, T.D., Harden, J.W., Peterson, M.L. 1996. Chemical weathering rates of a soil chronosequence on granite alluvium: I. Quantification of mineralogical and surface area changes and calculation of primary silicate reaction rates. *Geochimica et Cosmochimica Acta* 60(14): 2533-2550.

White, A.F., Bullen, T.D., Schulz, M.S., Blum, A.E., Huntington, T.G., Peters, N.E. 2001. Differential rates of feldspar weathering in granitic regoliths. *Geochimica et Cosmochimica Acta* 65(6): 847-869.

Zar, J.H. 1999. Simple Linear Regression in *Biostatistical Analysis 4th Edition*, chap. 17, pages 324-35, Prentice-Hall Inc. Upper Saddle River, New Jersey.

<http://water.usgs.gov/lab/>